

研究成果の刊行物印刷一覧表

1. Nozu K, Minamikawa S, Yamada S, Oka M, Yanagita M, Morisada N, Fujinaga S, Nagano C, Gotoh Y, Takahashi E, Morishita T, Yamamura T, Ninchoji T, Kaito H, Morioka I, Nakanishi K, Vorechovsky I, Iijima K. Characterization of contiguous gene deletions in COL4A6 and COL4A5 in Alport syndrome-diffuse leiomyomatosis. *J Hum Genet*. 2017 Mar 9. doi: 10.1038/jhg.2017.28. [Epub ahead of print] PMID: 28275241
2. Horinouchi T, Nozu K, Kamiyoshi N, Kamei K, Togawa H, Shima Y, Urahama Y, Yamamura T, Minamikawa S, Nakanishi K, Fujimura J, Morioka I, Ninchoji T, Kaito H, Nakanishi K, Iijima K. Diagnostic strategy for inherited hypomagnesemia. *Clin Exp Nephrol*. 2017 Mar 1. doi: 10.1007/s10157-017-1396-7. [Epub ahead of print] PMID: 28251383
3. Nagao R, Suzuki S, Kawashima H, Nozu K, Iijima K. Acute kidney injury in type 3 Bartter syndrome: Angiotensin-converting enzyme inhibitors as a cause. *Pediatr Int*. 2016;58(12):1373-1374. doi: 10.1111/ped.13100. PMID: 28008741
4. Uchida N, Kumagai N, Nozu K, Fu XJ, Iijima K, Kondo Y, Kure S. Early RAAS Blockade Exerts Renoprotective Effects in Autosomal Recessive Alport Syndrome. *Tohoku J Exp Med*. 2016;240(3):251-257. DOI: 10.1620/tjem.240.251. PMID: 27904025
5. Yokota K, Nozu K, Minamikawa S, Yamamura T, Nakanishi K, Kaneda H, Hamada R, Nozu Y, Shono A, Ninchoji T, Morisada N, Ishimori S, Fujimura J, Horinouchi T, Kaito H, Nakanishi K, Morioka I, Taniguchi-Ikeda M, Iijima K. Female X-linked Alport syndrome with somatic mosaicism. *Clin Exp Nephrol*. 2016 Oct 31. [Epub ahead of print] PMID: 27796712
6. Nozu K, Nozu Y, Nakanishi K, Konomoto T, Horinouchi T, Shono A, Morisada N, Minamikawa S, Yamamura T, Fujimura J, Nakanishi K, Ninchoji T, Kaito H, Morioka I, Taniguchi-Ikeda M, Vorechovsky I, Iijima K. Cryptic exon activation in SLC12A3 in Gitelman syndrome. *J Hum Genet*. 2017;62(2):335-337. doi: 10.1038/jhg.2016.129. PMID: 27784896
7. Iwafuchi Y, Morioka T, Oyama Y, Nozu K, Iijima K, Narita I. A Case of Transforming Growth Factor- β -Induced Gene-Related Oculorenal Syndrome: Granular Corneal Dystrophy Type II with a Unique Nephropathy. *Case Rep Nephrol Dial*. 2016;6(3):106-113. eCollection 2016 Sep-Dec. DOI: 10.1159/000449129. PMID: 27781206
8. Abe Y, Iyoda M, Nozu K, Hibino S, Hihara K, Yamaguchi Y, Yamamura T, Minamikawa S, Iijima K, Shibata T, Itabashi K. A Novel Mutation in a Japanese Family with X-linked Alport Syndrome. *Intern Med*. 2016;55(19):2843-2847. Epub 2016 Oct 1. DOI: 10.2169/internalmedicine.55.6873. PMID: 27725546
9. Kamiyoshi N, Nozu K, Fu XJ, Morisada N, Nozu Y, Ye MJ, Imafuku A, Miura K, Yamamura T, Minamikawa S, Shono A, Ninchoji T, Morioka I, Nakanishi K, Yoshikawa N, Kaito H, Iijima K.

Genetic, Clinical, and Pathologic Backgrounds of Patients with Autosomal Dominant Alport Syndrome. *Clin J Am Soc Nephrol*. 2016;11(8):1441-9. doi: 10.2215/CJN.01000116. Epub 2016 Jun 8. PMID: 27281700

10. Iijima T, Hoshino J, Mise K, Sumida K, Suwabe T, Hayami N, Ueno T, Takaichi K, Fujii T, Ohashi K, Morisada N, Iijima K, Ubara Y. Daughter and mother with orofaciodygital syndrome type 1 and glomerulocystic kidney disease. *Hum Pathol*. 2016;55:24-9. doi: 10.1016/j.humpath.2016.04.005. Epub 2016 Apr 27. PMID: 27131853
11. Ohtsubo H, Okada T, Nozu K, Takaoka Y, Shono A, Asanuma K, Zhang L, Nakanishi K, Taniguchi-Ikeda M, Kaito H, Iijima K, Nakamura S. Identification of mutations in FN1 leading to glomerulopathy with fibronectin deposits. *Pediatr Nephrol*. 2016;31(9):1459-67. doi: 10.1007/s00467-016-3368-7. Epub 2016 Apr 7. PMID: 27056061
12. Yamamura T, Morisada N, Nozu K, Minamikawa S, Ishimori S, Toyoshima D, Ninchoji T, Yasui M, Taniguchi-Ikeda M, Morioka I, Nakanishi K, Nishio H, Iijima K. Rare renal ciliopathies in non-consanguineous families that were identified by targeted resequencing. *Clin Exp Nephrol*. 2017;21(1):136-142. doi: 10.1007/s10157-016-1256-x. Epub 2016 Mar 11. PMID: 26968886
13. Kanda S, Morisada N, Kaneko N, Yabuuchi T, Nawashiro Y, Tada N, Nishiyama K, Miyai T, Sugawara N, Ishizuka K, Chikamoto H, Akioka Y, Iijima K, Hattori M. New-onset diabetes after renal transplantation in a patient with a novel HNF1B mutation. *Pediatr Transplant*. 2016;20(3):467-71. doi: 10.1111/petr.12690. Epub 2016 Feb 21. PMID: 26899772
14. Fu XJ, Nozu K, Eguchi A, Nozu Y, Morisada N, Shono A, Taniguchi-Ikeda M, Shima Y, Nakanishi K, Vorechovsky I, Iijima K. X-linked Alport syndrome associated with a synonymous p.Gly292Gly mutation alters the splicing donor site of the type IV collagen alpha chain 5 gene. *Clin Exp Nephrol*. 2016 Oct;20(5):699-702. DOI: 10.1007/s10157-015-1197-9. PMID: 26581810
15. Hirano D, Ishikura K, Uemura O, Ito S, Wada N, Hattori M, Ohashi Y, Hamasaki Y, Tanaka R, Nakanishi K, Kaneko T, Honda M. Association between low birth weight and childhood-onset chronic kidney disease in Japan: a combined analysis of nationwide survey for paediatric CKD and National Report of Vital Statistics. *Nephrol Dial Transplant*. 2016 Nov;31(11):1895-1900. DOI: 10.1093/ndt/gfv425. PMID: 26953592
16. Okuda Y, Ishikura K, Terano C, Harada R, Hamada R, Hataya H, Ogata K, Honda M. Irreversible severe kidney injury and anuria in a 3-month-old girl with atypical haemolytic uraemic syndrome under administration of eculizumab. *Nephrol (Carlton)*. 2016 Mar;21(3):261-265. DOI: 10.1111/nep.12582. PMID: 26818219
17. Yoshizawa C, Kobayashi Y, Ikeuchi Y, Tashiro M, Kakegawa S, Watanabe T, Goto Y, Nakanishi K, Yoshikawa N, Arakawa H. Congenital nephrotic syndrome with a novel NPHS1 mutation.

- Pediatr Int. 2016 Nov;58(11):1211-1215. doi: 10.1111/ped.13118. PMID: 27882743
18. Inaba A, Hamasaki Y, Ishikura K, Hamada R, Sakai T, Hataya H, Komaki F, Kaneko T, Mori M, Honda M. Long-term outcome of idiopathic steroid-resistant nephrotic syndrome in children. *Pediatr Nephrol*. 2016 Mar;31(3):425-434. doi: 10.1007/s00467-015-3174-7. Epub 2015 Sep 3. PMID: 26335197
 19. Kato H, Nangaku M, Hataya H, Sawai T, Ashida A, Fujimaru R, Hidaka Y, Kaname S, Maruyama S, Yasuda T, Yoshida Y, Ito S, Hattori M, Miyakawa Y, Fujimura Y, Okada H, Kagami S: Joint Committee for the Revision of Clinical Guides of Atypical Hemolytic Uremic Syndrome in Japan. *Clinical Guides for atypical hemolytic uremic syndrome in Japan*. *Clin Exp Nephrol* 20: 536-543, 2016. doi: 10.1007/s10157-016-1276-6. Review. PMID: 27422619
 20. Satoh N, Yamada H, Yamazaki O, Suzuki M, Nakamura M, Suzuki A, Ashida A, Yamamoto D, Kaku Y, Sekine T, Seki G, Horita S. A pure chloride channel mutant of CLC-5 causes Dent's disease via insufficient V-ATPase activation. *Pflugers Arch* 468: 1183-1196, 2016. DOI: 10.1007/s00424-016-1808-7. PMID: 27044412
 21. Udagawa T, Jo T, Yanagihara T, Shimizu A, Mitsui J, Tsuji S, Morishita S, Onai R, Miura K, Kanda S, Kajiho Y, Tsurumi H, Oka A, Hattori M, Harita Y. Altered expression of Crb2 in podocytes expands a variation of CRB2 mutations in steroid-resistant nephrotic syndrome. *Pediatr Nephrol* 2016 Dec 10 [Epub ahead of print] DOI:10.1007/s00467-016-3549-4. PMID: 27942854
 22. Sugimoto K, Miyazawa T, Enya T, Nishi H, Miyazaki K, Okada M, Takemura T. Clinical and genetic characteristics of Japanese nephronophthisis patients. *Clin Exp Nephrol*. 20:637-649, 2016. DOI: 10.1007/s10157-015-1180-5. PMID: 26499951
 23. Nishimura H, Yaoita E, Nameta M, Yamaguchi K, Sato M, Ihoriya C, Zhao L, Kawachi H, Sasaki T, Ikezumi Y, Ouchi Y, Kashihara N, Yamamoto T. Restricted nutrition-induced low birth weight, low number of nephrons and glomerular mesangium injury in Japanese quail. *J Dev Orig Health Dis* 6:1-14, 2017. DOI: 10.1017/S2040174416000787. PMID: 28162133
 24. Sakiyama M, Matsuo H, Nakaoka H, Yamamoto K, Nakayama A, Nakamura T, Kawai S, Okada R, Ooyama H, Shimizu T, Shinomiya N. Identification of rs671, a common variant of ALDH2, as a gout susceptibility locus. *Sci Rep*. 2016 May 16;6:25360. doi: 10.1038/srep25360. PMID: 27181629
 25. Higashino T, Matsuo H, Sakiyama M, Nakayama A, Nakamura T, Takada T, Ogata H, Kawamura Y, Kawaguchi M, Naito M, Kawai S, Takada Y, Ooyama H, Suzuki H, Shinomiya N. Common variant of PDZ domain containing 1 (PDZK1) gene is associated with gout susceptibility: A replication study and meta-analysis in Japanese population. *Drug Metab Pharmacokinet*. 2016 Dec;31(6):464-466. doi: 10.1016/j.dmpk.2016.07.004. Epub 2016 Jul 30. PMID: 27720648

26. Matsuo H, Tsunoda T, Ooyama K, Sakiyama M, Sogo T, Takada T, Nakashima A, Nakayama A, Kawaguchi M, Higashino T, Wakai K, Ooyama H, Hokari R, Suzuki H, Ichida K, Inui A, Fujimori S, Shinomiya N. Hyperuricemia in acute gastroenteritis is caused by decreased urate excretion via ABCG2. *Sci Rep.* 2016 Aug 30;6:31003. doi: 10.1038/srep31003. PMID: 27571712
27. Nakayama A, Nakaoka H, Yamamoto K, Sakiyama M, Shaukat A, Toyoda Y, Okada Y, Kamatani Y, Nakamura T, Takada T, Inoue K, Yasujima T, Yuasa H, Shirahama Y, Nakashima H, Shimizu S, Higashino T, Kawamura Y, Ogata H, Kawaguchi M, Ohkawa Y, Danjoh I, Tokumasu A, Ooyama K, Ito T, Kondo T, Wakai K, Stiburkova B, Pavelka K, Stamp LK, Dalbeth N; Eurogout Consortium., Sakurai Y, Suzuki H, Hosoyamada M, Fujimori S, Yokoo T, Hosoya T, Inoue I, Takahashi A, Kubo M, Ooyama H, Shimizu T, Ichida K, Shinomiya N, Merriman TR, Matsuo H; Eurogout Consortium.. GWAS of clinically defined gout and subtypes identifies multiple susceptibility loci that include urate transporter genes. *Ann Rheum Dis.* 2017 May;76(5):869-877. doi: 10.1136/annrheumdis-2016-209632. Epub 2016 Nov 29. PMID: 27899376
28. 先天性腎尿路異常(CAKUT)のガイドライン[オンライン版]
29. 腎性低尿酸血症診療ガイドライン

Long-term outcome of idiopathic steroid-resistant nephrotic syndrome in children

Aya Inaba¹ · Yuko Hamasaki² · Kenji Ishikura^{3,7} · Riku Hamada³ · Tomoyuki Sakai⁴ · Hiroshi Hataya³ · Fumiyo Komaki⁵ · Tetsuji Kaneko^{6,8} · Masaaki Mori¹ · Masataka Honda³

Received: 8 December 2014 / Revised: 13 July 2015 / Accepted: 15 July 2015 / Published online: 3 September 2015
© IPNA 2015

Abstract

Background Several recent studies have shown improved short-term outcome of steroid-resistant nephrotic syndrome (SRNS) in children; however, only a few studies have evaluated the long-term outcome. The aims of our study were to obtain detailed data and analyze the long-term outcome of children with SRNS.

Methods Sixty-nine children with idiopathic SRNS were enrolled and divided into two groups based on initial histopathological patterns: focal segmental glomerulosclerosis (FSGS) and minimal change (MC)/diffuse mesangial proliferation (DMP). The effects of initial treatment with the

immunosuppressant of choice (cyclosporine or cyclophosphamide) on renal survival, remission, and incidence of complications were analyzed in both groups (4 subgroups).

Results The renal survival rate was significantly different among the four different subgroups based on different combinations of initial histopathological pattern (FSGS vs. MC/DMP) and initial immunosuppressant used for treating SRNS (cyclosporine vs. cyclophosphamide) ($P=0.013$), with renal survival in the FSGS (cyclophosphamide) subgroup being especially low (54.6 %). Disease- and/or treatment-associated complications were relatively low; however, hypertension at last examination was observed in a considerable number of patients (31.9 %).

Conclusions Our results suggest that a recently developed therapeutic regimen with cyclosporine considerably improves both the initial remission rate and the long-term renal survival rate of children with idiopathic SRNS.

Electronic supplementary material The online version of this article (doi:10.1007/s00467-015-3174-7) contains supplementary material, which is available to authorized users.

✉ Yuko Hamasaki
yuhamasaki@med.toho-u.ac.jp

- ¹ Department of Pediatrics, Yokohama City University Medical Center, Kanagawa, Japan
- ² Department of Pediatric Nephrology, Toho University Faculty of Medicine, 6-11-1, Omori-Nishi, Ota-ku, Tokyo 143-8541, Japan
- ³ Department of Nephrology, Tokyo Metropolitan Children's Medical Center, Tokyo, Japan
- ⁴ Department of Pediatrics, Shiga University of Medical Science, Shiga, Japan
- ⁵ Community Health Welfare Division, Kawasaki Saiwai Ward Office Health and Welfare Center, Kanagawa, Japan
- ⁶ Department of Clinical Research, Tokyo Metropolitan Children's Medical Center, Tokyo, Japan
- ⁷ Department of Nephrology and Rheumatology, National Center for Child Health and Development, Tokyo, Japan
- ⁸ Teikyo Academic Research Center, Teikyo University, Tokyo, Japan

Keywords Children · Steroid-resistant nephrotic syndrome · Long-term outcome · Immunosuppressant · Minimal change · Diffuse mesangial proliferation · Focal segmental glomerulosclerosis

Introduction

In general, 10 % of children with idiopathic nephrotic syndrome (INS) show steroid resistance. Early studies reported that 30–40 % of children with steroid-resistant nephrotic syndrome (SRNS) progress to end stage-kidney disease (ESKD) during follow-up of 10 years [1, 2].

Methylprednisolone pulse therapy and/or immunosuppressant therapy, such as cyclophosphamide or cyclosporine, have been used for many years to treat children with SRNS. Cyclophosphamide has been used since the 1960s, and in the 1990s,

uncontrolled trials had found that up to 60 % of children treated with the combination of methylprednisolone pulse therapy and cyclophosphamide or chlorambucil achieved complete remission [3]. Cyclosporine was added to the battery of therapeutic strategies in 1987, and many recent studies have shown the efficacy of cyclosporine for SRNS [4–6]. Hamasaki et al. recently reported a high remission rate (88.6 %) and high renal survival rate (94.3 %) in a prospective 12-month protocol treatment trial using a combined cyclosporine/prednisolone therapeutic regimen for children with SRNS [7]. However, the long-term outcome of children with SRNS, including the renal survival rate, permanent remission rate, and incidence of treatment-related complications, as well as the impact of each therapeutic regimen on these rates have not yet been sufficiently evaluated.

The aims of this retrospective cohort study were to analyze the clinical and histopathological parameters of children with SRNS and to evaluate the remission rate of the initial SRNS episode, renal survival rate, permanent remission rate, and long-term complications. We also analyzed whether the remission rate of the initial SRNS episode and the long-term outcome differ according to the choice of initial immunosuppressant used to treat the SRNS, namely, cyclosporine or cyclophosphamide. The incidence of complications related to SRNS and treatment for SRNS was also evaluated.

Methods

Patients

This study was a retrospective analysis of children with SRNS who were followed in Tokyo Metropolitan Kiyose Children's Hospital (predecessor of Tokyo Metropolitan Children's Medical Center), a tertiary care center for children with kidney disease. Data were retrieved from the hospital's database on children with nephrotic syndrome who fulfilled the following criteria: (1) INS initially diagnosed between 1 January 1990 and 1 January 2005; (2) SRNS, either initial non-responder or late non-responder; (3) followed up for ≥ 4 years. Children were excluded if they (1) had underlying secondary causes [Henoch–Schönlein nephritis, systemic lupus erythematosus, immunoglobulin (Ig) A nephropathy, membranous nephropathy, membranoproliferative glomerulonephritis, among others]; (2) had congenital or inherited forms of nephrotic syndrome; (3) were younger than 1 year or older than 15 years when diagnosed with nephrotic syndrome; (4) had not undergone renal biopsy.

The database and medical records were reviewed to collect relevant data over the period from diagnosis of INS to last examination, including the date on which each child was diagnosed as having INS and SRNS, demographic characteristics (age, gender) at the time of diagnosis of SRNS, initial

histopathological pattern [minimal change (MC), diffuse mesangial proliferation (DMP), or focal segmental glomerulosclerosis (FSGS)], steroid response (primary or late non-responder), therapeutic strategies of immunosuppressant, the date on which each child achieved complete remission of the initial SRNS episode, the date of diagnosis of ESKD, the date on which each child achieved complete remission after last relapse episode, clinical aspects (height, weight, and blood pressure), the usage of anti-hypertensive agents, renal function, the condition of nephrotic syndrome, the complications of nephrotic syndrome or treatment-related complications at the last examination, and the findings of chronic cyclosporine nephrotoxicity at the last renal biopsy.

Definitions

Nephrotic syndrome was diagnosed if the urinary protein/creatinine ratio was ≥ 1.8 mg/mg and the serum albumin level was ≤ 2.5 g/dl [7]. SRNS was diagnosed if complete remission was not achieved after treatment with 2 mg/kg prednisolone daily for 4 weeks [8]. Complete remission was defined as negative or trace proteinuria (by the dipstick method or a urinary protein/creatinine ratio of ≤ 0.20 mg/mg) on urinalysis and a serum albumin level of >2.5 g/dl. Partial remission was defined as a serum albumin level of >2.5 g/dl, but persisting proteinuria on urinalysis (dipstick method +1 or greater, or urinary protein/creatinine ratio of >0.2 mg/mg). The state of remission included both complete remission and partial remission. Non-remission was defined as persisting nephrotic syndrome. Relapse of nephrotic syndrome was defined as increased proteinuria and a serum albumin level of ≤ 2.5 g/dl. Permanent remission was defined as the relapse-free state without any immunosuppressant or steroid over the previous 2 years or more up to the last examination. Frequently relapsing nephrotic syndrome (FRNS) was defined as four or more relapses within any 12-month period or the condition in which any immunosuppressant was used to control relapse of steroid-sensitive nephrotic syndrome (SSNS). ESKD was defined as the requirement for dialysis or kidney transplantation. Late non-response to steroids was defined as an initial response to steroid therapy but none during a subsequent relapse.

The estimated glomerular filtration rate (eGFR) was calculated using the Schwartz formula for patients aged ≤ 17 years [9]: $194 \times \text{SCr}^{-1.094} \times \text{Age}^{-0.278}$ in male patients aged ≥ 18 years, and $194 \times \text{SCr}^{-1.094} \times \text{Age}^{-0.278} \times 0.739$ in female patients aged ≥ 18 years, where SCr is the serum creatinine level [10]. Hypertension was defined as the need for anti-hypertensive therapy, except when given for renoprotective purpose. The height measurements were expressed as the height standard deviation score (SDS) compared with normal stature values for age- and sex-matched healthy Japanese children. Short stature was defined as a height of less than -2.0 SDS.

Histopathology

Renal biopsy was performed after the diagnosis of SRNS. Repeat biopsy was performed for the patients who were treated with cyclosporine to evaluate cyclosporine-related nephrotoxicity. Renal pathologists at our institution evaluated the initial histopathological findings and the development of chronic cyclosporine nephrotoxicity, defined as cyclosporine-associated arteriolopathy and/or cyclosporine-induced tubulointerstitial lesions showing characteristic striped tubulointerstitial lesions.

Treatment

All patients were treated initially with prednisolone at a dose of 2 mg/kg per day administered in three separate doses for 4 weeks (maximum 80 mg/day) and diagnosed with SRNS if they did not achieve complete remission during this period.

Up until the 1990s, following a diagnosis of SRNS, oral cyclophosphamide, methylprednisolone pulse therapy, or a combination of these therapies were administered. Cyclophosphamide was used at a dose 2.5 mg/kg per day (maximum 100 mg per day) orally for 12 weeks (with a total cumulative dose of 210 mg/kg). The basic protocol of methylprednisolone pulse therapy consisted of the administration of methylprednisolone 30 mg/kg per day (2-h infusion, maximum 1000 mg) every day for 3 days—considered to be one course; one course per week was given in weeks 1 and 2, then one course per month was given from week 4 to month 6, followed by one course per 3 months from month 7 to year 2 [11]. Beginning in the mid-1990s, the main immunosuppressant used to treat SRNS was changed to cyclosporine combined with prednisolone, the dose of which was adjusted to maintain a whole-blood trough level of 120–150 ng/ml for the initial 3 months, followed by 80–100 ng/ml for months 4–12, and 60–80 ng/ml for months 13–24, with subsequent tapering of the cyclosporine dose after 2 years of therapy. Among those patients treated with cyclosporine, some additionally received methylprednisolone pulse therapy consisting of methylprednisolone 30 mg/kg per day (2-h infusion, maximum 1000 mg) every day for 3 days—considered to be one course; one course per week was given in weeks 1, 2, 5, 9, and 13 [7]. Prednisolone was started at 1 mg/kg per day in three separate doses for 4 weeks and then was reduced to 1 mg/kg in a single dose every other day for generally 1 year in those patients diagnosed with SRNS.

If a therapeutic regimen failed to induce remission, another regimen or a combination of regimens was considered. That is, if the regimen with cyclosporine failed to induce remission, we switched to the regimen with cyclophosphamide, and if the cyclophosphamide regimen failed to induce remission, we switched to one with cyclosporine. We considered a therapeutic regimen as having failed to induce remission if remission

was not induced within 4–6 months after commencement of administration.

Statistical analyses

Results were expressed in terms of median, range, and percentage. The endpoints were the incidences of complete remission of the initial SRNS episode, ESKD, and permanent remission. The duration from the date of diagnosis of SRNS to the date on which each respective endpoint was reached was measured and evaluated using Kaplan–Meier analysis according to subgroup analysis of the initial histopathological patterns (FSGS or MC/DMP) and initial immunosuppressant used for SRNS (cyclosporine or cyclophosphamide). Thus, there were four subgroups. Differences between subgroups were compared using the log-rank test. Regarding renal survival rate, variables, including gender, age at time of SRNS diagnosis, initial histopathological pattern (FSGS or MC/DMP), and initial immunosuppressant used for SRNS were assessed by multivariate analysis with Cox regression. A two-sided *P*-value of <0.05 was considered to be statistically significant. All statistical analyses were performed using the SAS software package for Windows (release 9.3; SAS Institute Inc., Cary, NC, USA).

Results

In total, 230 patients were diagnosed with INS between 1 January 1990 and 1 January 2005, of whom 147 showed SSNS. Among the remaining 83 SRNS patients, ten patients had been followed for <4 years and four patients had not undergone renal biopsy. Therefore, 69 children were ultimately enrolled in the analysis (Fig. 1). Basic characteristics of these children are shown in Table 1. The first renal biopsy showed MC in 39 children (57 %), FSGS in 22 (32 %), and DMP in eight (11 %). Among the eight patients who showed DMP, two showed mild IgM deposition on immunofluorescence staining, one showed mild C1q deposition, one showed intense C3 deposition and mild IgM and C1q deposition, two showed no deposition, and two had no data about immunofluorescence staining. The median age at diagnosis of SRNS was 3.2 (range 1.1–15.3) years. In children with FSGS diagnosed on the first renal biopsy, cyclophosphamide and cyclosporine were used as the initial immunosuppressant for the initial SRNS episodes in 11 and ten patients, respectively; one patient did not receive any immunosuppressant. In children with MC/DMP on the first renal biopsy, cyclophosphamide was used as the initial immunosuppressant for initial SRNS episodes in 13 patients, cyclosporine was used in 29 patients, and no immunosuppressant was used in five patients, two of whom underwent methylprednisolone pulse therapy. Therapeutic strategies from the time of the initial diagnosis of SRNS to achievement of first complete remission or

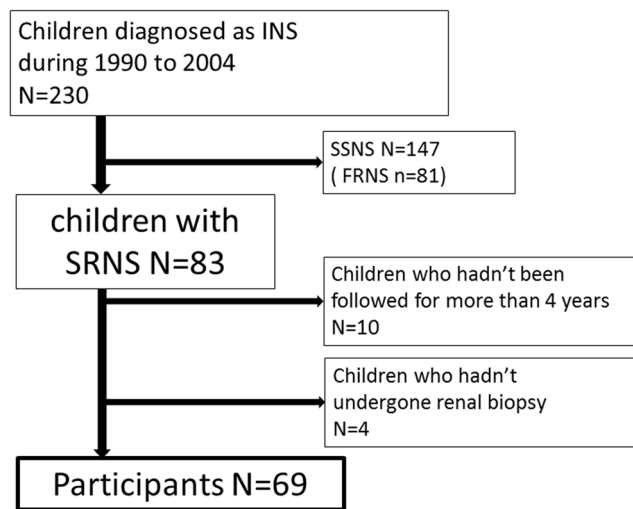


Fig. 1 Overview of idiopathic nephrotic syndrome (INS) patients in this study. Of the 230 children diagnosed with INS between 1 January 1990 and 1 January 2005, 69 patients with steroid-resistant nephritic syndrome (SRNS) met the entry criteria. SSNS, steroid-sensitive nephrotic syndrome; FRNS, frequently relapsing nephrotic syndrome

progression to ESKD are shown in Table 2. During the observation period of this study we did not use rituximab, mycophenolate mofetil, or tacrolimus. The overall median follow-up period was 10.1 (range 4.5–19.3) years.

No immunosuppressant was used in six patients (1 in FSGS, 5 in MC/DMP). Of these, three patients attained complete remission early and maintained that condition; one patient was diagnosed with SRNS and had been treated with

prednisolone for 1 year only at another institution and did not require any immunosuppressant when she came to our hospital for the first time; one patient had relatively mild proteinuria and spontaneously attained complete remission after prednisolone was discontinued; one patient was treated with prednisolone only and achieved partial remission but not complete remission within 1 month of the start of prednisolone, prednisolone therapy was discontinued after 2 months, and complete remission was finally achieved 7 years after the initial diagnosis of SRNS and maintained to date. Because the above six patients achieved complete remission without any immunosuppressant, they were excluded from the analysis, and the analyses of remission rate, renal survival rate, and permanent remission rate were conducted using only the data of the remaining 63 patients.

Kaplan–Meier analysis revealed that the complete remission rate of the initial SRNS episode at 4 months in those patients whose initial histopathological pattern was FSGS and initial immunosuppressant was cyclosporine [FSGS (cyclosporine) subgroup] was 40 %. In comparison, that of the patients whose initial histopathological pattern was FSGS and initial immunosuppressant was cyclophosphamide [FSGS (cyclophosphamide) subgroup] was 0 %. The complete remission rate of those patients whose initial histopathological pattern was MC/DMP and initial immunosuppressant was cyclosporine [MC/DMP (cyclosporine) subgroup] was 69.0 %. In comparison, that of the patients whose initial histopathological pattern was MC/DMP and initial immunosuppressant was cyclophosphamide [MC/DMP (cyclophosphamide)

Table 1 Basic (background) characteristics of participants in the study

Basic (background) characteristics of participants							
First renal biopsy finding:	FSGS			MC/DMP			Total
First immunosuppressant used to treat SRNS:	CP	CSA	None	CP	CSA	None	
Number of patients	11	10	1	13	29	5	69
Gender (n)							
Male	6	7	0	8	21	3	45
Female	5	3	1	5	8	2	24
Age when diagnosed with SRNS (years)							
<3	4	5	0	5	15	1	30
≥3, <7	5	1	0	5	7	2	20
≥7, <11	2	1	0	2	4	2	11
≥11	0	3	1	1	3	0	8
Median age (years) at last follow-up (range)	19.7 (13.6–26.9)	12 (10.0–28.1)	23.3	17.7 (8.2–23.6)	12.1 (6.9–24.9)	16.8 (15.5–27.6)	13.9 (6.9–28.1)
Steroid response							
Late non-responder	0	2	1	3	9	0	15

SRNS, Steroid-resistant nephritic syndrome; MC, minimal change; DMP, diffuse mesangial proliferation; FSGS, focal segmental glomerulosclerosis; CP, cyclophosphamide; CSA, cyclosporine

Table 2 Therapeutic strategies in each initial treatment from the initial diagnosis of steroid-resistant nephrotic syndrome to the first complete remission or progression to end-stage kidney disease

Therapeutic strategies	FSGS			MC/DMP			All patients		
	Number of patients	CR	Progressing to ESKD	Number of patients	CR	Progressing to ESKD	Number of patients	CR	Progressing to ESKD
CSA (n=39)									
CSA alone	1	0	1	20	20	0	21	20	1
CSA+MPT	7	7	0	8 ^b	7	0	15 ^b	14	0
CSA+MPT→CP→CSA+MZB	0	0	0	1	0	1	1	0	1
CSA→CP+MPT→CSA+MPT→CSA+MZB→MPT→LDL apheresis→CSA	1	0	1	0	0	0	1	0	1
CSA→CP+MPT→MZB	1	1	0	0	0	0	1	1	0
Total	10	8	2	29^b	27	1	39^b	35	3
Median follow-up period (years) (range)	9.0 (6.3–16.1)			8.6 (4.5–16.4)			8.7 (4.5–16.4)		
Median duration (years) to CR (range)	0.4 (0.1–5.1)			0.2 (0.0–1.5)			0.2 (0.0–5.1)		
Median duration (years) to ESKD (range)	11.5 (10.1–12.8)			1.8 (–)			10.1 (1.8–12.8)		
CP (n=24)									
CP alone	2	2	0	7	7	0	9	9	0
CP→CSA	3	2	1	0	0	0	3	2	1
CP→CSA→MZB	1	0	1	0	0	0	1	0	1
CP→CSA→CP	1	0	1	0	0	0	1	0	1
CP→CSA→CP+MPT	1	1	0	0	0	0	1	1	0
CP→CSA→MPT	0	0	0	1	1	0	1	1	0
CP→CSA→MPT→CSA	0	0	0	1	1	0	1	1	0
CP→CSA→MPT→CSA→LDL apheresis	0	0	0	1	0	1	1	0	1
CP+MPT ^a	1	0	1	2	2	0	3	2	1
CP+MPT→CSA→CP ^a	1	0	1	0	0	0	1	0	1
CP+MPT→CSA→MPT ^a	1	1	0	1	1	0	2	2	0
Total	11	6	5	13	12	1	24	18	6
Median follow-up period (years) (range)	14.6 (10.4–19.0)			11.5 (5.3–16.3)			12.1(5.3–19.0)		
Median duration (years) to CR (range)	2.5 (0.7–8.6)			1.5 (0.1–3.8)			2.0 (0.1–8.6)		
Median duration (years) to ESKD (range)	2.2 (1.0–3.7)			8.5 (–)			2.3(1.0–8.5)		
Others (n=6)									
MPT ^a	0	0	0	2	2	0	2	2	0
PSL only	1	1	0	3	3	0	4	4	0
Total	1	1	0	5	5	0	6	6	0
Median follow-up period (years) (range)	19.3 (–)			12.8 (6.9–17.7)			15.1(6.9–19.3)		
Median duration (years) to CR (range)	2.4 (–)			1.4 (0.0–7.4)			1.2 (0.0–7.4)		
Median duration (years) to ESKD (range)	–			–			–		

Data are presented as numbers unless stated otherwise

MPT, methylprednisolone pulse therapy; MZB, mizoribine; PSL, prednisolone; CR, complete remission; ESKD, end-stage kidney disease; LDL apheresis, low-density lipoprotein apheresis

^a The maximum number and median number of courses of methylprednisolone pulse therapy were 16 and 3.5, respectively

^b Of those, one patient did not achieve CR and remained as partial remission until the last examination

subgroup] was 38.5 % ($P=0.001$) (Fig. 2). After exclusion of patients with DMP from the analysis, the complete remission rate of the initial SRNS of the MC (cyclosporine) subgroup was 75.0 % and that of the MC (cyclophosphamide) subgroup was 45.4 % (not shown).

The actual renal survival rate at 10 years in the FSGS (cyclosporine) subgroup was 100 %, as calculated by Kaplan–Meier analysis ($P=0.013$). However, actual renal survival rate in the FSGS (cyclophosphamide) subgroup, MC/DMP (cyclosporine) subgroup, and MC/DMP (cyclophosphamide) subgroup was 54.6, 96.6, and 90.9 %,

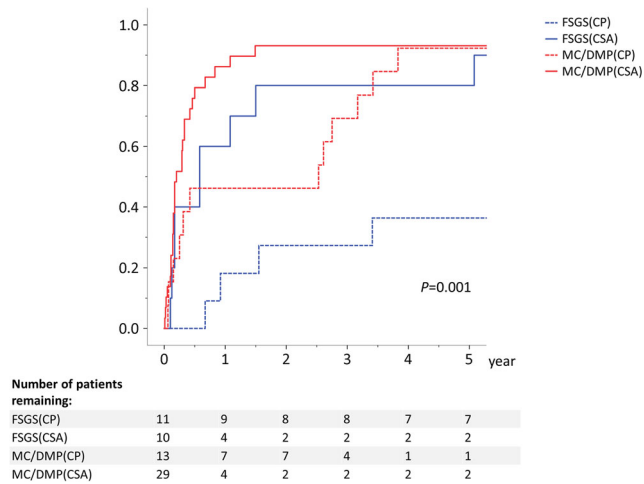


Fig. 2 The complete remission rate of the initial SRNS episode, analyzed by Kaplan-Meier analysis according to subgroup {initial histopathological patterns [minimal change (MC)/diffuse mesangial proliferation (DMP) vs. focal segmental glomerulosclerosis (FSGS)] and initial immunosuppressive agents used to treat for SRNS [cyclosporine (CSA) vs. cyclophosphamide (CP)]}. Number of children at risk at each time point is shown below the x-axis

respectively (Fig. 3). The risk of ESKD was assessed by multivariate analysis, revealing that the initial immunosuppressant of cyclophosphamide [hazard rate (HR) 20.2; 95 % confidence interval (CI) 1.6–260.6; $P=0.021$], initial histopathological pattern of FSGS (HR 10.7; 95 % CI 1.3–89.7; $P=0.029$), and age of >11 years when diagnosed with SRNS (HR 36.3; 95 % CI 2.2–604.6; $P=0.012$) were significant risk factors for progression to ESKD (Table 3). After exclusion of patients with DMP from the analysis, the renal survival rate at 10 years was 100 % in both the MC

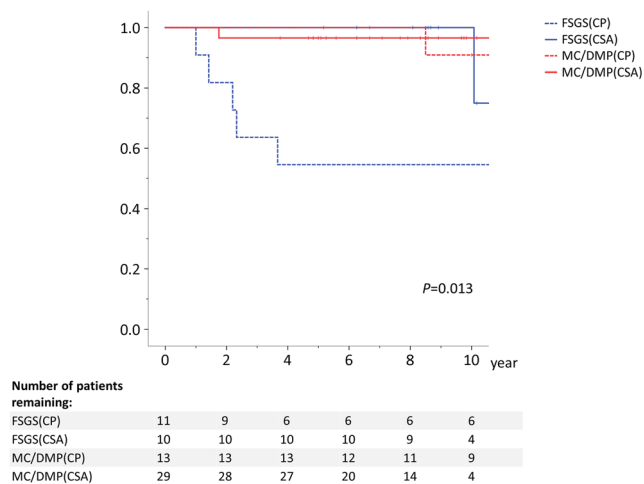


Fig. 3 Renal survival rate in subgroups based on the initial histopathological patterns [minimal change (MC)/diffuse mesangial proliferation (DMP) vs. focal segmental glomerulosclerosis (FSGS)] and initial immunosuppressive agents [cyclosporine (CSA) vs. cyclophosphamide (CP)] used to treat SRNS. Number of children at risk at each time point is shown below the x-axis

(cyclosporine) group and MC (cyclophosphamide) subgroup (not shown).

As calculated by Kaplan–Meier analysis, the permanent remission rate at 10 years in the FSGS (cyclosporine) group, FSGS (cyclophosphamide) group, MC/DMP (cyclosporine) group, and MC/DMP (cyclophosphamide) group was 10.0, 27.3, 24.1, and 23.1 %, respectively (Fig. 4). Significant differences between groups were not found ($P=0.747$).

At the last follow-up examination, the disease was in remission in 57 (83 %) patients, was not in remission in three (4 %) patients, and had progressed to ESKD in nine (13 %; see Electronic Supplementary Material for the detailed clinical course of these 9 patients) patients (Fig. 5). Of those patients who achieved remission at the last follow-up examination ($n=57$), 48 (84 %) were in complete remission but only 18 (31 %) were in permanent remission.

Nephrotic syndrome- or treatment-related complications at the last examination are listed in Table 4. No patient died during the follow-up period. The median eGFR, excluding children with ESKD at the last examination, was 121.4 ml/min/1.73 m² (81.0–180.8 ml/min/1.73 m²), that of FSGS group was 121.0 ml/min/1.73 m² (82.5–180.8 ml/min/1.73 m²), and that of the MC/DMP group was 123.0 ml/min/1.73 m² (81.0–170.4 ml/min/1.73 m²).

In total, 55 patients underwent repeat renal biopsy, and six of these patients (10.9 %) exhibited significant cyclosporine-related nephrotoxicity in the last renal biopsy (FSGS group, 3/19; MC/DMP group, 3/36). Of these six patients, three showed tubulointerstitial fibrosis only, one showed arteriolar hyalinosis only, and two showed both arteriolar hyalinosis and tubulointerstitial fibrosis. The median duration from the date of starting of cyclosporine therapy to the date on which cyclosporine toxicity was found was 4.8 (range 2.0–5.8) years.

Discussion

In this retrospective cohort study, we found that children with SRNS treated with cyclosporine had better outcome than those treated with cyclophosphamide, particularly those with FSGS, in terms of both induction of complete remission and long-term renal survival. On the other hand, most of the patients had been suffering frequent relapse for a long-term period, up to 10 years.

Among our study subjects, our analysis showed that the renal survival rates of those who received cyclosporine as the initial immunosuppressant were better than those of patients who received cyclophosphamide, regardless of the initial histopathological patterns. Those who received cyclosporine as initial immunosuppressant showed both higher short-term remission rate and higher long-term renal survival rate, suggesting that early induction of complete remission by cyclosporine might lead to better renal survival. SRNS has been recognized

Table 3 Risk factor for end-stage kidney disease by multivariate analysis

Variable	Hazard ratio	95 % Confidence interval	P value
Female gender (vs. male)	1.7	0.2–12.6	0.624
Age at time of SRNS diagnosis (years) (vs. <3 years)			
≥3, <7	0.8	0.1–6.6	0.834
≥7, <11	0.6	0.0–7.4	0.672
≥11	36.3	2.2–604.6	0.012
FSGS as the first renal biopsy finding (vs. MC/DMP)	10.7	1.3–89.7	0.029
CP as the first immunosuppressive agent for SRNS (vs. CSA)	20.2	1.6–260.6	0.021

The data are presented as numbers unless stated otherwise

SRNS, Steroid-resistant nephritic syndrome; MC, minimal change; DMP, diffuse mesangial proliferation; FSGS, focal segmental glomerulosclerosis; CP, cyclophosphamide; CSA, cyclosporine

as a disease associated with a high risk to progress to ESKD over the long term, although several recent studies have reported good short-term remission rate in patients with SRNS and, consequently, the effect of cyclosporine to induce remission in SRNS patients is beginning to be established [7, 12–14]. However, there have been only a few reports of children with SRNS in which the observation time was >10 years [15, 16]. In our study, we assessed long-term renal survival rate in children with SRNS mainly with respect to the initial immunosuppressant and showed for the first time the higher effectiveness of cyclosporine.

Our results show that the immunosuppressant used to treat SRNS, the initial histopathological pattern, and the age of patient diagnosis of SRNS were significant predictive factors of renal survival. Children who received cyclosporine had a significantly higher renal survival, even after adjustment for the other factors. In previous studies, FSGS as the initial

histopathological pattern was found to be a predictive factor of progression to ESKD, particularly in those who could not attain remission [16–20]. In this regard, our results are compatible with those reported previously. Moreover, our results demonstrate that those children with FSGS treated with oral cyclophosphamide had a much lower renal survival rate (Fig. 3). Treatment regimens for patients with SRNS that include oral cyclophosphamide have been tentatively advocated by the authors of a number of reports (including patients with FSGS) [16, 21]; however, the results of our study suggest that the treatment regimen of oral cyclophosphamide can not be recommended—at least not to patients with SRNS with the FSGS histopathological pattern. Our institution has not adopted regimens with intravenous cyclophosphamide for the treatment of children with SRNS, but the results of other studies evaluating the efficacy of such therapeutic regimens are conflicting [12, 22, 23]. The older children in our study

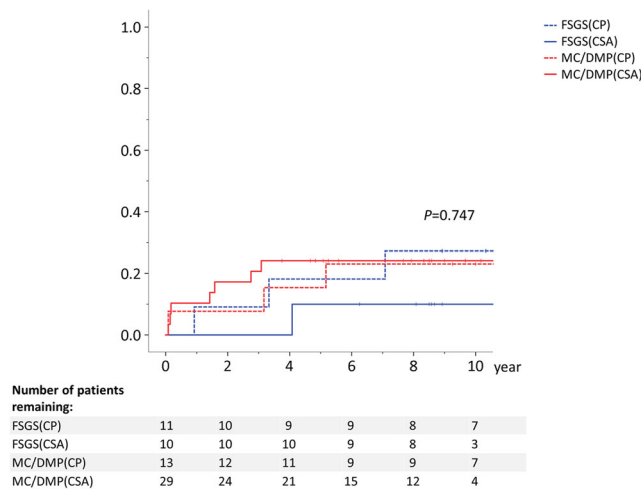


Fig. 4 The permanent remission rate in subgroups based on the initial histopathological patterns [minimal change (MC)/diffuse mesangial proliferation (DMP) vs. focal segmental glomerulosclerosis (FSGS)] and initial immunosuppressive agents [cyclosporine (CSA) vs. cyclophosphamide (CP)] used to treat SRNS. Number of children at risk at each time point is shown below the x-axis

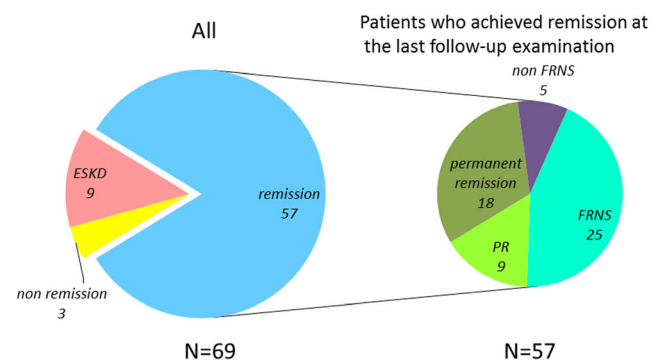


Fig. 5 Condition of patients at the last follow-up examination. Of 69 patients with SRNS, 57 patients had achieved remission by the last follow-up examination (right pie chart). SRNS, steroid-resistant nephritic syndrome; ESKD, end-stage kidney disease; PR, partial remission; FRNS, frequently relapsing nephrotic syndrome. The median duration of follow-up for patients with permanent remission was 10.3 (range, 5.2–15.9) years; with non-FRNS, 8.7 (5.5–12.5) years; with FRNS, 8.6 (4.9–15.8) years; with PR, 16.3 (4.5–19.3) years; with non-remission, 10.1 (6.3–16.4) years; with ESKD, 14.6 (9.2–19.0) years

Table 4 Nephrotic syndrome or treatment-related complications at the last examination

Variable	Total	Initial renal biopsy finding	
		FSGS	MC/DMP
Number of patients	69	22	47
Short stature	5 (7.2)	1 (4.5)	4 (8.5)
Excessive body weight ^a	9 (13.0)	3 (13.6)	6 (12.8)
Obesity ^b	4 (5.8)	1 (4.5)	3 (6.4)
Hypertension	22 (31.9)	11 (50.0)	11 (23.4)
Number of patients with ESKD	9	7	2
Hypertension among patients with ESKD	5 (55.6)	3 (42.8)	2 (100)
Number of patients undergoing repeat renal biopsy	55	19	36
CSA-related nephrotoxicity	6 (10.9)	3 (15.8)	3 (8.3)

The data are presented as numbers with the percentage in parenthesis

ESKD, end-stage kidney disease; FSGS, focal segmental glomerulosclerosis; MC, minimal change; DMP, diffuse mesangial proliferation; CSA, cyclosporine

^a Defined as the body mass index (BMI): weight (kg)/square of height (m²) of >25 in men and >24 in women

^b Defined as a BMI of >30

cohort showed a significantly lower renal survival rate, which is a similar result to that reported previously [15]

On the other hand, the permanent remission rate among our study cohort was relatively low regardless of the initial immunosuppressant, and we found no evidence of any superiority of cyclosporine in achieving permanent remission. Moreover, many children in our study showed were in the state of FRNS at the last follow-up examination (Fig. 5). These results support those which we reported previously [24] and suggest that treatment strategies for children with SRNS to achieve long-term remission without immunosuppressant or steroid therapy still need to be improved.

Disease- and/or treatment-associated complications were relatively low among our study cohort and were comparable with those of the previous studies on long-term outcomes in patients with SSNS, except for hypertension [25, 26]. Excluding those who deteriorated to ESKD, only a few children showed mild kidney dysfunction. There were also only a few children who showed short stature or obesity, which might be attributable to the treatment, such as alternate-day administration of prednisolone. The rate of children who showed chronic cyclosporine nephrotoxicity in repeated biopsy was 10.9 %, which is lower than that reported in previous studies [27–31], possibly due to the advantage of trough control of cyclosporine. Close attention should be paid to cyclosporine nephrotoxicity. The rate of children who showed hypertension at last examination was relatively high, which might be attributed to the use of prednisolone or cyclosporine. However, the frequency of hypertension in our children with SRNS and in children with SRNS in previously reported studies was higher than that of children with FRNS [24, 32], which suggests that SRNS might itself be a significant risk factor for developing hypertension.

Our study has a number of strengths. First, a relatively large number of patients were included in the analysis, among whom 22 showed FSGS as the initial histopathological pattern. Second, we analyzed a rare refractory disease. Third, patient data for the analysis were collected over a relatively long term. These strengths should be balanced against this study's limitations. First, there was a diversity with the patient study groups, with the analysis including patients with MC and those with DMP in the same group. Second, the study cohort consisted of a homogeneous population. This study was confined to Japanese patients and did not include other races, such as Black Africans who typically show poorer long-term outcome. The homogeneity of our patient population might have contributed to the better outcome demonstrated in this study. Third, no genetic analyses were performed. Several recent papers have reported lack of efficacy of immunosuppression in SRNS secondary to genetic causes. We did not perform genetic analyses; however, none of our patients were indicated for this at the time of diagnosis. Fourth, the immunosuppression treatment course (including methylprednisolone pulse therapy) was quite complex, making the analysis of any given variable impossible. Patients who used cyclosporine only as the first immunosuppressive agent for SRNS and those who used cyclosporine plus methylprednisolone pulse therapy were not analyzed separately; as such, it is very difficult to compare the results of this study with those having other protocols. Finally, our assessment of the side effects in this study relied mainly on medical records, and thus some side effects might not have been identified and the assessment might be insufficient.

In conclusion, our results suggest that the recently reported therapeutic regimen with cyclosporine could

considerably improve both the initial remission rate and the long-term renal survival rate of children with idiopathic SRNS, regardless of initial histopathological pattern (i.e., FSGS or MC/DMP). However, further studies are required to resolve remaining problems, such as the management of SRNS in children who show frequent relapse after SRNS remission, and the establishment of a new therapeutic regimen for those who show resistance to the existing therapeutic regimens.

Acknowledgments The results presented in this paper have not been published previously in whole or part. The authors would like to thank Drs. Kentaro Ogata (Tokyo), Ryugo Hiramoto (Chiba), Takeshi Matsuyama (Tokyo), Hitoshi Wakaki (Tokyo), and Kaori Kikunaga (Tokyo) for their contributions to this study.

Financial declaration Kenji Ishikura has received lecture fees from Novartis Pharma and Asahi Kasei Pharma. Yuko Hamasaki has received research grants from Novartis Pharma and lecture fees from Novartis Pharma, Astellas Pharma, and Pfizer Japan. Hiroshi Hataya has received lecture fees from Asahi Kasei Pharma, Astellas Pharma, Baxter, JMS, and Meiji Seika Pharma Co. Ltd. Masataka Honda has received lecture fees from Novartis Pharma, Takeda Pharmaceutical Co. Ltd., Chugai Pharmaceutical Co. Ltd., Japan Blood Products Organization, JCR Pharmaceuticals Co. Ltd., and Asahi Kasei Pharma. Masaaki Mori has received lecture fees from Astellas Pharma, Pfizer Japan, Asahi Kasei Pharma, Meiji Seika Pharma Co. Ltd., and Chugai Pharmaceutical Co. Ltd.

Ethical approval The study was conducted in accordance with the ethical principles set out in the Declaration of Helsinki, and with the ethical guideline for epidemiological studies issued by the Ministry of Health, Labor and Welfare in Japan. The study was approved by the ethics committee of Tokyo Metropolitan Children's medical Center (H25-2).

Informed Consent Because data were reported retrospectively based on patient charts, informed consent was not obtained, in accordance with the above guidelines.

References

- Mendoza SA, Reznik VM, Griswold WR, Krensky AM, Yorgin PD, Tune BM (1990) Treatment of steroid-resistant focal segmental glomerulosclerosis with pulse methylprednisolone and alkylating agents. *Pediatr Nephrol* 4:303–307
- Catran DC, Rao P (1998) Long-term outcome in children and adults with classic focal segmental glomerulosclerosis. *Am J Kidney Dis* 32:72–79
- Tune BM, Kirpekar R, Sibley RK, Reznik VM, Griswold WR, Mendoza SA (1995) Intravenous methylprednisolone and oral alkylating agent therapy of prednisone-resistant pediatric focal segmental glomerulosclerosis: a long-term follow-up. *Clin Nephrol* 43: 84–88
- Garin EH, Orak JK, Hiott KL, Sutherland SE (1988) Cyclosporine therapy for steroid-resistant nephrotic syndrome. A controlled study. *Am J Dis Child* 142:985–988
- Ponticelli C, Rizzoni G, Edefonti A, Altieri P, Rivolta E, Rinaldi S, Ghio L, Lusvardi E, Gusmano R, Locatelli F, Pasquali S, Castellani A, Casa-Alberighi OD (1993) A randomized trial of cyclosporine in steroid-resistant idiopathic nephrotic syndrome. *Kidney Int* 43:1377–1384
- Lieberman KV, Tejani A (1996) A randomized double-blind placebo-controlled trial of cyclosporine in steroid-resistant idiopathic focal segmental glomerulosclerosis in children. *J Am Soc Nephrol* 7:56–63
- Hamasaki Y, Yoshikawa N, Hattori S, Sasaki S, Iijima K, Nakanishi K, Matsuyama T, Ishikura K, Yata N, Kaneko T, Honda M (2009) Cyclosporine and steroid therapy in children with steroid-resistant nephrotic syndrome. *Pediatr Nephrol* 24:2177–2185
- Ishikura K, Matsumoto S, Sako M, Tsuruga K, Nakanishi K, Kamei K, Saito H, Fujinaga S, Hamasaki Y, Chikamoto H, Ohtsuka Y, Komatsu Y, Ohta T, Nagai T, Kaito H, Kondo S, Ikezumi Y, Tanaka S, Kaku Y, Iijima K (2015) Clinical practice guideline for pediatric idiopathic nephrotic syndrome 2013: medical therapy. *Clin Exp Nephrol* 19:6–33
- Schwartz GJ, Haycock GB, Edelmann CM Jr, Spitzer A (1976) A simple estimate of glomerular filtration rate in children derived from body length and plasma creatinine. *Pediatrics* 58:259–263
- Matsuo S, Imai E, Horio M, Yasuda Y, Tomita K, Nitta K, Yamagata K, Tomino Y, Yokoyama H, Hishida A (2009) Revised equations for estimated GFR from serum creatinine in Japan. *Am J Kidney Dis* 53:982–992
- Mori K, Honda M, Ikeda M (2004) Efficacy of methylprednisolone pulse therapy in steroid-resistant nephrotic syndrome. *Pediatr Nephrol* 19:1232–1236
- Plank C, Kalb V, Hinkes B, Hildebrandt F, Gefeller O, Rascher W (2008) Cyclosporin A is superior to cyclophosphamide in children with steroid-resistant nephrotic syndrome—a randomized controlled multicentre trial by the Arbeitsgemeinschaft für Padiatrische Nephrologie. *Pediatr Nephrol* 23:1483–1493
- Ehrich JH, Geerlings C, Zivicnjak M, Franke D, Geerlings H, Gellermann J (2007) Steroid-resistant idiopathic childhood nephrosis: overdiagnosed and undertreated. *Nephrol Dial Transplant* 22: 2183–2193
- Choudhry S, Bagga A, Hari P, Sharma S, Kalaivani M, Dinda A (2009) Efficacy and safety of tacrolimus versus cyclosporine in children with steroid-resistant nephrotic syndrome: a randomized controlled trial. *Am J Kidney Dis* 53:760–769
- Mekahli D, Liutkus A, Ranchin B, Yu A, Bessenay L, Girardin E, Van Damme-Lombaerts R, Palcoux JB, Cachat F, Lavocat MP, Bourdat-Michel G, Nobili F, Cochat P (2009) Long-term outcome of idiopathic steroid-resistant nephrotic syndrome: a multicenter study. *Pediatr Nephrol* 24:1525–1532
- Kirpekar R, Yorgin PD, Tune BM, Kim MK, Sibley RK (2002) Clinicopathologic correlates predict the outcome in children with steroid-resistant idiopathic nephrotic syndrome treated with pulse methylprednisolone therapy. *Am J Kidney Dis* 39:1143–1152
- Abrantes MM, Cardoso LS, Lima EM, Penido Silva JM, Diniz JS, Bambirra EA, Oliveira EA (2006) Predictive factors of chronic kidney disease in primary focal segmental glomerulosclerosis. *Pediatr Nephrol* 21:1003–1012
- Paik KH, Lee BH, Cho HY, Kang HG, Ha IS, Cheong HI, Jin DK, Moon KC, Choi Y (2007) Primary focal segmental glomerular sclerosis in children: clinical course and prognosis. *Pediatr Nephrol* 22:389–395
- Gipson DS, Chin H, Presler TP, Jennette C, Ferris ME, Massengill S, Gibson K, Thomas DB (2006) Differential risk of remission and ESRD in childhood FSGS. *Pediatr Nephrol* 21:344–349
- Martinelli R, Okumura AS, Pereira LJ, Rocha H (2001) Primary focal segmental glomerulosclerosis in children: prognostic factors. *Pediatr Nephrol* 16:658–661
- Mantan M, Sriram CS, Hari P, Dinda A, Bagga A (2008) Efficacy of intravenous pulse cyclophosphamide treatment versus combination of intravenous dexamethasone and oral cyclophosphamide treatment in steroid-resistant nephrotic syndrome. *Pediatr Nephrol* 23:1495–1502

22. Hari P, Bagga A, Jindal N, Srivastava RN (2001) Treatment of focal glomerulosclerosis with pulse steroids and oral cyclophosphamide. *Pediatr Nephrol* 16:901–905
23. Bajpai A, Bagga A, Hari P, Dinda A, Srivastava RN (2003) Intravenous cyclophosphamide in steroid-resistant nephrotic syndrome. *Pediatr Nephrol* 18:351–356
24. Hamasaki Y, Yoshikawa N, Nakazato H, Sasaki S, Iijima K, Nakanishi K, Matsuyama T, Ishikura K, Ito S, Kaneko T, Honda M (2013) Prospective 5-year follow-up of cyclosporine treatment in children with steroid-resistant nephrosis. *Pediatr Nephrol* 28:765–771
25. Fakhouri F, Bocquet N, Taupin P, Presne C, Gagnadoux MF, Landais P, Lesavre P, Chauveau D, Knebelmann B, Broyer M, Grunfeld JP, Niaudet P (2003) Steroid-sensitive nephrotic syndrome: from childhood to adulthood. *Am J Kidney Dis* 41:550–557
26. Ruth EM, Kemper MJ, Leumann EP, Laube GF, Neuhaus TJ (2005) Children with steroid-sensitive nephrotic syndrome come of age: long-term outcome. *J Pediatr* 147:202–207
27. Niaudet P, Fuchshuber A, Gagnadoux MF, Habib R, Broyer M (1997) Cyclosporine in the therapy of steroid-resistant idiopathic nephrotic syndrome. *Kidney Int Suppl* 58:S85–S90
28. Iijima K, Hamahira K, Tanaka R, Kobayashi A, Nozu K, Nakamura H, Yoshikawa N (2002) Risk factor for cyclosporine-induced tubulointerstitial lesions in children with minimal change nephrotic syndrome. *Kidney Int* 61:1801–1805
29. Kengne-Wafo S, Massella L, Diomedi-Camassei F, Gianviti A, Vivarelli M, Greco M, Stringini GR, Emma F (2009) Risk factors for cyclosporin A nephrotoxicity in children with steroid-dependent nephrotic syndrome. *Clin J Am Soc Nephrol* 4:1409–1416
30. Sinha A, Sharma A, Mehta A, Gupta R, Gulati A, Hari P, Dinda AK, Bagga A (2013) Calcineurin inhibitor induced nephrotoxicity in steroid resistant nephrotic syndrome. *Indian J Nephrol* 23:41–46
31. Fujinaga S, Shimizu T (2013) Chronic cyclosporine-induced nephrotoxicity in children with steroid-resistant nephrotic syndrome. *Pediatr Nephrol* 28:2065–2066
32. Ishikura K, Yoshikawa N, Nakazato H, Sasaki S, Iijima K, Nakanishi K, Matsuyama T, Ito S, Yata N, Ando T, Honda M (2012) Two-year follow-up of a prospective clinical trial of cyclosporine for frequently relapsing nephrotic syndrome in children. *Clin J Am Soc Nephrol* 7:1576–1583

Clinical and genetic characteristics of Japanese nephronophthisis patients

Keisuke Sugimoto¹ · Tomoki Miyazawa¹ · Takuji Enya¹ · Hitomi Nishi¹ · Kohei Miyazaki¹ · Mitsuru Okada¹ · Tsukasa Takemura¹

Received: 30 August 2015 / Accepted: 4 October 2015
© Japanese Society of Nephrology 2015

Abstract

Background Nephronophthisis (NPH) accounts for 4–5 % of end-stage renal disease occurring in childhood.

Method We investigated the clinical context and characteristics of renal and extrarenal symptoms, as well as the *NPHP* genes, in 35 Japanese patients with clinical and histologic features suggesting NPH.

Results NPH occurred fairly uniformly throughout Japan irrespective of region or gender. In three families, NPH affected siblings. The median age of patients was 12.5 years. Renal abnormalities attributable to NPH discovered through mass screening, such as urine tests in school. However, NPH accounted for less than 50 % of children with abnormal findings, including incidentally discovered renal dysfunction during evaluation of extrarenal symptoms or during routine check-ups. Typical extrarenal manifestations led to discovery including anemia and delayed physical development. The urine often showed low gravity specific density and low molecular weight proteinuria. Frequent renal histologic findings included cystic dilation of tubules, mainly in the medulla, and irregularity of tubular basement membranes. Genetically abnormalities of *NPHP1* were not common, with large deletions frequently noted. Compound heterozygotes showing single abnormalities in each of *NPHP1*, *NPHP3*, and *NPHP4* were observed.

Conclusions Our findings resemble those reported in Western populations.

Keywords End-stage renal disease · Renal cysts · *NPHP* genes · Children · Renal tubules

Introduction

Nephronophthisis (NPH) is a disease characterized by renal medullary cyst formation. Additional histologic findings include tubulointerstitial nephritis accompanied by progressive sclerosis and hyaline glomeruli. Although NPH characteristically shows autosomal recessive inheritance, it may occur sporadically [1]. NPH accounts for approximately 4–5 % of end-stage renal disease (ESRD) in childhood. Disease subtypes include: infantile NPH (NPH2), which progresses to ESRD around the age of 5 years; juvenile NPH (NPH1), which develops from early childhood to school age and usually progresses to ESRD by an age of about 13 or 14 years; and adolescent NPH (NPH3), with development of ESRD at an average age of 19 years. Juvenile NPH is reported to be the most common subtype [1].

NPHP1, the gene most often responsible for juvenile nephronophthisis, encodes the nephrocystin-1 molecule. This gene has an extent of approximately 11 kbp, and is located on chromosome 2q12-13 [2]. The nephrocystin-1 protein consists of 677 amino acids and includes three coiled domains; two highly acidic negatively charged glutamic acid-rich domains; and an Src-homology 3 domain. Nephrocystin-1 has a molecular weight of 83 kD. As this protein is located in the transition zone of primary cilia of renal tubular epithelial cells, its abnormalities typically cause dysfunction of these primary cilia (ciliopathy) [1, 2].

NPHP4, whose abnormalities cause a second form of NPH1, is located on chromosome 1p36 and encodes the nephrocystin-4 (nephroretinin) molecule. Nephrocystin-4

✉ Keisuke Sugimoto
ksugimo@med.kindai.ac.jp

¹ Department of Pediatrics, Kinki University Faculty of Medicine, 377-2 Ohno-higashi, Osaka-Sayama 589-8511, Japan

Primers for *NPHP1*

exon	F primer	5'-nucleotide sequence -3'	R primer	5'-nucleotide sequence -3'	Amplified fragment length (bp)
exon1	NPHP1E01F010	GACCACCGCAAGAGAACATT	NPHP1E01R010	AAGCTCCAGGATTAGGTGGG	319
exon2	NPHP1E02F010	GGTATATGGGTTTTCACTGTA	NPHP1E02R010	TTCCATTGATTCCAAGGAC	319
exon3	NPHP1E03F010	TAATTGCCTTGCCTGCTCAAC	NPHP1E03R010	CAGACTTAGCAAGCCTGTTCG	320
exon4	NPHP1E04F010	GATAGGTGTAATGTCACACTG	NPHP1E04R010	CATGGGATCTAACACCTTCTA	418
exon5	NPHP1E05F010	CCAGCTCCAATATGGGATAT	NPHP1E05R010	CAGGTGTACAGGCAGAGTTTTTC	380
exon6	NPHP1E06F010	GGGAAGCTTTTGATAAACCTT	NPHP1E06R010	GTCATCACTAGTCAACTGAC	349
exon7	NPHP1E07F010	GTTTTGTTTTTACTGGAGGG	NPHP1E07R010	GTTGCTCCATTCAAGAAAG	306
exon8	NPHP1E08F010	CTCGTTTTTCACTGAAAACCTG	NPHP1E08R010	GGAAAGCAGGATCAATGAGAA	443
exon9	NPHP1E09F010	CTTCCACTAAAGTCTGTATGT	NPHP1E09R010	GTGAGATTCAACATCTTCTTC	322
exon10	NPHP1E10F010	TTTGAAGTGCCTGTACTCTA	NPHP1E10R010	GTCCAAATCTGCCTTAGTTA	360
exon11	NPHP1E11F010	GCCTGCCAATATTTATTGTTC	NPHP1E11R010	TACTCTTTGGGAATGGGGA	494
exon12	NPHP1E12F010	TCCTCACTTAGTGTAGCCACT	NPHP1E12R010	GTCCTCAAAGAACACCAAAGA	302
exon13	NPHP1E13F010	CACCTCAACATTTGGGATTAC	NPHP1E13R010	CATTCTATTCCTCAAGGGAT	365
exon14	NPHP1E14F010	GCAAAATGAGATTCTACTGTG	NPHP1E14R010	AGTTATTGGCATGCTCATAGA	342
exon15	NPHP1E15F010	GGCATAAATGAAATGTCTGAG	NPHP1E15R010	GTCTCATATGTGTACCAAGA	374
exon16	NPHP1E16F010	GCACTACTGGGTGGTATATTT	NPHP1E16R010	GGGAAGAATTAAGAGGACAA	330
exon17	NPHP1E17F010	GAAGCAAATTTGGGACTGTT	NPHP1E17R010	AAAGTACAACCAGAAACAGA	316
exon18	NPHP1E18F010	CCTAGAAGTCAAAGTGTGTAG	NPHP1E18R010	GGAGACATCATCTAGTAACA	326
exon19	NPHP1E19F010	CAGCATTTTTAAACCCTGTCCA	NPHP1E19R010	GGGATTATGACTATGGCTACT	261
exon20	NPHP1E20F010	CCCTCATCTACCTCTTAGG	NPHP1E20R010	CTAAGTTGAAAGTGACAGTG	478

Primers for *NPHP2*

exon	F primer	5'-nucleotide sequence -3'	R primer	5'-nucleotide sequence -3'	Amplified fragment length (bp)
5UTR	I5Uf1	TTTCCATTGGGCTCTCGGCC	I5Ur1	TGAGTCTGCAGCAGGGGCCAA	366
exon1	IEx1F	CCCCTTGGAACTGATGAGAC	IEx1R	AACAACTTCTCAGGACAAAC	265
exon2	IEx2F	ATAATAAACAGCGAATATAGTCTTAC	IEx2R	TGTCCATTGCATAGTCCAC	327
exon3	IEx3F	GTGGAATTACAAGCATTTTTCC	IEx3R	AATTCAGGCCCTTCTCCTTG	411
exon4	IEx4F	TTGTTACTGTTGTTATTCGAGAACC	IEx4R	ACTTCTGGGGGATGAGTCC	356
exon5	IEx5F	CACCAAATGTAATTTATTGAGGATTC	IEx5R	AGTGAAGGGGAAGGCACAG	317
exon6	IEx6F	CTGCTGTTCAGAAACCGTTG	IEx6R	GGTGTAGGAGTGCAAAAAGC	421
exon7	IEx7F	AGGGGAAAATGCTTTGCTTC	IEx7R	AATTTATAGCAACATCTACACTTTGG	351
exon8	IEx8F	GATGGGGAAAATCAAGAGAGG	IEx8R	TGTGCAGCTTTCTGCTAAGG	348
exon9	IEx9F	CCATAAGAATAAAGCATTAAAGGAAC	IEx9R	TGTGGGTGATCTTCTCATCTTG	494
exon10	IEx10F	CCACATATCCAAAATACTTACTCC	IEx10R	AGAAAGGATGTATGATAAAGAGCAC	528
exon11	IEx11F	TTCCACATCTTGAATGAAGTTTCC	IEx11R	CTCATCTGTTCCCTCTCCTG	427
exon12	IEx12F	CACACAGAGACTTGAGGAGGTG	IEx12R	CGGCAGAAGATGACAAAGG	382
exon13	IEx13F	TGTAAGTCCACTATTATGGTGATG	IEx13R	CACCACATGGAACACTCTGG	939
exon14	IEx14F	AATGGGAGCTGAATGAACC	IEx14R	TGGTACTCTGGGGTACTTG	410
exon15	IEx15F	CACACACCTGCAAGCTCAAG	IEx15R	TCTTGGGGATGAAACAAAGG	255
exon16	IEx16F	CCAATGAACTATTCCCTCAGC	IEx16R	GCAGAAAATCTGAACTCTGCAC	242

Fig. 1 Genomic DNA extraction, PCR, and determination of *NPHP1*, *2*, *3* and *4* gene sequence. PCR primers were prepared to amplify approximately 200–300 bp fragments based on *NPHP 1–4* gene sequences registered in GenBank, the following primers were used as shown

has been shown to carry out signal transmission between renal tubular epithelial cells, in cooperation with nephrocystin-1 [3].

NPHP2, the gene responsible for infantile NPH (NPH2), is located on 9q22–31 [4]. *NPHP2* encodes a protein termed inversin (INVS). An abnormality in INVS can cause situs inversus, pancreatic islet-cell dysplasia, cardiovascular

abnormalities, and hepato-biliary disorders. In addition, INVS abnormalities can cause cyst formation resembling that in juvenile nephronophthisis. However, the renal prognosis is worse progression to ESRD in early childhood.

The gene responsible for adolescent NPH (NPH3), *NPHP3* is located on chromosome 3q21–22 [5]. *NPHP3* is believed to encode a protein involved in signal

Primers for *NPHP3*

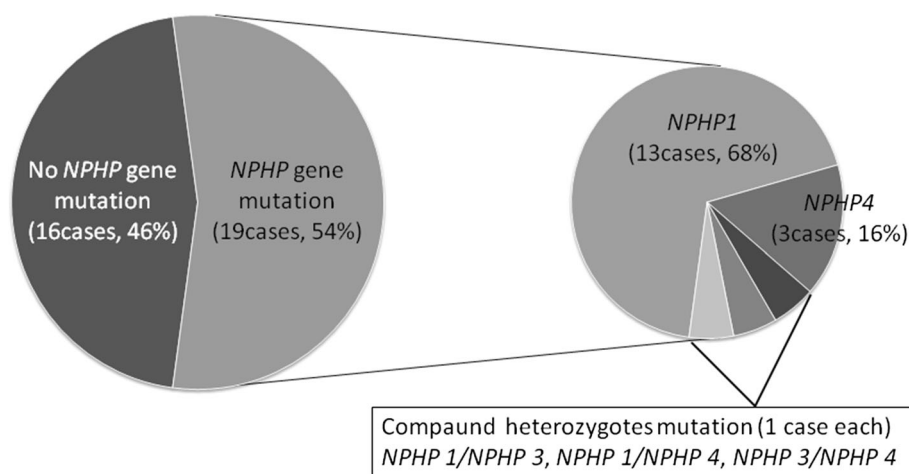
exon	F primer	5'- nucleotide sequence -3'	R primer	5'- nucleotide sequence -3'	Amplified fragment length (bp)
exon1	NPHP4E01F010	ATGCAATCAGGATGGGCCCG	NPHP4E01R010	AACCCACGTAGCCAAACGGCA	598
exon2	NPHP4E02F010	AGGTTCTCTGGGATTAGTG	NPHP4E02R010	AATCAAAGCATCGTAAGCCAG	373
exon3	NPHP4E03F010	TGATATCTGAGCGAGGTGGCC	NPHP4E03R010	AAGTCTGAGACGCCTGTGAG	368
exon4	NPHP4E04F010	TGCTGTGGCACGTGTAGGAAG	NPHP4E04R010	ACTGCACTCTAGCTGTGTTGA	379
exon5	NPHP4E05F010	AAAGCTCTAGTGGCGTGGTG	NPHP4E05R010	CAGATAGCAGTTTACACTGAG	273
exon6	NPHP4E06F010	CCTGTTGTGGTGTCTTAAC	NPHP4E06R010	TTCCATCTCTCCACTGTCC	426
exon7	NPHP4E07F030	TGGAGGAGGTTGGGGTAGAT	NPHP4E07R020	AGGGGAAAAGACAGAATACTACA	569
exon8	NPHP4E08F010	CTGCTCCAGTTTCTCTCT	NPHP4E08R010	TCCACGTGGGTGAGTCAACA	383
exon9	NPHP4E09F010	ACTTGCTGTGCAGCAGCACC	NPHP4E09R010	CCATCTCATCTGTATCCTTTG	446
exon10	NPHP4E10F010	CACTGAGCTCTGTTGAATT	NPHP4E10R010	GGCATACCCATGACATGAAAA	420
exon11	NPHP4E11F010	GACTTTGTTTTAGGGCAGAGC	NPHP4E11R010	ATGTGGTATTACCGTACTAG	339
exon12	NPHP4E12F010	AGACAAGGTGGTGAGGCCTGT	NPHP4E12R010	AAGCACGCAGGGATCCACTGT	274
exon13	NPHP4E13F010	TTGAGAAGCGTCCCAGGTTT	NPHP4E13R010	TGCCACCTAACTAAGGACAGG	384
exon14	NPHP4E14F010	CCAGAGGCAATTAATCGATGA	NPHP4E14R010	ATTGATGCACCTCCCTGTGGA	354
exon15	NPHP4E15F010	CAGACTGTGGACCTGTGAA	NPHP4E15R010	TCAGCACAGACAGTCTGCCA	392
exon16	NPHP4E16F010	GACTAAGTGCCTGGACCATC	NPHP4E16R010	GGTCCAGTATGATTCTAATG	419
exon17	NPHP4E17F010	GTAGCTATGACAGAAAGCAGAA	NPHP4E17R010	ACAAGTCTGTGGCGGATAGC	392
exon18	NPHP4E18F010	AGGGTCTTATCTGCGCACAC	NPHP4E18R010	ATTCTCCCGTTTTCTCTCGG	441
exon19	NPHP4E19F010	AGGCCATTGAAAGCCACAGC	NPHP4E19R010	CACATGCACACAGCATGCAC	326
exon20	NPHP4E20F010	CCCTCCATATAGTGGTCC	NPHP4E20R010	AGGTAAGAGAGAAATCATGTGG	404
exon21	NPHP4E21F010	AATGTCTCTCTGAGATGCGC	NPHP4E21R010	AGAGAAGTCAAATGCCCCGG	444
exon22	NPHP4E22F010	TCTCTCCACTCTCTGAGCA	NPHP4E22R010	TGCACAGTAAGGGAGGAGCA	391
exon23	NPHP4E23F010	TCAGTGTGAGGGAGGCTGGT	NPHP4E23R010	AAAAGGCCATCCAGGCCCA	346
exon24	NPHP4E24F010	GTCTGGCAACAGTGGAGATA	NPHP4E24R010	ACCAGGGCATGAAGCCATGAG	360
exon25	NPHP4E25F010	TGACGAGCTGTCTGTCTTA	NPHP4E25R010	CCTAAATGAAGAGGATCCCA	286
exon26	NPHP4E26F010	AGATGCGTCTGGGAGGGACT	NPHP4E26R010	TTTAGGAAGGGGCAAGCCCA	308
exon27	NPHP4E27F010	TTCCCTGCACAGCTCTCTGT	NPHP4E27R010	AAAAGTCTGTGTCAGGGCCAC	390
exon28	NPHP4E28F010	AACCACCATGACCTGGGCT	NPHP4E28R010	TGTATCCAGTGTCCGAGTCA	392
exon29	NPHP4E29F010	TCTTATCTGTGGGGTCC	NPHP4E29R010	GCTGTGATTGAGGAACTCG	364
exon30	NPHP4E30F010	CAGCTCCCTGGAAATAAC	NPHP4E30R020	AAACTGCCAAGGGAGACGTG	768

Primers for *NPHP4*

exon	F primer	5'- nucleotide sequence -3'	R primer	5'- nucleotide sequence -3'	Amplified fragment length (bp)
exon1	NPHP3E01F020	TGCTCCGCCAGTCTGCTCT	NPHP3E01R020	GAGAATATGGCCTCTCAAATT	694
exon2	NPHP3E02F010	CATGAAGTCTCTGATAATTGG	NPHP3E02R010	GAATCTCATGACTTACTTC	387
exon3	NPHP3E03F010	GAGGACCAAAATGAATATTGGT	NPHP3E03R020	GCAGCTGACAGAGAAACACA	420
exon4	NPHP3E04F020	CAGTATCTTTGAACCTTTGCCA	NPHP3E04R020	GATGGTTTGTCAATGGAAAGC	459
exon5	NPHP3E05F020	GGTATGGCAGTATTAACATGT	NPHP3E05R020	GCTTCTGTCTTTAAGACAT	391
exon6	NPHP3E06F020	GTATTGAGAGAAACTTGCCCT	NPHP3E06R020	GCTATATTGCCAAACTCTGA	595
exon7	NPHP3E07F020	GTTGGACCTTTCTGGCCACT	NPHP3E07R020	GTTCCAGCCACACTGTTTCT	401
exon8	NPHP3E08F010	CCTAAGGTTGTTGTGAAGATA	NPHP3E08R010	TTCAAAAAGACAAGGAAAGTGG	320
exon9	NPHP3E09F020	AAGGCTGTATGTTGAACCTTG	NPHP3E09R020	CACATCTCAACATGGAATATC	440
exon10	NPHP3E10F010	CAGCTTTTCTCCAGTATTTTC	NPHP3E10R020	GGGCATGAACCTATTGTTTA	350
exon11	NPHP3E11F020	AGTAACTGACCACCTGATTGC	NPHP3E11R020	GACCCGATTGTATCGAATATT	390
exon12	NPHP3E12F020	ATATTGCATAAATCGGGTCC	NPHP3E12R020	CTGTGGGCATACGATATATT	458
exon13	NPHP3E13F010	CAGAGTTCAGATTGGTGATAA	NPHP3E13R010	CCTCACTGCAAGTTACATAAA	406
exon14	NPHP3E14F010	GTTGTGATTCAATGCTCAAAG	NPHP3E14R010	CCTTATAACAGATCCCTTATA	410
exon15	NPHP3E15F010	TTTCTGTGGGGTACTTGTG	NPHP3E15R010	CAGACTGGTGTAGTGATCAGT	283
exon16	NPHP3E16F020	TGACTTAGCAGCCCATAAA	NPHP3E16R020	GGCTATCAGCATTCTGCATA	435
exon17	NPHP3E17F020	GTTATCTTGGTGTGCTAGAT	NPHP3E17R010	CTTTGGCAGAAAATATCTTGC	487
exon18	NPHP3E18F010	CATTCACACTTCTGAGATT	NPHP3E18R010	GAATAGGGAGAGGATTTAATC	496
exon19	NPHP3E19F020	GGTCTGCATATCACTGAATT	NPHP3E19R020	GGAAAAGCAGATCTAATAGAG	492
exon20	NPHP3E20F010	CAGTACTGCCTACTAATAAA	NPHP3E20R020	GCAAGATCTGCTCATGTATTA	440
exon21	NPHP3E21F020	CTCTCTCTTTTCCAAGATG	NPHP3E21R020	CCACATGAAGACTAGGCACAG	497
exon22	NPHP3E22F020	CTAGACTGTCTTGTTTTGTG	NPHP3E22R020	CTTTAAAGAACTGAGGTAGCT	614
exon23	NPHP3E23F010	GTTGCCATGTGAAAATATTTG	NPHP3E23R010	CATACATGAAATTTTGCCTGG	436
exon24	NPHP3E24F010	GGAAAAGTAAGATTTGAGCTG	NPHP3E24R020	GTTCTGTGCTGATCTGTTTA	536
exon25	NPHP3E25F020	GCTTTTCTATACAGTGTAGCT	NPHP3E25R010	CCTTCATACAAGTCTAACTTC	485
exon26	NPHP3E26F010	CCCATCTTTAGGAGGATATT	NPHP3E26R010	CCCCACTTAAGAAAAACAT	341
exon27	NPHP3E27F010	AGGGGAAATGGGCAATATTT	NPHP3E27R020	CCTTGGATACATATAATAGG	512

Fig. 1 continued

Fig. 2 Percentage of NPH patients with *NPHP* gene mutation. *NPHP* gene mutation was detected in 19 patients. No *NPHP* gene aberration detected within the sequences analyzed in the other 16 patients with suspicion of NPH clinicopathologically



transmission in renal tubular epithelial cells, such as signaling involving diacylglycerol kinase-zeta and receptor-like tyrosine kinase. Abnormalities of the protein disrupt urinary concentrating ability and the structure of cilia of renal tubules, as in the other types of NPH.

Previous reports describe occurrence of *NPHP1* mutations in approximately 30–50 % of juvenile nephronophthisis patients in Western countries [1, 6], where genetic analysis of *NPHP1* is performed initially when juvenile NPH is suspected. If mutation is detected, kidney biopsy usually is deferred [7]. Genetic diagnosis is made less frequently in Japan; so kidney biopsy often is performed to obtain a definitive diagnosis. Not infrequently, NPH is discovered in the advanced or end stage in many Japanese patients, in whom treatment no longer can slow progression. Unfortunately, symptoms typically seen in early stages are incompletely characterized.

In the present study, we investigated clinical, histologic, and genetic features in 35 Japanese patients clinically and histologically suspected to have NPH, aiming to promote early diagnosis. We studied many exons as many as 13 *NPHP* genes. Since such genetic analysis involves significant cost and time, we also screened biopsy specimens by immunohistologic methods employing antibodies against relevant peptides.

Methods

Patient registration and informed consent

Our subjects included 35 patients with clinicopathologic findings suggestive of NPH who were referred to our department from various regions of Japan. The study was performed following approval by the Ethics Committee of Kinki University Faculty of Medicine and acquisition of

written informed consent from patients or their parents (Actual state of Japanese juvenile nephronophthisis patients and identification of gene aberrations; approval number 20–99).

Genomic DNA extraction, polymerase-chain reaction (PCR), and determination of *NPHP* gene sequence.

After approximately 5 mL of peripheral blood was collected from patients into tubes containing Na-EDTA, genomic DNA was extracted using NucleoSpin for Blood (TaKaRa Bio Inc, Shiga, Japan). Human genomic DNA (TaKaRa Clontech, code 636401; Shiga, Japan) was used as a control. Patient samples and control genomic DNA were diluted with sterile water to prepare 10 ng/ μ L solutions. PCR was performed using these as templates and TaKaRa PCR Thermal Cycler Dice Gradient (TaKaRa Bio Inc, Shiga, Japan). To determine extent of deletions and identify break points, PCR primers were prepared to amplify approximately 200–300 bp fragments based on *NPHP* gene sequences registered in GenBank (Fig. 1). For PCR, annealing temperatures and times were 63 °C and 15 s for *NPHP1* and *NPHP3*; 60 °C and 15 s for *NPHP2*; and 60 °C and 20 s for *NPHP4*, respectively. For sequence analysis, PCR products were purified by an enzyme reaction, and templates for sequencing were prepared. The sequencing reaction was carried out using the prepared template DNA and a BigDye Terminator v.3.1 Cycle Sequencing Kit (Applied Biosystems, CA, USA), employing the dye terminator method. Reaction products were purified by gel filtration, and sequence analysis was performed using a capillary-type sequencer, ABI3730xl (Applied Biosystems, CA, USA). The algorithm established by Salomon et al. [8]. was adapted for use in our analytical procedure. In children with renal dysfunction

Table 1 Characteristics of patients found to have NPHP gene mutations

Age/gender	Motive of discovery	BUN/ Om (mg/ dL) ^a	UP	Urinary LMP	Low gravity urine	Extrarenal symptom	Diagnosis at first biopsy	NPHP/mutation	The other NPHP mutation	Consanguineous marriage	Family history of renal disease
14 years/M	Anemia	49/3.3	(-)	(-)	(-)	n.f	n.d	Large deletion (>2.0kbp)	(-)	(-)	(-)
13 years/F	Nocturnal enuresis	27/1.3	(-)	(-)	(-)	n.f	n.d	Large deletion	(-)	(-)	NPH (younger brother)
11 years/M	Sibling with NPH	17/0.6	(-)	(+)	(+)	n.f	n.d	Large deletion	(-)	(-)	NPH (elder sister)
15 years/F	Protein uria (school urinalysis)	21.3/1.3	(±)	(-)	(-)	n.f	TIN	(-)	D1980G (NPHP4, hetero)	(-)	(-)
15 years/F	Protein uria (school urinalysis)	89.6/ 11.6	(-)	(+)	(+)	RP	NPH	Partial deletion (=300bp)	(-)	(-)	Acute glomerulonephritis (mother)
14 years/M	Chance discovery of the RD (heatstroke)	17/0.9	(±)	(+)	(+)	n.f	n.d	n.d	L939 (NPHP4, hetero)	(-)	(-)
11 years/F	Enuresis, polyuria	74/5.2	(1+)	(+)	(+)	SS(-2.5SD)	NPH	E677Q (hetero)	E642L (NPHP4, hetero)	(-)	(-)
18 years/F	Enuresis, polydipsia	82/8.1	(±)	(+)	(+)	SS(-1.8SD)	NPH	Gln547 (hetero)	S80L (NPHP3, hetero)	(-)	Protein uria (father)
8 years/M	Glycosuria (school urinalysis)	159/ 11.1	(2+)	(+)	(+)	n.f	Similar NPH	E677Q (hetero)	NPHP4(-)	(-)	(-)
14 years/M	Glycosuria (school urinalysis)	48/5.0	(±)	(+)	(+)	RP	NPH	Large deletion	(-)	(-)	NPH (younger sister)
13 years/F	Sibling with NPH	58/2.7	(1+)	(+)	(+)	RP	NPH	Large deletion	(-)	(-)	NPH (elder brother)
20 years/F	Chance discovery of the RD (medical examination)	44.6/2.4	(1+)	(+)	(+)	n.f	n.d	(-)	L939Q (NPHP4, homo)	(-)	(-)
8 years/F	Chance discovery of the RD	32.2/1.4	(-)	(+)	(+)	n.f	NPH	Large deletion	(-)	(-)	(-)
15 years/F	Protein uria (school urinalysis)	37/2.6	(-)	(+)	(+)	n.f	Tubular enlargement medullary cysts	Large deletion	(-)	(-)	(-)
7 years/F	Chance discovery of the RD (urine tract infection)	40/3.0	(1+)	(+)	(+)	Joubert syndrome	n.d	(-)	AA/OO→AG/ OT (exon 26/exon 20)	(-)	(-)
19 years/F	Chance discovery of the RD (bronchitis)	90.3/8.4	(1+)	(+)	(+)	n.f	n.d	(-)	A150V (NPHP3, hetero)	(-)	(-)

Table 1 continued

Age/gender	Motive of discovery	BUN/ Om (mg/ dL) ^a	UP	Urinary LMP	Low gravity urine	Extrarenal symptom	Diagnosis at first biopsy	<i>NPHP</i> /mutation	The other <i>NPHP</i> mutation	Consanguineous marriage	Family history of renal disease
8 years/M	Visual impairment	46.5/1.9	(-)	(+)	(+)	RP	NPH	Large deletion	D1980G (<i>NPHP4</i> , hetero)	(-)	(-)
16 years/F	Protein uria (school urinalysis)	43.3/2.6	(1+)	(+)	(+)	n.f	NPH	Large deletion		(-)	(-)
13 years/F	Anemia, fatigue	39/2.2	(-)	(+)	(-)	n.f	TIN, tubular enlargement	Large deletion		(-)	(-)

RD renal dysfunction, *n.f.* not found, *n.d* not done, *UP* urinary protein, *LMP* low molecule protein, *SS* short stature, *RP* retinitis pigmentosa, *TIN* tubulo interstitial nephritis
^a Renal function at the time of the discovery

who were 5 years old or younger, the gene responsible for infantile *NPHP* (*NPHP2*) was analyzed first. In patients older than 5 years, *NPHP1* was analyzed first; if no mutation was detected, *NPHP4* was examined. *NPHP3* analysis was added when no mutation was detected in other genes in patients whose disease progressed to end-stage renal disease at an age of 16 years or older.

Clinical data

Data originally collected at our department as well as data provided by other institutions were surveyed using a questionnaire. Questionnaire consists of personal data including the patient's age, motive of discovery, urinary abnormality and renal dysfunction, detailed clinical data, extrarenal symptom, renal tissue diagnosis at the first biopsy, consanguineous marriage, and family history of renal disease.

Results

NPHP gene analysis

Among 35 patients, an *NPHP* gene mutation was identified in 19 patients. Although NPH was suspected clinicopathologically in the other 16 patients, no *NPHP* gene aberration was detected within the sequences analyzed (Fig. 2). Characteristics of patients with *NPHP1* gene mutations (Table 1) and without *NPHP* gene mutations (Table 2) were shown. A mutation was detected only in *NPHP1* in 13 patients; deletion was extensive in 10 (Fig. 3a) and partial in 1. Two other patients had a point mutation (E677Q and K334 N, both heterozygous). In all, these mutations accounted for 37.1 % (13/35) of patients. In another candidate gene responsible for the juvenile type, *NPHP4*, the mutation L939* was detected in 2 patients (Fig. 3b), while a D1980G mutation was detected in 1, accounting for 8.6 % (3/35) of all patients. Compound heterozygotes containing 1 mutation each in *NPHP1* G547* and *NPHP3* S80L (Fig. 4a), 1 mutation each in *NPHP1* E677Q and *NPHP4* E642L (Fig. 4b), and 1 mutation each in *NPHP3* A150 V and *NPHP4* D1089G (Fig. 4c) also were observed. The disease progressed to ESRD before 20 years of age in these patients, similar to the course of other patients with a single-gene mutation. No *NPHP2* mutation was detected in any patient.

Clinical and demographic features of patients

Patient background

Patients were reported from 46 prefectures without evident selection bias, and with no important regional

Table 2 Characteristics of patients without apparent NPHP gene mutations

Age/gender	Motive of discovery	BUN/Orn (mg/dL) ^a	UP	Urinary LMP	Low gravity urine	Extrarenal symptom	Diagnosis at first biopsy	NPHP1 mutation	NPHP3 mutation	NPHP4 mutation	Consanguineous marriage	Family history of renal disease
6 years/M	Lagging physical development	34/1.2	(-)	(-)	(-)	SS (-1.3SD)	NPH	(-)	n.d	(-)	(-)	(-)
12 years/M	SS, fatigue	48/1.3	(-)	(+)	(-)	Sensory deafness	Chronic interstitial nephritis, glomerulosclerosis	(-)	n.d	(-)	(-)	(-)
26 years/M	Chance discovery of the RD (medical examination)	21/1.6	(-)	(+)	(-)	n.f	Interstitial nephritis	(-)	(-)	(-)	(-)	Renal dysfunction (father, young sister)
11 years/M	Pallor, anemia	27.4/1.5	(-)	(+)	(+)	SS (-2.2SD)	n.d	(-)	n.d	(-)	(-)	(-)
17 years/M	SS	34/1.5	(±)	(+)	(+)	SS (-3.8SD)	n.d	(-)	n.d	(-)	(-)	(-)
22 years/M	Hypertension	32.5/1.5	(1+)	(+)	(-)	RP	TIN	(-)	(-)	(-)	(-)	(-)
11 years/F	polydipsia, polyuria	15.4/0.7	(-)	(+)	(+)	n.f	n.d	(-)	n.d	(-)	(-)	(-)
12 years/F	Chance discovery of the RD (protein uria at 3 years old)	32/1.6	(2+)	(+)	(+)	n.f	TIN, tubular enlargement	(-)	(-)	(-)	(-)	(-)
14 years/M	Protein uria (school urinalysis)	58/4.2	(1+)	(+)	(+)	n.f	TIN, tubular enlargement	(-)	(-)	(-)	(-)	(-)
26 years/M	Hypertension (medical examination)	38.7/1.5	(-)	(+)	(+)	n.f	TIN, glomerulosclerosis	(-)	(-)	(-)	(-)	(-)
10 years/M	Pallor, anemia	53.6/1.0	(1+)	(+)	(+)	n.f	NPH	(-)	n.d	(-)	(-)	(-)
28 years/F	Chance discovery of the RD anemia	47.5/2.9	(1+)	n.d	(+)	n.f	TIN, similar NPH	(-)	(-)	(-)	(-)	(-)
11 years/F	Pallor, polydipsia, polyuria	27.4/1.5	(-)	(+)	(+)	SS(-2.2SD)	n.d	(-)	n.d	(-)	(-)	(-)
18 years/M	Crud, fatigability	49.6/4	(±)	(+)	(+)	Specific complexon	Similar NPH	(-)	(-)	(-)	(-)	NPH (young sister)
16 years/F	Sibling with NPH	38.3/1.8	(-)	(+)	(-)	Specific complexon	Similar NPH	(-)	(-)	(-)	(-)	NPH (elder brother)
46 years/F	Protein uria, hematuria (at 30 years old)	33/1.8	(1+)	(+)	(-)	Sensory deafness	Chronic interstitial nephritis, glomerulosclerosis	(-)	(-)	(-)	(-)	NPH (elder brother)

RD renal dysfunction, n.f not found, n.d not done, UP urinary protein, LMP low molecule protein, SS short stature, RP retinitis pigmentosa, TIN tubular interstitial nephritis

^a Renal function at the time of the discovery

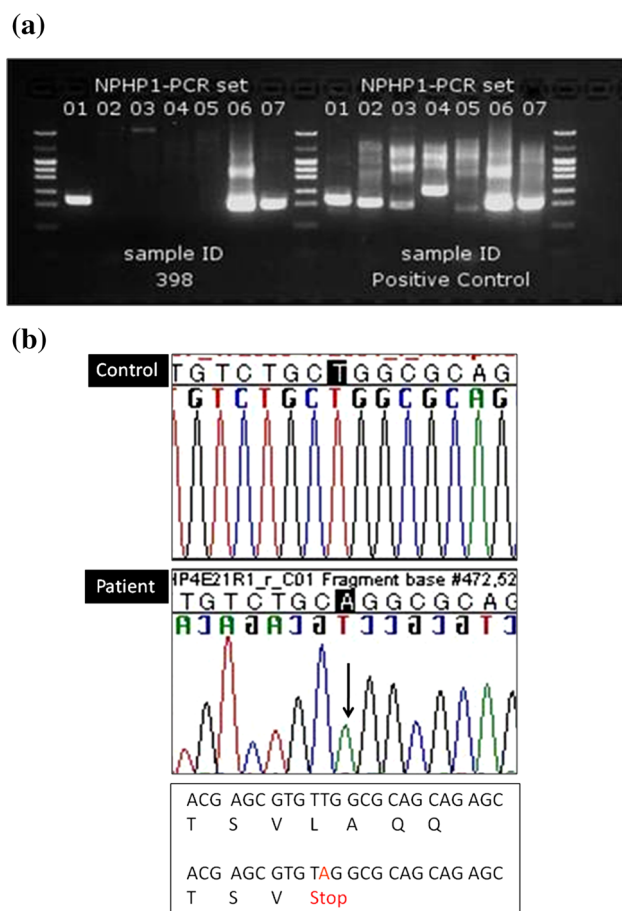


Fig. 3 Analysis of deletion in *NPHP1* (a) and analysis of *NPHP4* (b). In a lane 1 and lanes 6 and 7, contain PCR products of regions within and outside *NPHP1*, respectively; Lane 2 contains PCR products from the junction between *NPHP1* and the adjacent *MALL* gene. Lanes 3–5 show the PCR products of *NPHP1* obtained with primers amplifying fragments of approximately 300 bp. *NPHP1* was nearly completely deleted (1.2 kbp deletion). In b, substitution of TAG for TTG formed a stop codon, prematurely terminating peptide synthesis

differences (Fig. 5). The male:female ratio was 16:19, with evident gender difference. Ages of patients ranged from 2 to 38 years (median; 12.5). Familial occurrence was noted in 3 families. Other occurrences were solitary, with no family member showing a urinary abnormality, a diagnosis of NPH, or any renal dysfunction of unknown cause.

Initial abnormality deletion

NPH sometimes was discovered following an abnormal urinary finding by mass screening, such as proteinuria detected in a urine test at school (18 %), or renal dysfunction discovered incidentally in working up other medical symptoms, or during medical check-ups (23 %). Approximately 20 % of cases were discovered because of urinary tract symptoms such as polyuria with or without

polydipsia, enuresis (often nocturnal), or mellituria. Some 38 % were discovered because of either extrarenal manifestations such as lagging physical development, dwarfism, anemia, pallor, hypertension, or visual disturbance arising from pigmentary retinal degeneration; a prior diagnosis of NPH in a sibling; or both (Fig. 6).

Urinary findings

Urine specific gravity frequently was low (not greater than 1.010); approximately 75 % of cases. Low molecular weight proteinuria, such as β 2-microglobulinuria, also was common (85 %), even though inclusion of renal function shown such as between blood urea nitrogen and serum creatinine was relatively mild at that time.

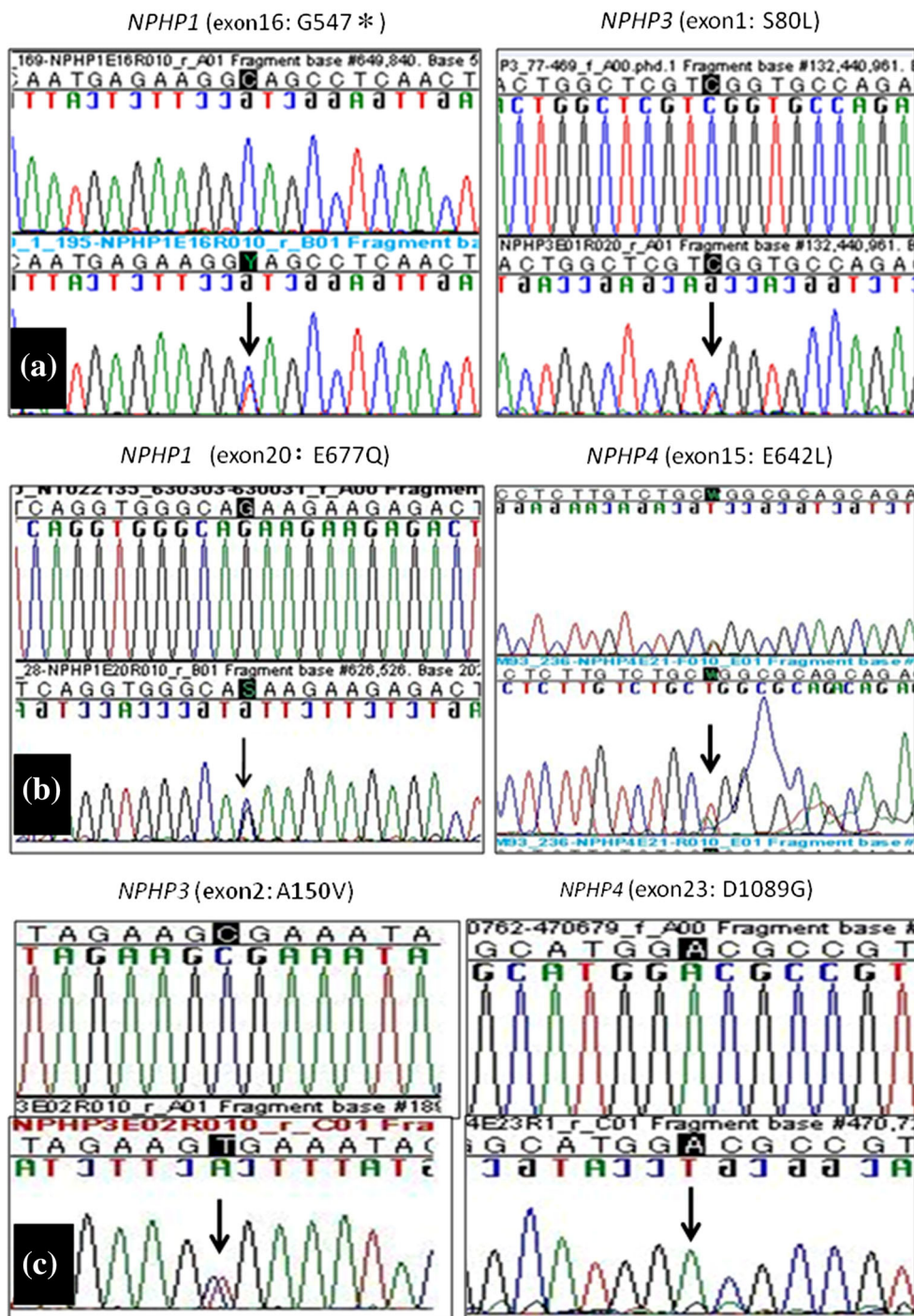
Renal histologic findings

Renal biopsy was performed in 25 patients (71 %). These included 13 patients demonstrated to have an *NPHP* gene mutation and in 12 with no *NPHP* gene mutation identified (suspected cases). Histologic findings included suspected NPH; interstitial nephritis, renal tubular dilation, and glomerulosclerosis. Cystic dilation of renal tubules and irregular contours of tubular basement membranes were observed in most patients, mainly in the renal medulla (Fig. 7a). Sclerotic glomeruli, inflammatory cell infiltration in the renal tubules and interstitium, and fibrosis were frequent, although not seen in all patients (Fig. 7b).

Discussion

Renal tubular epithelial cells are attached to the basement membrane through integrin cross-linking, which transmits extracellular signals to the cell nucleus [2]. Nephrocystin acts importantly in signal transmission between tubular epithelial cells and between these epithelial cells and the extracellular matrix functioning as a docking protein. Nephrocystin also is involved in cell adhesion, together with *N*-cadherin, catenin, and β -catenin [2, 8]. Furthermore, nephrocystin influences actin cytoskeleton structure together with β -tubulin, contributing to maintenance of the cytoskeleton and determination of cell polarity. Nephrocystin forms a complex with Crk-associated substrate, which promotes phosphorylation of Pyk2 and transmits intracellular information through a Pyk2-dependent pathway [2]. Furthermore, nephrocystin is present on primary cilia, where it functions in cooperation with α -tubulin; nephrocystin also is involved in signal transmission in organelles [9]. Accordingly, abnormalities in the nephrocystin molecule disrupt signal transmission between cells

Fig. 4 Compound heterozygotes with heterozygous mutations in different *NPHP* genes. In **a**, a compound heterozygote has one heterozygous mutation involving each of *NPHP1* (G547*) and *NPHP3* (S80L). In **b**, a compound heterozygote has one heterozygous mutation involving each of *NPHP1* (E677Q) and *NPHP4* (E642L). In **c**, a compound heterozygote has one heterozygous mutation involving each of *NPHP3* (A150 V) and *NPHP4* (D1089G)



and the extracellular matrix, intercellular adhesion, cytoskeletal integrity, cell polarity, primary cilia function, and intracellular signal transmission to the nucleus. Structural and functional disorders involving the renal tubular epithelium result.

An *NPHP* gene mutation was detected in about 54 % of all patients, but no mutation was noted within the sequences analyzed in the other 46 %. However, nephronophthisis was suspected clinically and histologically, suggesting possible

mutation in some other *NPHP* gene. An *NPHP1* mutation was most frequent among our Japanese patients, most often representing a large deletion rather than a point mutation. Frequency of an *NPHP1* mutation was similar to that reported in Western populations [10].

On the other hand, mutation in the gene responsible for the infantile type, *NPHP2*, a patient in a compound heterozygous stable with another abnormal *NPHP* gene such as that responsible for NPH3 recently has been

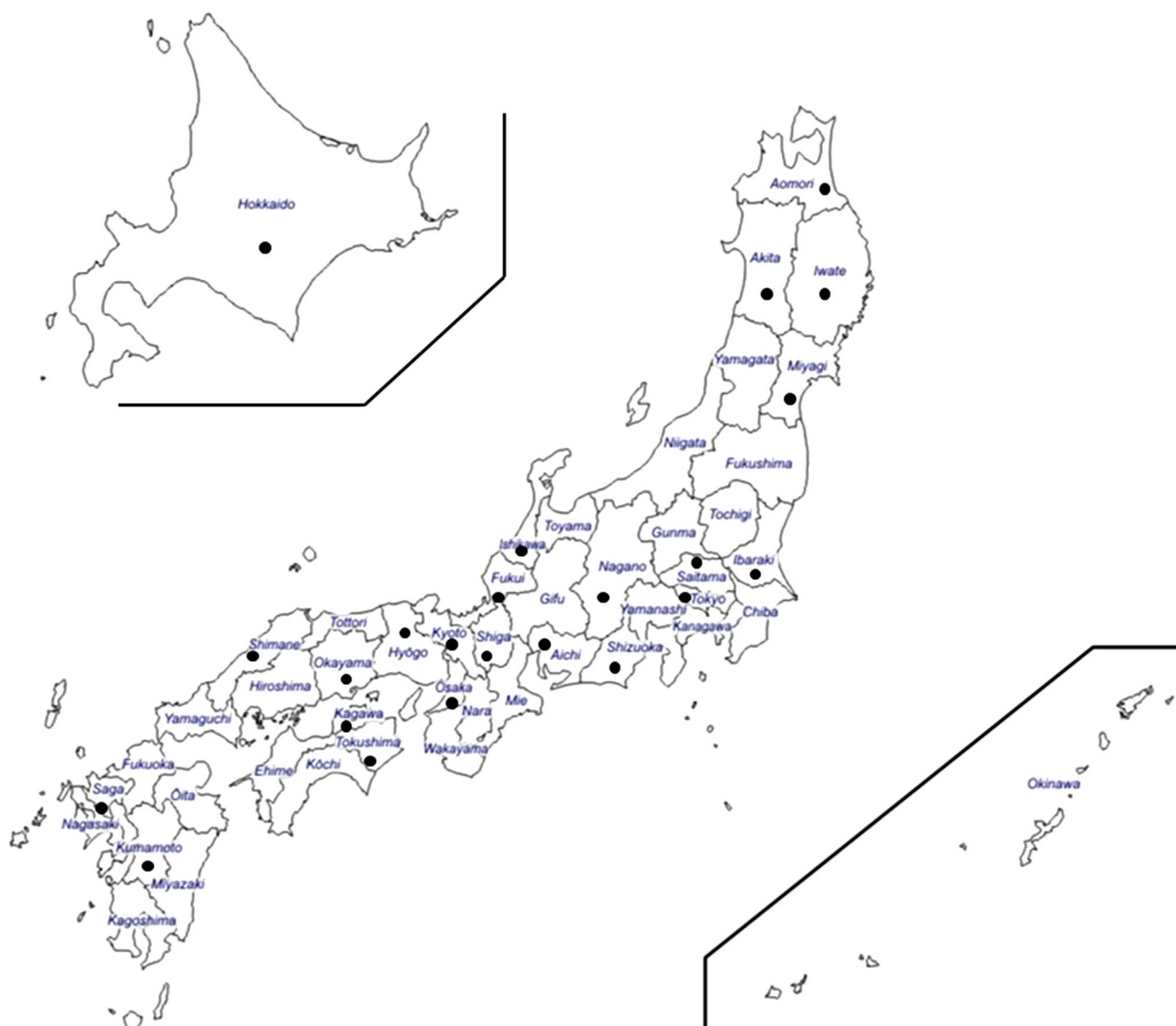


Fig. 5 Demographic features of patients in Japan. Regional distribution of study subjects within Japan, show as a *dot* for each patient

reported [11, 12]. We also found compound heterozygosity across multiple *NPHP* genes in some of our Japanese nephronophthisis patients. In *NPHP4*, L939* (IVS-20T > A) was detected in two geographically distant patients who were not consanguineous. The mutation formed a stop codon by substituting TAG for TTG in exon 21, terminating peptide synthesis. This might prove to be a ‘hot spot’ among Japanese patients.

We detected in three patients with two mutations in either *NPHP1*, *NPHP3*, or *NPHP4* in this study. As similar to the results of the other studies [13, 14], the age of the initial discovery of this disease and the course of progression to end-stage renal disease were not significantly different from those of the patients having mutation in single *NPHP* gene. An analysis of patient backgrounds revealed that NPH was distributed fairly evenly Japan,

including the suspected cases where no causative mutation was identified. Heterozygotes carrying *NPHP* gene mutations also were rather evenly distributed nationwide. No gender difference was evident from our analysis. Although the median age at time of disease discovery was 12.5 years, individual presentation ranged from infancy to adulthood.

Frequency of disease discovery in mass screening programs, such as school urine tests, was low, as previously reported [15]. Incidental discovery of renal dysfunction during diagnostic workup of possibly unrelated symptoms, or during routine check-ups, accounted for less than 50 % of cases. Often symptoms that led to the discovery of NPH represented extrarenal manifestations such as incomplete physical development reported previously [15]. In particular, currently used urine test strips, intended mainly to detect albuminuria, are insensitive to this disease.

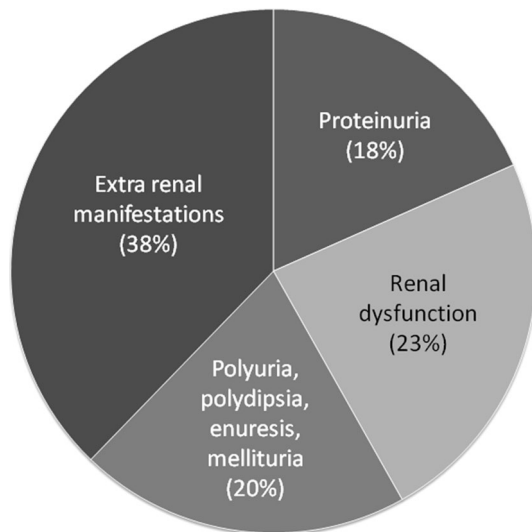


Fig. 6 Clinical suspicion and motivation to discover for NPH. Proteinuria is detected in a urine test at school (18 %), renal dysfunction discovered incidentally (23 %), urinary tract symptoms such as polyuria with or without polydipsia, enuresis, or mellituria (approximately 20 %). Some 38 % were discovered because of either extrarenal manifestations such as lagging physical development, dwarfism, anemia, pallor, hypertension, or visual disturbance arising from pigmentary retinal degeneration

Development in siblings was noted in three families, suggesting autosomal recessive inheritance. However, many cases appear to be sporadic. Familial genetic analysis centering on patients, parents is needed.

In contrast to albuminuria, urinary findings such as low specific gravity and low-molecular-weight proteinuria are relatively helpful in early discovery. According to the results of this study, we suggest that the findings of the low-molecular weight proteinuria and hypotonic urine reflecting renal tubular disorder coupled with the histologic abnormalities involving cystic dilation of renal tubules and the irregularity of tubular basement membrane could be a convincing diagnostic criterion of this disease. Extrarenal manifestations, such as short stature, delayed physical development, and anemia also were frequent. Unfortunately, these tended to coincide with were progression of renal dysfunction rather than early NPH. Nonetheless, NPH needs to be considered in children with such presentations. Some patients have been reported to show somewhat distinctive extrarenal manifestations [13] such as pigmentary retinal degeneration (Senior-Loken syndrome), ocular dysmetria (Cogan's syndrome), cerebral ataxia, hepatic fibrosis, and skeletal and facial abnormalities [13, 16, 17]. Even the most frequent of these extrarenal manifestations, pigmentary retinal degeneration, was present only in some patients and not in others, even among children showing the same *NPHP1* deletion. Similar lesions also have been reported in Jeune, Joubert, oro-facial-digital (OFD1), and

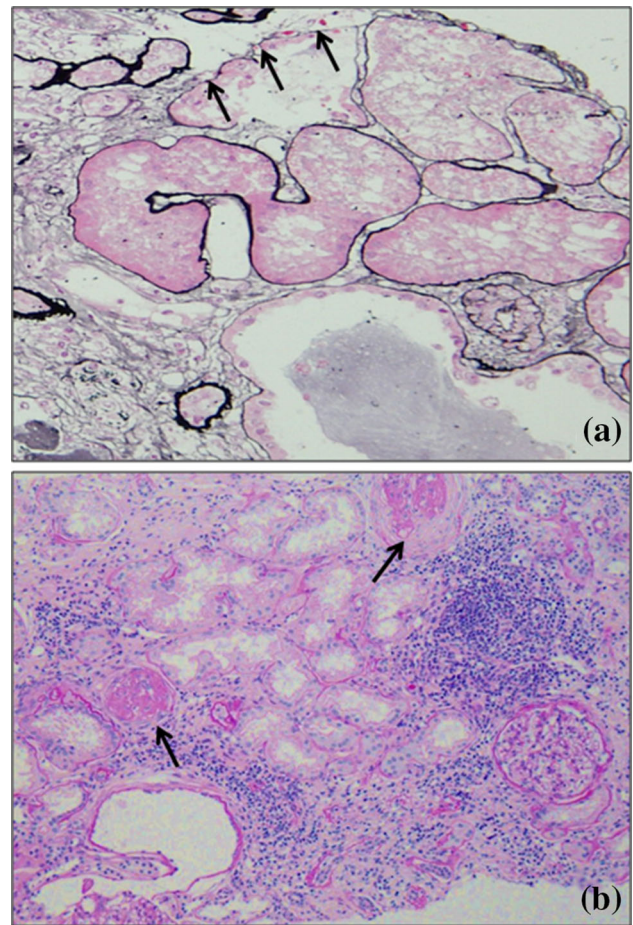


Fig. 7 Pathologic findings in the kidney in nephronophthisis patients. In **a** irregularity (*arrow*) of the renal tubular basement membrane was evident (methenamine silver stain, $\times 200$). In **b**, Inflammatory cell infiltration involved the renal tubular interstitium, and sclerotic glomeruli (*arrow*) were present (periodic acid-Schiff stain, $\times 100$)

Meckel syndromes [13, 18, 19]. *NPHP1* mRNA is expressed predominantly in a wide range of extrarenal tissues including pituitary gland, spine, testis, lymph nodes, and thyroid [14]. Expression also is high in the central nervous system, which could account for associated cerebellar ataxia. However, associated symptoms may develop in organs with low *NPHP1* expression, such as hepatic fibrosis. The role of nephrocystin in extrarenal manifestations remains poorly understood. The 11 kb interval between the 3' end of *NPHP1* and an inverted repeat containing the distal deletion breakpoint was found to contain the first exon of a second gene, *MALL* [20]. Although the detail of the *MALL* gene function has not been clarified, recent report suggested the involvement of the age-related macular degeneration (AMD) [21]. Interestingly, associations have also been reported between AMD and chronic kidney disease [22]. Since pigmentary retinal degeneration is the most common extrarenal

manifestation of NPH, similar to AMD, *MALL* gene may involve the pathogenesis of this eye disorder found in NPH patients as the contiguous gene syndrome.

No truly effective treatment currently is available for NPH. Dietary therapy and administration of ion exchange resins and bicarbonate are carried out to manage hyponatremia, hyperkalemia, or metabolic acidosis. Studies possibly relevant to drug therapy have been conducted in various animals, even protozoa [23, 24]. Previous studies reported that renal cyst expression was inhibited by stimulating the G-protein-coupled calcium sensing receptor and elevating Ca^{2+} and cAMP in the renal tubular epithelial cells of pcy mice. Morphology and function of cilia in zebrafish with ciliopathy may be improved by the administration of rapamycin and rescovitin [25, 26]; however, applicability to human NPHP is unknown. Living-donor kidney transplantation was found to have favorable outcome in many reports including the North American Pediatric Renal Trials and Collaborative Studies (NAPRTCS) [27].

Acknowledgments This study was performed after approval by the Ethics Committee of Kinki University Faculty of Medicine. Written informed consent was obtained from the patient's guardian for genetic examination. We thank Ai Itoh for technical support in tissue staining and manuscript preparation.

Compliance with ethical standards

Conflicts of interest This study was partly supported by a Grant-in-Aid for Scientific Research from Morinaga Hoshikai to Tsukasa Takemura (2013–2014) and from Ministry of Health, Labour and Welfare Japan (grant number: 26070201, Representative investigator: Kazumoto Iijima, Pediatrics, Kobe University School of Medicine). The authors declare that they have no competing interests involving this work.

References

- Hildebrandt F, Otto E. Molecular genetics of the nephronophthisis-medullary cystic disease complex. *J Am Soc Nephrol*. 2000;11:1753–61.
- Donaldson JC, Dise RS, Ritchie MD, Hanks SK. Nephrocystin-converted domains involved in targeting to epithelial cell-cell functions, interaction with filaments, and establishing cell polarity. *J Biol Chem*. 2002;277:29028–35.
- Mollet G, Salomon R, Gribouval O, Silbermann F, Bacq D, Landthaler G, Milford D, Nayir A, Rizzoni G, Antignac C, Saunier S. The gene mutated in juvenile nephronophthisis type 4 encodes a novel protein that interacts with nephrocystin. *Nat Genet*. 2002;32:300–5.
- Otto EA, Schermer B, Obara T, O'Toole JF, Hiller KS, Mueller AM, Ruf RG, Hoefele J, Beekmann F, Landau D, Foreman JW, Goodship JA, Strachan T, Kispert A, Wolf MT, Gagnadoux MF, Nivet H, Antignac C, Walz G, Drummond IA, Benzing T, Hildebrandt F. Mutations in *INVS* encoding inversin cause nephronophthisis type 2, linking renal cystic disease to the function of primary cilia and left-right axis determination. *Nat Genet*. 2003;34:413–20.
- Omran H, Fernandez C, Jung M, Häffner K, Fargier B, Vilaquiran A, Waldherr R, Gretz N, Brandis M, Rüschemdorf F, Reis A, Hildebrandt F. Identification of a new gene locus for adolescent nephronophthisis, on chromosome 3q22 in a large Venezuelan pedigree. *Am J Hum Genet*. 2000;66:118–27.
- Broyer M, Kleinknecht C. Structural tubulointerstitial disease: nephronophthisis. In: Morgan SH, Grunfeld JP, editors. *Inherited disorders of the kidney. Investigation and management*. Oxford: Oxford University Press; 1998. p. 340–8.
- Hildebrandt F, Rensing C, Betz R, Sommer U, Birnbaum S, Imm A, Omran H, Leioldt M, Otto E. Arbeitsgemeinschaft für Paediatrische Nephrologie (APN) Study Group. Establishing an algorithm for molecular genetic diagnostics in 127 families with juvenile nephronophthisis. *Kidney Int*. 2001;59:434–45.
- Salomon R, Saunier S, Niaudet P. Nephronophthisis. *Pediatr Nephrol*. 2009;24:2333–44.
- Hurd TW, Hildebrandt F. Mechanisms of nephronophthisis and related ciliopathies. *Nephron Exp Nephrol*. 2011;118:e9–14.
- Wolf MT. Nephronophthisis and related syndromes. *Curr Opin Pediatr*. 2015;27:201–11.
- Tory K, Rousset-Rouvière C, Gubler MC, Morinière V, Pawtowski A, Becker C, Guyot C, Gié S, Frishberg Y, Nivet H, Deschènes G, Cochat P, Gagnadoux MF, Saunier S, Antignac C, Salomon R. Mutations of *NPHP2* and *NPHP3* in infantile nephronophthisis. *Kidney Int*. 2009;75:839–47.
- Hoefele J, Wolf MT, O'Toole JF, Otto EA, Schultheiss U, Deschenes G, Attanasio M, Utsch B, Antignac C, Hildebrandt F. Evidence of oligogenic inheritance in nephronophthisis. *J Am Soc Nephrol*. 2008;18:2789–95.
- Benzing T, Schermer B. Clinical spectrum and pathogenesis of nephronophthisis. *Curr Opin Nephrol Hypertens*. 2012;21:272–8.
- Hildebrandt F, Zhou W. Nephronophthisis-associated ciliopathies. *J Am Soc Nephrol*. 2007;18:1855–71.
- Hirano D, Fujinaga S, Ohtomo Y, Nishizaki N, Hara S, Murakami H, Yamaguchi Y, Hattori M, Ida H. Nephronophthisis cannot be detected by urinary screening program. *Clin Pediatr (Phila)*. 2013;52:759–61.
- Ronquillo CC, Bernstein PS, Baehr W. Senior-Løken syndrome: a syndromic form of retinal dystrophy associated with nephronophthisis. *Vision Res*. 2012;75:88–97.
- Deacon BS, Lowery RS, Phillips PH, Schaefer GB. Congenital ocular motor apraxia, the *NPHP1* gene, and surveillance for nephronophthisis. *J AAPOS*. 2013;17:332–3.
- Valente EM, Dallapiccola B, Bertini E. Joubert syndrome and related disorders. *Handb Clin Neurol*. 2013;113:1879–88.
- Bredrup C, Saunier S, Oud MM, Fiskerstrand T, Hoischen A, Brackman D, Leh SM, Midtbø M, Filhol E, Bole-Feysot C, Nitschké P, Gilissen C, Haugen OH, Sanders JS, Stolte-Dijkstra I, Mans DA, Steenbergen EJ, Hamel BC, Maignon M, Pfundt R, Jeanpierre C, Boman H, Rødahl E, Veltman JA, Knappskog PM, Knoers NV, Roepman R, Arts HH. Ciliopathies with skeletal anomalies and renal insufficiency due to mutations in the *IFT-A* gene *WDR19*. *Am J Hum Gene*. 2011;89:634–43.
- Hildebrandt F, Otto E, Rensing C, Nothwang HG, Vollmer M, Adolphs J, Hanusch H, Brandis M. A novel gene encoding an SH3 domain protein is mutated in nephronophthisis type 1. *Nat Genet*. 1997;17:149–53.
- Meyer KJ, Davis LK, Schindler EI, Beck JS, Rudd DS, Grundstad AJ, Scheetz TE, Braun TA, Fingert JH, Alward WL, Kwon YH, Folk JC, Russell SR, Wassink TH, Stone EM, Sheffield VC. Genome-wide analysis of copy number variants in AMD. *Hum Genet*. 2011;129:91–100.
- Cheung CM, Wong TY. Is age-related macular degeneration a manifestation of systemic disease? New prospects for early intervention and treatment. *J Intern Med*. 2014;276:140–53.

23. Sugiyama N, Kohno M, Yokoyama T. Inhibition of the p38 MAPK pathway ameliorates renal fibrosis in an NPHP2 mouse model. *Nephrol Dial Transplant*. 2012;27:1351–8.
24. Gattone VH 2nd, Sinders RM, Hornberger TA, Robling AG. Late progression of renal pathology and cyst enlargement is reduced by rapamycin in a mouse model of nephronophthisis. *Kidney Int*. 2009;76:178–82.
25. Chen NX, Moe SM, Eggleston-Gulyas T, Chen X, Hoffmeyer WD, Bacallao RL, Herbert BS, Gattone VH 2nd. Calcimimetics inhibit renal pathology in rodent nephronophthisis. *Kidney Int*. 2011;80:612–9.
26. Wang S, Dong Z. Primary cilia and kidney injury: current research status and future perspectives. *Am J Physiol Renal Physiol*. 2013;305:F1085–98.
27. Hamiwka LA, Midgley JP, Wade AW, Martz KL, Grisaru S. Outcomes of kidney transplantation in children with nephronophthisis: an analysis of the North American Pediatric Renal Trials and Collaborative Studies (NAPRTCS) Registry. *Pediatr Transplant*. 2008;12:878–82.

X-linked Alport syndrome associated with a synonymous p.Gly292Gly mutation alters the splicing donor site of the type IV collagen alpha chain 5 gene

Xue Jun Fu¹ · Kandai Nozu¹ · Aya Eguchi² · Yoshimi Nozu¹ · Naoya Morisada¹ · Akemi Shono¹ · Mariko Taniguchi-Ikeda¹ · Yuko Shima³ · Koichi Nakanishi³ · Igor Vorechovsky⁴ · Kazumoto Iijima¹

Received: 4 October 2015 / Accepted: 10 November 2015 / Published online: 18 November 2015
© Japanese Society of Nephrology 2015

Abstract

Background X-linked Alport syndrome (XLAS) is a progressive hereditary nephropathy caused by mutations in the type IV collagen alpha chain 5 gene (*COL4A5*). Although many *COL4A5* mutations have previously been identified, pathogenic synonymous mutations have not yet been described.

Methods A family with XLAS underwent mutational analyses of *COL4A5* by PCR and direct sequencing, as well as transcript analysis of potential splice site mutations. In silico analysis was also conducted to predict the disruption of splicing factor binding sites. Immunohistochemistry (IHC) of kidney biopsies was used to detect $\alpha 2$ and $\alpha 5$ chain expression.

Results We identified a hemizygous point mutation, c.876A>T, in exon 15 of *COL4A5* in the proband and his brother, which is predicted to result in a synonymous amino acid change, p.(Gly292Gly). Transcript analysis showed that this mutation potentially altered splicing because it disrupted the splicing factor binding site. The

kidney biopsy of the proband showed lamellation of the glomerular basement membrane (GBM), while IHC revealed negative $\alpha 5(\text{IV})$ staining in the GBM and Bowman's capsule, which is typical of XLAS.

Conclusions This is the first report of a synonymous *COL4A5* substitution being responsible for XLAS. Our findings suggest that transcript analysis should be conducted for the future correct assessment of silent mutations.

Keywords Synonymous mutation · *COL4A5* · Splicing · Silent mutation

Introduction

Alport syndrome is a hereditary disorder of type IV collagen characterized by hearing loss and ocular abnormalities, which progresses to chronic kidney disease. X-linked Alport syndrome (XLAS) accounts for approximately 85 % of Alport syndrome patients. Affected patients have mutations in the type IV collagen $\alpha 5$ ($\alpha 5(\text{IV})$) gene (*COL4A5*) gene, leading to abnormal $\alpha 5(\text{IV})$ expression. Male patients typically have a complete absence of $\alpha 5(\text{IV})$ in the glomerular basement membrane (GBM) and Bowman's capsule, while female patients demonstrate a mosaic expression pattern [1, 2]. The median renal survival rate in male XLAS patients is 25 years, and the risk of developing end-stage renal disease (ESRD) before the ages of 30 and 40 is 70 and 90 %, respectively [3].

To date, many variants have been identified including splice site variants: according to the ARUP database 771 variants (http://www.arup.utah.edu/database/alport/alport_welcome.php), HGMD, 852 variants (<http://www.hgmd.cf.ac.uk/ac/index.php>), and LOVD, 1168 variants (<http://www.lovd.nl/3.0/home>) at the point of 21 Oct 2015.

Electronic supplementary material The online version of this article (doi:10.1007/s10157-015-1197-9) contains supplementary material, which is available to authorized users.

✉ Kandai Nozu
nozu@med.kobe-u.ac.jp

¹ Department of Pediatrics, Kobe University Graduate School of Medicine, 7-5-1 Kusunoki-cho, Chuo-ku, Kobe 6500017, Japan

² Department of Nephrology, Saiseikai Kawaguchi General Hospital, Saitama, Japan

³ Department of Pediatrics, Wakayama Medical University, Wakayama, Japan

⁴ Faculty of Medicine, University of Southampton, Southampton, UK

However, none of these involve a synonymous substitution leading to production of an abnormal splice site. Here, we report the first known case of an XLAS family possessing an apparently synonymous *COL4A5* variant.

Materials and methods

Patients and ethical considerations

All procedures were reviewed and approved by the Institutional Review Board of Kobe University School of Medicine. Informed consent was obtained from the patients or their parents.

Mutational analyses

Genomic DNA was isolated from patient peripheral blood leukocytes using the Quick Gene Mini 80 System (Kurabo Industries Ltd, Tokyo, Japan) according to the manufacturer's instructions. Mutational analyses of *COL4A5* were carried out using PCR and direct sequencing of genomic DNA of all exons and exon–intron boundaries. If a suspected splice site mutation was detected, or we failed to detect a mutation by PCR/direct sequencing, reverse-transcription (RT)-PCR and direct sequencing of abnormal mRNA products were carried out [4, 5].

All 51 specific exons of *COL4A5* were amplified by PCR, as described previously [6]. PCR-amplified products were then purified and subjected to direct sequencing using a Dye Terminator Cycle Sequencing Kit (Amersham Biosciences, Piscataway, NJ) with an automatic DNA sequencer (ABI Prism 3130; Perkin Elmer Applied Biosystems, Foster City, CA). Total RNA was extracted from blood leukocytes, and/or urinary sediments. RNA from leukocytes was isolated using a Paxgene Blood RNA Kit (Qiagen Inc., Chatsworth, CA) and was then reverse-transcribed into cDNA using random hexamers and a Superscript III Kit (Invitrogen, Carlsbad, CA). RNA from urinary sediments was isolated as described previously [7]. cDNA was amplified by nested PCR using the following *COL4A5* primer pairs: first PCR Forward: 5'-CCTCG GGGACAAAAGGG-3', and Reverse: 5'-TGGAGTCC TTTATCACCTGG-3'; 2nd PCR Forward: 5'-CAGGAC-CAAAGGAATCAGAGG-3', and Reverse: 5'-CCGTCA AGTCCAGGAGG-3'. PCR-amplified products were purified and subjected to direct sequencing.

Immunohistochemical analyses

Immunohistochemical analyses were performed using frozen sections of kidney tissue as described previously [8–10]. A mixture of fluorescein isothiocyanate-conjugated rat

monoclonal antibody for the human $\alpha 5(\text{IV})$ chain (H53) and Texas red-conjugated rat monoclonal antibody for the human $\alpha 2(\text{IV})$ chain (H25) was purchased from Shigei Medical Research Institute (Okayama, Japan). Their epitopes were EAIQP at position 675–679 of the $\alpha 2(\text{IV})$ chain, and IDVEF at position 251–255 of the $\alpha 5(\text{IV})$ chain.

Prediction of splicing factor binding sites

We used SFmap v1.8 to predict splicing factor binding sites of *COL4A5* exon 15 and the disruption of the sites with the c.876A>T substitution (<http://sfmap.technion.ac.il/index.html>).

Results

Patient history

Figure 1a shows the pedigree of this family. Individual I-1 died at the age of 30 as a result of uremia caused by ESRD after receiving dialysis for 10 years. The exact age of ESRD onset is unknown. Individual II-1 is a 49-year-old female who was diagnosed with microhematuria and proteinuria at the age of 10. She currently has hypertension, persistent microhematuria, and mild proteinuria (0.2 g/g Cr). Her estimated glomerular filtration rate (eGFR) is 60.7 ml/min/1.73 m². Individual II-2 is a 43-year-old female also diagnosed with microhematuria and proteinuria at the age of 10. She currently demonstrates persistent microhematuria and moderate proteinuria (0.5 g/g Cr) with an eGFR of 19.8 ml/min/1.73 m².

Individual III-1 is the proband. He is a 23-year-old male diagnosed with microhematuria and proteinuria at 2 years of age. He underwent a kidney biopsy at the age of 3, and was diagnosed with Alport syndrome with lamellation of the GBM and negative expression of $\alpha 5(\text{IV})$. His eGFR is 32.4 ml/min/1.73 m². Individual III-2 is a 19-year-old male diagnosed with microhematuria and proteinuria at 3 years of age. He underwent a kidney biopsy at the age of 6 and was diagnosed with Alport syndrome with negative expression of $\alpha 5(\text{IV})$. He developed ESRD when he was 18 years old. Individual III-3 is a 20-year-old male diagnosed with microhematuria and proteinuria when he was 3 years old. He had a kidney biopsy at the age of 5 and was diagnosed with Alport syndrome with lamellation of the GBM and negative expression of $\alpha 5(\text{IV})$. He developed ESRD when he was 19 years old.

Genetic analysis

Genomic sequences of *COL4A5* exon 15-containing fragments from the proband (III-1) and individual III-2 revealed a hemizygous point mutation, c.876A>T, which is the predicted synonymous mutation of p.(Gly292Gly) (Fig. 1b). No other

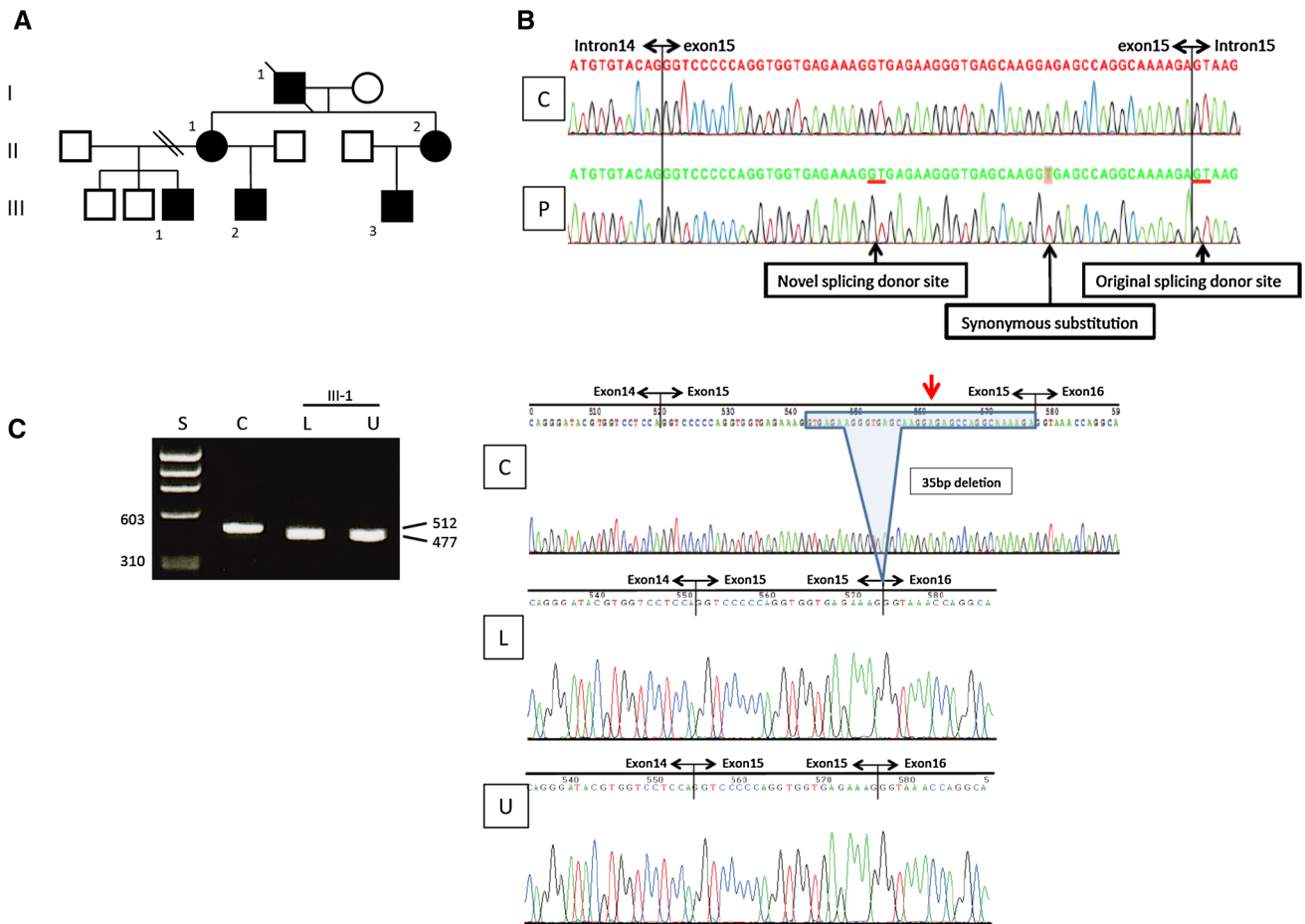


Fig. 1 **a** Family pedigree. **b** Genomic DNA sequencing of family members. Individuals III-1 and III-2 possess a hemizygous c.876A>T mutation in exon 15 of COL4A5, resulting in a predicted synonymous amino acid change of p.(Gly292Gly); individual II-1 possesses the same mutation in heterozygous form. **C** genomic DNA extracted from control, **P** genomic DNA extracted from patient III-1. **c** Sequencing of

cDNA extracted from leukocytes and urinary sediments from the proband, III-1. cDNA analysis shows deletion of the last 35 bp of exon 15. **C** cDNA extracted from control, **L** cDNA prepared from RNA extracted from leukocytes of patient III-1. **U** cDNA extracted from urine sediments of patient III-1

pathogenic mutations were detected by genomic DNA analysis. The analysis of RNA products including exon 15 by RT-PCR revealed a shorter transcript for the patient and his brother (Fig. 1c), which when sequenced revealed a 35-nt deletion of the 5' portion of exon 15. Alignment of the deleted sequence with wild-type revealed a change in the splicing donor site (Fig. 2). This change was not a natural DNA variant and was absent from 200 control DNA samples, suggesting that the A>T substitution created a splicing silencer that inhibited the authentic 5' splice site of exon 15. T is a preferred nucleotide in splicing silencers.

Prediction analyses of wild-type and mutated COL4A5 exon 15 sequences using SFmap (supplementary material) suggested that the mutation may result in the loss of binding sites for several splicing factors, including 9G8 (also known as serine/arginine-rich splicing factor 7) and Tra2alpha, which are SR proteins that may bind to exon 15 to stimulate its inclusion in COL4A5 mRNA.

Discussion

This case illustrates the pitfalls of classifying functional consequences of disease mutations into simple categories. Many mutations in coding sequences have been shown to alter RNA processing [11]. Our case illustrates that a synonymous substitution, generally classified as a silent change not related to disease, can dramatically affect pre-mRNA splicing. As shown, in the absence of RT-PCR analysis of RNA products, DNA sequencing could fail to identify the causative mutation.

XLAS has previously been reported to show a clear genotype–phenotype linkage [3, 12, 13]. Although male XLAS patients typically develop ESRD at the median age of 25 years, patients with missense and in-frame mutations tend to show milder phenotypes and develop ESRD later (median age, 32 years) than those with nonsense mutations, and deletions or insertions that change the reading frame



Fig. 2 Alignment of *COL4A5* exon 15 and its boundaries. The single nucleotide substitution activates a novel splicing donor site

(median age of developing ESRD, 20 years) [3]. Similar results were also reported by other groups [12, 13].

The affected male patients reported here developed ESRD at the ages of 18, and 19 which is in line with those XLAS male patients with truncating mutations and severe phenotypes. In agreement with this, the predicted synonymous mutation detected in this family is a splice site mutation leading to a 35 nt deletion, i.e., a truncating mutation.

In conclusion, we report a synonymous mutation in *COL4A5* which resulted in a potential alteration of splicing caused by disruption of the splice factor binding site. Our findings indicate that transcript analysis and cDNA sequencing should be conducted to correctly assess synonymous mutations and for further genotype–phenotype correlation analysis. This is the first report of a synonymous *COL4A5* substitution being responsible for XLAS which is supported by transcript analysis.

Acknowledgments This study was supported by a grant from the Ministry of Education, Culture, Sports, Science and Technology of Japan (Subject ID: 15K09691 to Kandai Nozu) and a Health Labour Sciences Research Grant for Research on Measures for Intractable Diseases (H26-nanchitou-ippan-036 to Kazumoto Iijima).

Compliance with ethical standards

Conflict of interest Kandai Nozu has received lecture fees from Novartis Pharma K.K. and Taisho Pharm. Co. Kazumoto Iijima has received grants from Pfizer Japan, Inc., Daiichi Sankyo Co., Ltd., Japan Blood Product Organization, Miyarisan Pharmaceutical Co., Ltd., AbbVie LLC, CSL Behring, JCR Pharmaceuticals Co., Ltd., and Teijin Pharma Ltd.; lecture fees from MSD, ALEXION Pharmaceuticals, AstraZeneca K.K., Meiji Seika Pharma Co., Ltd., Novartis Pharma K.K., Zenyaku Kogyo Co., Ltd., Chugai Pharmaceutical Co., Ltd., Astellas Pharma Inc., Daiichi Sankyo, Co., Ltd., Springer Japan, and Asahi Kasei Pharma Corp; and consulting fees from Chugai Pharmaceutical Co., Ltd., Astellas Pharma Inc., and Takeda Pharmaceutical Company Ltd.

References

- Kashtan CE. Alport syndrome and thin glomerular basement membrane disease. *J Am Soc Nephrol.* 1998;9(9):1736–50.
- Savage J, Gregory M, Gross O, Kashtan C, Ding J, Flinter F. Expert guidelines for the management of Alport syndrome and thin basement membrane nephropathy. *J Am Soc Nephrol.* 2013;24(3):364–75.
- Jais JP, Knebelmann B, Giatras I, De Marchi M, Rizzoni G, Renieri A, Weber M, Gross O, Netzer KO, Flinter F, et al. X-linked Alport syndrome: natural history in 195 families and genotype-phenotype correlations in males. *J Am Soc Nephrol.* 2000;11(4):649–57.
- Nozu K, Iijima K, Ohtsuka Y, Fu XJ, Kaito H, Nakanishi K, Vorechovsky I. Alport syndrome caused by a *COL4A5* deletion and exonization of an adjacent *AluY*. *Mol Genet Genom Med.* 2014;2(5):451–3.
- Nozu K, Vorechovsky I, Kaito H, Fu XJ, Nakanishi K, Hashimura Y, Hashimoto F, Kamei K, Ito S, Kaku Y, et al. X-linked Alport syndrome caused by splicing mutations in *COL4A5*. *Clin J Am Soc Nephrol.* 2014;9(11):1958–64.
- Hashimura Y, Nozu K, Kaito H, Nakanishi K, Fu XJ, Ohtsubo H, Hashimoto F, Oka M, Ninchoji T, Ishimori S, et al. Milder clinical aspects of X-linked Alport syndrome in men positive for the collagen IV alpha5 chain. *Kidney Int.* 2014;85(5):1208–13.
- Kaito H, Nozu K, Fu XJ, Kamioka I, Fujita T, Kanda K, Krol RP, Suminaga R, Ishida A, Iijima K, et al. Detection of a transcript abnormality in mRNA of the *SLC12A3* gene extracted from urinary sediment cells of a patient with Gitelman's syndrome. *Pediatr Res.* 2007;61(4):502–5.
- Naito I, Kawai S, Nomura S, Sado Y, Osawa G. Relationship between *COL4A5* gene mutation and distribution of type IV collagen in male X-linked Alport syndrome. *Japanese Alport Network. Kidney Int.* 1996;50(1):304–11.
- Nakanishi K, Iijima K, Kuroda N, Inoue Y, Sado Y, Nakamura H, Yoshikawa N. Comparison of alpha5(IV) collagen chain expression in skin with disease severity in women with X-linked Alport syndrome. *J Am Soc Nephrol.* 1998;9(8):1433–40.
- Sado Y, Kagawa M, Kishiro Y, Sugihara K, Naito I, Seyer JM, Sugimoto M, Oohashi T, Ninomiya Y. Establishment by the rat lymph node method of epitope-defined monoclonal antibodies recognizing the six different alpha chains of human type IV collagen. *Histochem Cell Biol.* 1995;104(4):267–75.
- Cartegni L, Chew SL, Krainer AR. Listening to silence and understanding nonsense: exonic mutations that affect splicing. *Nat Rev Genet.* 2002;3(4):285–98.
- Bekheirnia MR, Reed B, Gregory MC, McFann K, Shamshirsaz AA, Masoumi A, Schrier RW. Genotype-phenotype correlation in X-linked Alport syndrome. *J Am Soc Nephrol.* 2010;21(5):876–83.
- Gross O, Netzer KO, Lambrecht R, Seibold S, Weber M. Meta-analysis of genotype-phenotype correlation in X-linked Alport syndrome: impact on clinical counselling. *Nephrol Dial Transpl.* 2002;17(7):1218–27.

Brief Communication

Irreversible severe kidney injury and anuria in a 3-month-old girl with atypical haemolytic uraemic syndrome under administration of eculizumabYUSUKE OKUDA,^{1,2} KENJI ISHIKURA,^{1,3} CHIKAKO TERANO,¹ RYOKO HARADA,¹ RIKU HAMADA,¹ HIROSHI HATAYA,¹ KENTARO OGATA⁴ and MASATAKA HONDA¹

¹Department of Nephrology, Tokyo Metropolitan Children's Medical Center, and ³Department of Nephrology and Rheumatology, National Center for Child Health and Development, and ⁴Division of Pathology, Federation of National Public Service Personnel Mutual Aid Associations, Tachikawa Hospital, Tokyo, and ²Department of Pediatrics, Shiga University of Medical Science, Otsu, Shiga, Japan

KEY WORDS:

anuria, atypical haemolytic uraemic syndrome, histopathology, infant, infusion reaction.

Correspondence:

Dr Kenji Ishikura, Department of Nephrology and Rheumatology, National Center for Child Health and Development, 2-10-1 Okura, Setagaya-ku, Tokyo 157-8535, Japan. Email: kenzo@ii.e-mansion.com

Accepted for publication 31 July 2015.

doi:10.1111/nep.12582

ABSTRACT:

Histopathological findings can play an important role in the management of atypical haemolytic uraemic syndrome (aHUS). We report a case of aHUS that did not recover from anuria, despite the administration of eculizumab, with impressive histopathological findings. A 3-month-old girl was admitted because of poor feeding, vomiting, and diarrhoea without haemorrhage. She had anuria and severe hypertension, and laboratory results showed haemolytic anaemia with schizocytes, thrombocytopenia, and renal impairment. Although no mutations in the complement system or diacylglycerol kinase epsilon were detected, she was diagnosed with aHUS owing to the clinical course and by the exclusion of *Escherichia coli* infection and thrombotic thrombocytopenic purpura. Plasma exchange was performed once at day 2 and eculizumab therapy was started from day 18, with a severe infusion reaction at the first administration. After the initiation of eculizumab, although the serum lactate dehydrogenase level improved gradually, she did not recover from anuria. Pathological findings of the kidney biopsy at day 37 included diffuse arteriolar and arterial luminal stenosis with remarkable thickness and sclerotic changes of the media and intima, which are suggestive of aHUS. In addition, most glomeruli had global sclerosis and were collapsed, and 80% of the tubulointerstitial compartment showed atrophic changes with infiltration of inflammatory cells. The present case is possibly a kidney-specific fulminant type of aHUS. Although showing efficacy against thrombotic microangiopathy, eculizumab did not improve kidney function. The pathological findings reflected the severe and irreversible kidney injury.

Atypical haemolytic uraemic syndrome (aHUS) is caused by uncontrolled activation of the complement system. Affected patients frequently develop end-stage kidney disease, which may be fatal.^{1,2} Eculizumab is a monoclonal antibody that binds to C5 to prevent the formation of C5a and the membrane attack complex.³ The outstanding efficacy and safety of eculizumab in the treatment of aHUS have been reported recently.⁴

Accurate diagnosis of aHUS is important in terms of not only the induction but also the maintenance of eculizumab therapy. Diagnosis of aHUS is a diagnosis of exclusion, and

genetic testing of the complement system required to increase the accuracy of the diagnosis.⁵ In patients negative for known gene mutations, meticulous ruling out of other thrombotic microangiopathies, especially Shiga toxin-producing *Escherichia coli*-associated HUS (STEC-HUS) and thrombotic thrombocytopenic purpura (TTP),⁶ is important for the differential diagnosis. However, an accurate diagnosis is often difficult, particularly in STEC-HUS.⁷ Therefore, histopathological findings are a key tool in the diagnosis of aHUS. Although the clinicopathological findings characteristic of aHUS have been previously identified,⁸ there are few

reports in the literature on the histopathological findings of aHUS.

Here, we report a case of an infant with aHUS who did not recover from anuria despite the administration of eculizumab. Histopathological findings showed marked arteriolar and arterial changes characteristic of aHUS, which played an important role in making the diagnosis of aHUS without known gene mutations.

CASE REPORT

The patient was a 3-month-old Japanese girl. She was admitted to our hospital with poor feeding in addition to a 1-week history of vomiting and diarrhoea without haemorrhage. She was in a state of anuria and had hypertension of 119/59 mm Hg, even with 1 µg/kg per min of nifedipine on admission. She was born by a normal vaginal delivery at a gestation of 38 weeks with a birth weight of 2480 g, and had no significant past history and no family history of hypertension, kidney disease, or HUS. Laboratory results indicated anaemia (haemoglobin 5.7 g/dL), thrombocytopenia (platelets $34 \times 10^3/\mu\text{L}$), and kidney dysfunction (creatinine 4.63 mg/dL). Serum lactate dehydrogenase (LDH) levels were elevated (780 U/L), C3 was decreased (28 mg/dL), C4 was normal (17 mg/dL), and schizocytes were detected.

Stool culture without the use of antibiotics and anti-lipopolysaccharide antibodies against the most frequent Shiga toxin-producing *Escherichia coli* (O157, O26, O111, O103, O145, O121, O165) were negative (performed by the Department of Bacteriology, National Institute of Infectious Diseases, Tokyo, Japan). A disintegrin and metalloprotease with thrombospondin type 1 motif 13 (ADAMTS13) activity was normal and the factor H haemolytic assay was negative (ADAMTS13 activity and factor H haemolytic assays were performed by the Department of Blood Transfusion Medicine, Nara Medical University, Nara, Japan). No known gene mutations in the complement system, including factor H, factor I, factor B, membrane cofactor protein, thrombomodulin, and C3, were detected (performed by the Department of Molecular Pathogenesis, National Cerebral and Cardiovascular Center, Osaka, Japan). Direct sequencing of the diacylglycerol kinase epsilon (DGKE) gene was also performed (at the Tokyo Metropolitan Children's Medical Center), and no mutations were detected.

Figure 1 shows the clinical course. Continuous haemodiafiltration (CHDF) was adopted for anuria and hypertension from the day of admission. CHDF was soon converted to continuous flow peritoneal dialysis owing to pineal haemorrhage on day 3. Plasma exchange, replacement of one plasma volume with fresh frozen plasma, was started because of the possibility of aHUS or TTP at day 2, but performed only once because of pineal haemorrhage. Although schizocytes had disappeared and the serum LDH level had decreased after plasma exchange, schizocytes reappeared and the LDH level increased again. Because the

diagnoses of STEC-HUS and TTP were previously excluded, we administered eculizumab owing to the diagnosis of aHUS at day 18. Eculizumab was not approved for aHUS in Japan at that time, so the administration of eculizumab was reviewed and approved by the ethics committee of Tokyo Metropolitan Children's Medical Center (ID: H25-13). Written informed consent from the parents was also obtained. Unfortunately, anaphylactoid reactions that required adrenaline administration, including systemic rash, dyspnoea, and blood pressure reduction, developed after eculizumab administration. Therefore, we halted the initial administration at half of the intended dose. We concluded that the adverse reactions were severe infusion reactions, which again developed as a rash at the fourth administration, owing to it being the first administration of eculizumab and the patient being negative for anti-eculizumab antibodies (performed by Alexion Pharmaceuticals). Although serum LDH level decreased after eculizumab administration, anuria persisted. We performed a kidney biopsy at day 37 and chronic peritoneal dialysis was adopted reflecting the severe pathological findings.

Figure 2 shows the histopathological findings of the kidney biopsy from day 37. A wedge biopsy consisting of cortex tissue was taken that included 15 glomeruli, almost all of which showed global sclerosis or collapse. Endothelial swelling, fibrillary appearance of mesangial matrix, and double contour of the glomerular basement membrane were detected in some glomeruli. Eighty percent of the tubulointerstitial compartment showed fibroedematous widening with infiltration of mononuclear leukocytes. Diffuse arteriolar and arterial luminal stenosis with thickening of the intima was evident. A small number of mononuclear cells infiltrated into the intima of arteries.

DISCUSSION

The present case has clinical significance for the following reasons: first, it has pathological findings that are characteristic of aHUS and so is useful for demonstrating the diagnosis of aHUS; and second, its clinical course, as the patient did not recover from anuria despite the administration of eculizumab.

In the present case, the histopathological findings, showing marked intimal thickening of arteries and arterioles resulting in luminal stenosis, are characteristic of aHUS and significantly contributed to the diagnosis. For the appropriate application of eculizumab, to make a definitive diagnosis of aHUS by detecting complement gene mutations or antibodies to complement factors is ideal, especially in terms of maintenance therapy that may require lifelong administration. However, because gene mutations in the complement system can only be detected in 50–60% of aHUS patients,⁹ other information that helps us to diagnose aHUS more accurately is required for the patients without gene mutations. Because arteriolar and arterial changes like those in the present case

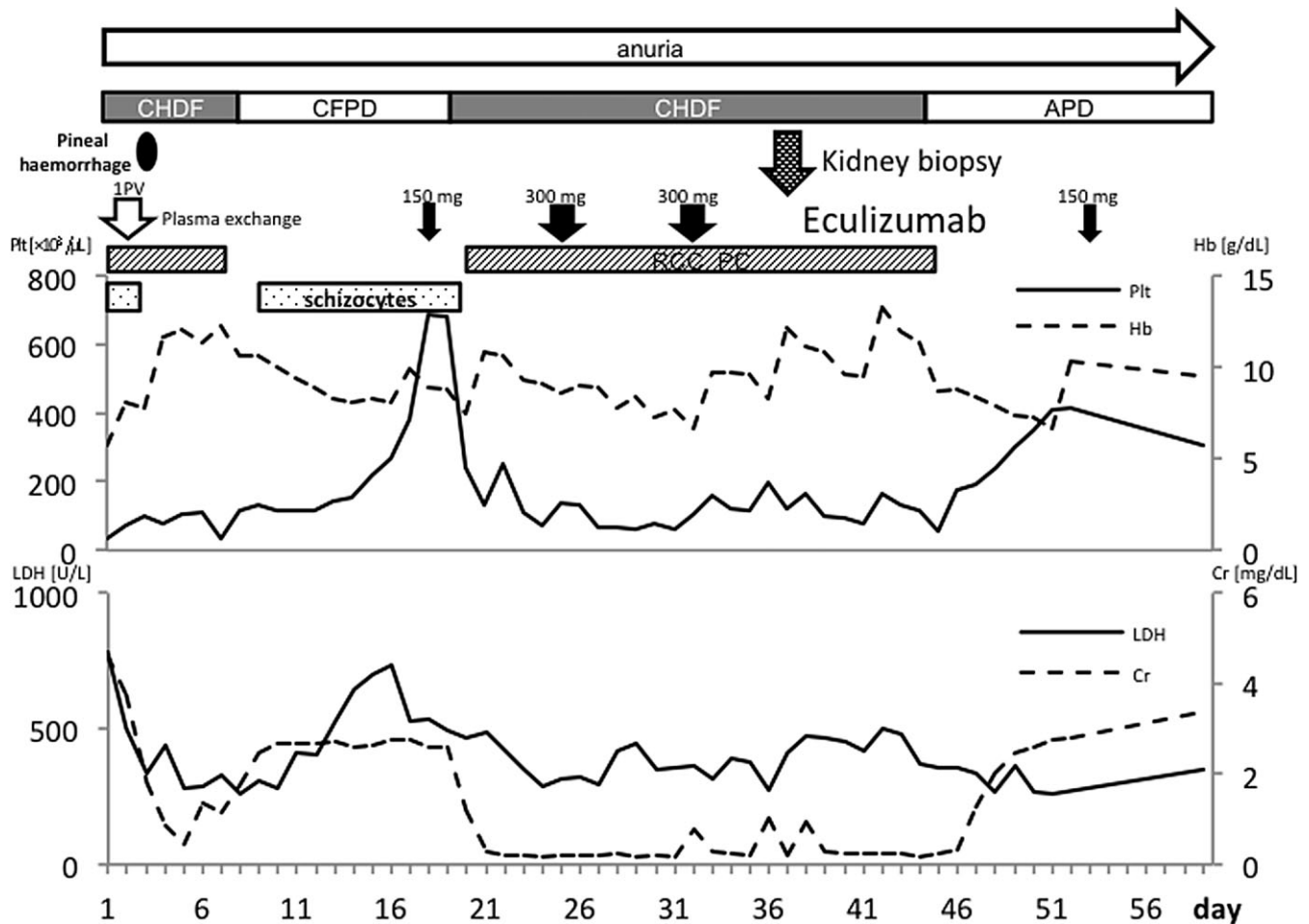


Fig. 1 Clinical course. Continuous haemodiafiltration (CHDF) was adopted for anuria and hypertension from the day of admission. CHDF was soon converted to continuous flow peritoneal dialysis (CFPD) owing to pineal haemorrhage on day 3. PE was performed at day 2 with 1 PV. Although schizocytes had disappeared and serum lactate dehydrogenase (LDH) level had decreased after PE, schizocytes reappeared and the LDH level increased again. Eculizumab was administered from day 18. Although the serum LDH level decreased after eculizumab administration, anuria persisted throughout the course of disease. Kidney biopsy was performed at day 37 and chronic peritoneal dialysis was adopted reflecting the severe pathological findings. The first and fourth administration of eculizumab was halted at half the intended dose owing to infusion reactions. (—) Plt, (---) Hb. (—) LDH, (---) Cr. APD, automated peritoneal dialysis; Cr, creatinine; Hb, haemoglobin; LDH, lactate dehydrogenase; PC, platelet concentrates; Plt, platelets; PV, plasma volume; RCC, red cell concentrates.

are known to be more common in patients with aHUS,⁸ histopathological findings can be useful in clinical practice. However, histopathological findings are not always used for the diagnosis of aHUS because of the lack of a sufficient number of reports on the histopathology. The present case adds information to the histopathological findings of aHUS and shows their significance in the diagnosis of aHUS. However, the diagnosis of the present case requires caution as no known gene mutations were detected, i.e. a definitive diagnosis has not been made. It would have been ideal to detect genetic mutations in the present case, and then to clarify the relationship between gene mutations and worse prognostic phenotype or severe pathological findings.

Histopathological findings provided clues not only to the diagnosis but also in the prediction of a prognosis. The severity of histopathological involvement, especially the degree of

vascular damage, may be a predictor of the prognosis.^{8,10} In the present case, renal blood flow obstruction caused by diffuse arterial and arteriolar luminal stenosis led to irreversible changes in kidney tissue. Diffuse tubular interstitial change and global sclerosis indicated the degree of blood flow obstruction and prognosis. In fact, the patient did not recover from anuria despite the administration of eculizumab.

The reasons for irreversible anuria despite the administration of eculizumab were unclear. Although the efficacy of eculizumab has been reported in many situations and a recent case series reported that aHUS patients with anuria all recovered from anuria after eculizumab administration,¹¹ no aHUS cases of irreversible anuria despite administration of eculizumab in the acute phase have been reported. The main reason for this may be that aHUS phenotype could be

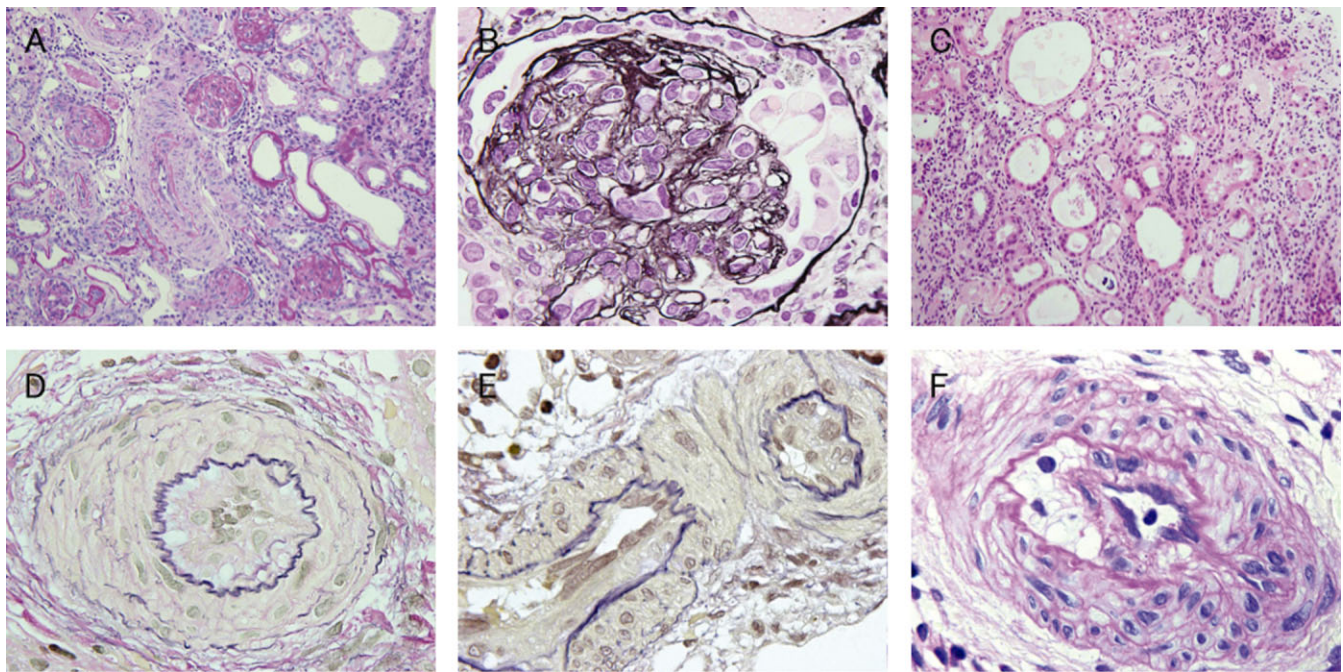


Fig. 2 Histopathological findings of the kidney biopsy taken at day 37. (A) Almost all glomeruli had evidence of global sclerosis or were collapsed (periodic acid Schiff stain [PAS]; $\times 100$). (B) Endothelial swelling was conspicuous and glomerular basement membranes were focally duplicated (periodic acid methenamine silver stain [PAM]; $\times 1000$). (C) Interstitial fibroedematous change and tubular atrophy were marked (haematoxylin and eosin stain [H&E]; $\times 200$). (D, E) Arterial and arteriolar lumina were stenosed or obstructed with intimal thickening (Elastica van Gieson stain [EVG]; $\times 1000$). (F) Mononuclear cells infiltrated into the intima of arteries (PAS; $\times 1000$).

fulminant, with manifestation limited to kidney. Although showing efficacy against thrombotic microangiopathy with improvement of serum LDH levels, eculizumab could not recover kidney function. Histopathological findings indicated the degree of kidney injury and the severity of aHUS. Other possible reasons for the irreversible anuria are discontinuation of plasma exchange, and delayed or insufficient administration of eculizumab (150, 300, 300 and 150 mg at days 18, 25, 32 and 53 respectively), or other factors resulting in kidney injury such as the use of multiple drugs in intensive care or the long duration of CHDF. Notably, 18 days passed before the first eculizumab administration and this delay may be the cause of the ineffective response. As Japanese health insurance did not cover eculizumab for aHUS at that time, we could not administer eculizumab immediately upon presentation.

In conclusion, histopathological findings in the kidney play an important role in the diagnosis of aHUS, particularly in patients without identified gene mutations. Furthermore, although an effective drug, eculizumab administration is not always successful in patients with aHUS. The present case is thus possibly a kidney-specific fulminant type of aHUS, as determined by clinical course and pathological findings.

ACKNOWLEDGEMENTS

The authors thank Dr. Sunao Iyoda, Department of Bacteriology, National Institute of Infectious Diseases, for testing for

STEC infection; Drs. Yoshihiro Fujimura and Yoko Yoshida, Department of Blood Transfusion Medicine, Nara Medical University, and Toshiyuki Miyata, Department of Molecular Pathogenesis, National Cerebral and Cardiovascular Center, for testing ADAMTS13 activity, factor H haemolytic assay and complement gene mutations; and Dr. Hiroshi Yoshihashi, Division of Medical Genetics, Tokyo Metropolitan Children's Medical Center, for testing DGKE gene mutations.

Hiroshi Hataya has received lecture fees from Alexion Pharmaceuticals. Riku Hamada has received lecture fees from Alexion Pharmaceuticals. The other authors have no conflicts of interest to declare.

The information of the present case was submitted to the Japanese national survey of eculizumab for aHUS.

REFERENCES

1. Noris M, Remuzzi G. Atypical hemolytic-uremic syndrome. *N. Engl. J. Med.* 2009; **361**: 1676–87.
2. Waters AM, Licht C. aHUS caused by complement dysregulation: New therapies on the horizon. *Pediatr. Nephrol.* 2011; **26**: 41–57.
3. Brodsky RA, Young NS, Antonioli E *et al.* Multicenter phase 3 study of the complement inhibitor eculizumab for the treatment of patients with paroxysmal nocturnal hemoglobinuria. *Blood* 2008; **111**: 1840–47.
4. Legendre CM, Licht C, Muus P *et al.* Terminal complement inhibitor eculizumab in atypical hemolytic-uremic syndrome. *N. Engl. J. Med.* 2013; **368**: 2169–81.

5. Loirat C, Fremeaux-Bacchi V. Atypical hemolytic uremic syndrome. *Orphanet J. Rare Dis.* 2011; **6**: 60.
6. Kavanagh D, Goodship TH, Richards A. Atypical hemolytic uremic syndrome. *Semin. Nephrol.* 2013; **33**: 508–30.
7. Mellmann A, Bielaszewska M, Zimmerhackl LB *et al.* Enterohemorrhagic *Escherichia coli* in human infection: In vivo evolution of a bacterial pathogen. *Clin. Infect. Dis.* 2005; **41**: 785–92.
8. Taylor CM, Chua C, Howie AJ, Risdon RA. Clinico-pathological findings in diarrhoea-negative haemolytic uraemic syndrome. *Pediatr. Nephrol.* 2004; **19**: 419–25.
9. Sellier-Leclerc AL, Fremeaux-Bacchi V, Dragon-Durey MA *et al.* Differential impact of complement mutations on clinical characteristics in atypical hemolytic uremic syndrome. *J. Am. Soc. Nephrol.* 2007; **18**: 2392–400.
10. Mehrazma M, Hooman N, Otukesh H. Prognostic value of renal pathological findings in children with atypical hemolytic uremic syndrome. *Iran. J. Kidney Dis.* 2011; **5**: 380–85.
11. Baskin E, Gulleroglu K, Kantar A, Bayrakci U, Ozkaya O. Success of eculizumab in the treatment of atypical hemolytic uremic syndrome. *Pediatr. Nephrol.* 2015; **30**: 783–9.

New-onset diabetes after renal transplantation in a patient with a novel *HNF1B* mutation

Kanda S, Morisada N, Kaneko N, Yabuuchi T, Nawashiro Y, Tada N, Nishiyama K, Miyai T, Sugawara N, Ishizuka K, Chikamoto H, Akioka Y, Iijima K, Hattori M. (2016) New-onset diabetes after renal transplantation in a patient with a novel *HNF1B* mutation. *Pediatr Transplant*, 20: 467–471. DOI: 10.1111/ptr.12690.

Abstract: CAKUT are the most frequent causes of ESRD in children. Mutations in the gene encoding *HNF1B*, a transcription factor involved in organ development and maintenance, cause a multisystem disorder that includes CAKUT, diabetes, and liver dysfunction. Here, we describe the case of a patient with renal hypodysplasia who developed NODAT presenting with liver dysfunction. The NODAT was initially thought to be steroid and FK related. However, based on the patient's clinical features, including renal hypodysplasia and recurrent elevations of transaminase, screening for an *HNF1B* mutation was performed. Direct sequencing identified a novel splicing mutation of *HNF1B*, designated c.344 + 2T>C. Because CAKUT is the leading cause of ESRD in children and *HNF1B* mutations can cause both renal hypodysplasia and diabetes, *HNF1B* mutations may account for a portion of the cases of NODAT in pediatric patients who have undergone kidney transplantation. NODAT is a serious and major complication of solid organ transplantation and is associated with reduced graft survival. Therefore, for the appropriate management of kidney transplantation, screening for *HNF1B* mutations should be considered in pediatric patients with transplants caused by CAKUT who develop NODAT and show extra-renal symptoms.

Shoichiro Kanda¹, Naoya Morisada², Naoto Kaneko¹, Tomoo Yabuuchi¹, Yuri Nawashiro¹, Norimasa Tada¹, Kei Nishiyama¹, Takayuki Miyai¹, Noriko Sugawara¹, Kiyonobu Ishizuka¹, Hiroko Chikamoto¹, Yuko Akioka¹, Kazumoto Iijima² and Motoshi Hattori¹

¹Department of Pediatric Nephrology, Tokyo Women's Medical University School of Medicine, Tokyo, Japan, ²Department of Pediatrics, Kobe University Graduate School of Medicine, Kobe, Japan

Key words: pediatric kidney transplantation – complications – NODAT – *HNF1B*

Motoshi Hattori, MD, PhD, Department of Pediatric Nephrology, Tokyo Women's Medical University School of Medicine, 8-1 Kawadacho, Shinjuku-ku, Tokyo 162-8666, Japan
Tel.: +81 3 3353 8111
Fax: +81 3 3359 4877
E-mail: hattori@kc.twmu.ac.jp

Accepted for publication 19 January 2016

NODAT, defined as newly diagnosed diabetes in a patient who has undergone organ transplantation, is a serious metabolic complication. NODAT is associated with a significant reduction of graft survival and an increase in cardiovascular morbidity. Thus, attenuation of the risk factors for NODAT based on an understanding of its etiology is necessary for the achievement of better graft function and survival (1). Recent research has identified several risk factors

involved in the pathogenesis of NODAT, which can also be divided into two categories: modifiable and non-modifiable (1). Notably, genetic susceptibility is a non-modifiable risk factor.

HNF1B is a homeodomain-containing transcriptional factor encoded by a gene located on chromosome 17q12. *HNF1B* functions either as a homodimer or as a heterodimer with *HNF1A* to regulate gene expression. Mutations in *HNF1B* were initially described in MODY5 (2). Today, more than 100 *HNF1B* mutations have been identified, including missense, nonsense, frame-shift, and splicing mutations (3). *HNF1B* is highly expressed in the kidney, and *HNF1B* mutations cause several types of CAKUT, including cystic disease, hypodysplasia, horseshoe kidney, and lateral renal agenesis (4). The ESCAPE study showed that *HNF1B* is mutated in 8.1% cases of renal hypodysplasia (5).

Abbreviations: ALT, alanine aminotransferase; AST, aspartate aminotransferase; CAKUT, congenital anomalies of the kidney and urinary tract; ESRD, end-stage renal disease; FK, tacrolimus; *HNF1B*, hepatocyte nuclear factor-1 β ; MMF, mycophenolate mofetil; MODY5, maturity-onset diabetes of the young type 5; NODAT, new-onset diabetes after transplantation; PD, peritoneal dialysis; RCAD, renal cyst and diabetes; RTx, renal transplantation.

Another pediatric cohort showed that *HNF1B* anomalies were detected in one-third of patients with renal cysts, hyperechogenicity, hypoplasia, or single kidney (4). The overall detection rate of *HNF1B* mutations is between 5% and 31% (4–7). Patients who show both a renal anomaly and diabetes mellitus are described as having RCAD syndrome.

CAKUT is the leading cause of ESRD in children (8, 9). Despite recognition of a role for *HNF1B* mutations in the development of both CAKUT (5) and diabetes (2), whether aberrant *HNF1B* expression also results in NODAT is unclear. In this report, we describe the case of a pediatric patient with renal hypodysplasia and a novel *HNF1B* mutation who developed NODAT and liver dysfunction. Our discussion includes a summary of the relevant literature. This case demonstrates the need for appropriate pre- and post-transplantation management of pediatric CAKUT patients scheduled for kidney transplantation.

Case report

The female patient was the second child of non-consanguineous Japanese parents. She was born in 2000 and had a weight at term birth of 3095 g. Her Apgar scores were eight at one min and nine at five min. The mother's pregnancy was uneventful. There was no family history of kidney disease or diabetes mellitus. At four days of age, the patient was admitted to a neonatal intensive care unit because of persistent vomiting. Her blood urea nitrogen was 115 mg/dL, and her serum creatinine was 4.1 mg/dL, indicative of chronic renal failure. Renal ultrasonography confirmed bilateral hypodysplastic kidneys. Renal function gradually worsened such that at three yr of age she received a living-related preemptive kidney transplant from her mother. The patient's immunosuppressive regimen comprised oral methylprednisolone, FK, and MMF. At four yr of age, a steroid pulse for acute rejection resulted in the development of diabetes mellitus; she was diagnosed with NODAT, and insulin therapy was started. Antibodies (anti-glutamic-acid-decarboxylase and anti-islet-antigen 2) were absent. The development of NODAT was attributed to methylprednisolone and FK use. Her post-transplant renal function continued to worsen; seven yr later, she started chronic PD. She continued to receive insulin treatment.

At 13 yr of age, she was seen in the emergency department of our hospital because of fever and acute right flank pain. Jaundice was not observed. Laboratory findings showed elevated

levels of transaminase (Table 1). Neither infection (hepatitis A virus, hepatitis B virus, hepatitis C virus, Epstein–Barr virus, cytomegalovirus, influenza virus, and mycoplasma pneumonia) nor autoantibodies (anti-liver-kidney microsomal type 1 and anti-M2 mitochondrial) were detected. Her serum levels of copper and ceruloplasmin were 86 µg/dL (normal range 68–128) and 21 mg/dL (21–37), respectively. Computed tomography showed a malformed bile duct, winding, and with partition walls (Fig. 1), but no abnormalities of the liver and spleen. Her clinical condition and laboratory findings improved promptly, and four days later, she had recovered completely with supportive therapies alone. Routine physical examinations revealed recurrent elevation of her liver enzymes approximately twice per year. AST and ALT were twofold to 20-fold higher than the upper limit of normal.

Given the patient's young age, hypodysplastic kidneys, NODAT, and liver dysfunction, screening for an *HNF1B* gene mutation was performed. After the provision of informed consent by her parents, a leukocyte genomic DNA sample obtained from the patient was amplified for the

Table 1. Laboratory results during hospitalization

Characteristics	Admission	Day4	Day8
AST, U/L (13–33)	805	74	33
ALT, U/L (6–30)	347	118	41
LDH, U/L (119–229)	717	304	221
T-Bil, mg/dL (0.2–1.2)	0.4	0.5	0.5
ALP, U/L (115–359)	2002	1476	1255
G-GTP, U/L (6–46)	87	77	N/A
ChE, U/L (175–420)	553	481	602

LDH, lactate dehydrogenase; T-Bil, total bilirubin; ALP, alkaline phosphatase; G-GTP, gamma-glutamyltransferase; ChE, cholinesterase.

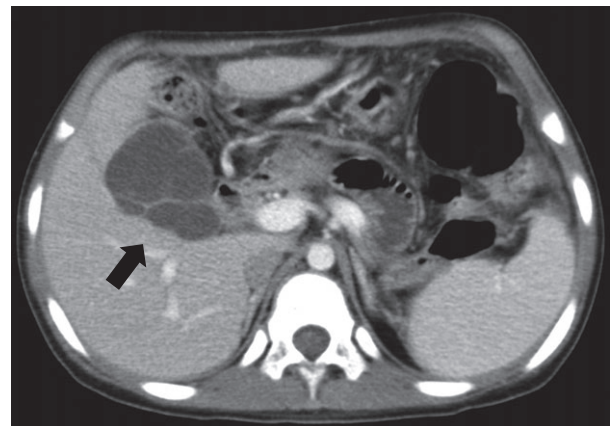


Fig. 1. The winding bile duct with partition walls can be seen on computed tomography imaging (arrow).

HNF1B coding regions of exons 1–9 and their splice sites. The PCR products were subjected to direct sequencing using previously described primer sequences and PCR conditions (6). Direct sequencing identified a novel heterozygous mutation in the *HNF1B* gene at the conserved splice-donor site of intron 1. The mutation, designated c.344 + 2T>C (Fig. 2), was predicted to lead to a splicing defect with either exon skipping or

intron retention. None of the other members of the family had the same mutation. The genetic analyses were approved by the Central Ethics Board of Tokyo Women's Medical University and Kobe University.

Discussion

This report presents the case of a patient with NODAT caused by an *HNF1B* mutation. She had disorders in multiple organs, including hypodysplastic kidneys, NODAT, elevated transaminase levels, and malformation of the bile duct. For a long period of time, it was presumed that her NODAT was caused by the immunosuppressants administered following RTx. However, the recurrent elevation of transaminase prompted screening for an *HNF1B* mutation. Detection of a novel mutation confirmed the underlying genetic condition of the patient.

This is the fifth reported case of NODAT attributed to a mutation of *HNF1B* (Table 2) (10–12). Of these patients, three were female and two were male. Regarding the use of a calcineurin inhibitor, three patients had been taking FK and two patients cyclosporine A. NODAT developed within one month in three patients. In the present case, steroid pulse therapy triggered NODAT one yr post-transplantation. Because

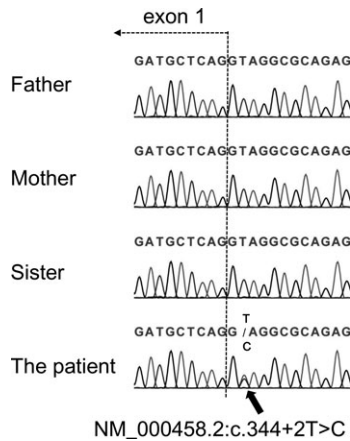


Fig. 2. Mutation analysis using DNA samples obtained from the patient and family members. The patient's *de novo* heterozygous c.344 + 2T>C *HNF1B* mutation is highlighted in yellow and indicated by the red arrow.

Table 2. Summary of all cases of new-onset diabetes after renal transplantation characterized by *HNF1B* mutations

Reference	Sex	Mutation	Kidney (diagnosis age)	ESRD (age)	RTx (age)	Immunosuppressant	Transplant function	Onset of diabetes treatment	Other symptoms
10	Male	H69fsdelAC	Cystic Kidneys (antenatal)	14 yr	CD-RTx, 14 yr, preemptive	AZA, CyA, PSL	Gradually worsening, HD (8 months after RTx)	Immediately after RTx, insulin	N/A
11	Male	c810-1045del A271SfsX10	rt renal agenesis (1 yr)	30 yr	LR-RTx, 37 yr	MMF, FK, PSL	Excellent renal function	One month after RTx, insulin	Gout (24 yr) Hepatitis C (30 yr) elevation of liver enzyme (after RTx)
11	Female	c244G>A D82N	Dysplastic cystic kidneys (N/A)	N/A	RTx, 41 yr	MMF, FK, PSL	N/A	5 months after RTx, insulin	Bicornuate and bicervical uterus, longitudinal vaginal partition Hepatitis C Elevation of liver enzyme (after RTx)
12	Female	c443C>G S148W	Hypodysplasia (antenatal)	9 yr	LR-RTx, 9 yr	BAS, MMF, CyA, PSL	N/A	21 days after RTx, insulin	Premature puberty Hypotrophy of the pancreatic head and atrophy of the body
Present study	Female	c344 + 2T>C	Hypodysplasia (antenatal)	3 yr	LR-RTx, 3 yr, preemptive	MMF, FK, PSL	Gradually worsening, PD (7 yr after RTx)	1 yr after RTx, insulin	Elevation of liver enzyme (after RTx) Bile duct anomaly

N/A, not available; CD, cadaveric grafts; LR, living donor; HD, hemodialysis; AZA, azathioprine; CyA, cyclosporine A; PSL, prednisolone.

HNF1B is expressed in several organs, including the pancreas, kidney, liver, intestines, and genital tract, mutations in the *HNF1B* gene result not only in MODY5 and RCAD syndrome but also in a multisystem disorder (3). The *HNF1B* score for selecting patients for *HNF1B* screening was proposed based on the combination of clinical characteristics, including family history and symptoms of kidney and urinary tract, pancreas, genital tract, and liver (13). Moreover, the spectrum of HNF1B-associated diseases is expanding, and symptoms besides renal failure and diabetes have often been confirmed in patients with NODAT associated with *HNF1B* mutation. Transaminase levels were elevated in three of the five patients, including ours. The development of liver dysfunction associated with *HNF1B* mutations is well documented and has been identified in 15.2% of carriers (14). Genital organ anomalies consisted of bicornuate and bicervical uterus with vaginal partition in one patient and premature puberty in another. *HNF1B* mutations also cause familial juvenile hyperuricemic nephropathy (3), with gout developing in one male patient. Hepatitis C virus infection, a modifiable risk factor (1) detected in two of the five patients, is thought to induce the development of NODAT by acting in concert with the *HNF1B* mutation. Furthermore, our patient had a unique phenotype of the bile duct. In mice, inactivation of HNF1B in bile duct cells causes abnormalities of the gallbladder, an irregularly shaped and dilated cystic duct, and liver dysfunction (15). In humans, ours is the first case to include a morphological anomaly of the gallbladder.

The reported incidence of NODAT varies between 3% and 20% in child and adolescent transplant recipients. This is because of differences in diagnostic criteria, length of follow-up, and type of immunosuppression (16). The diagnosis of NODAT should be made according to the American Diabetes Association criteria, which are based on the results of a random plasma glucose, a fasting plasma glucose, and oral glucose tolerance test. Although an oral glucose tolerance test had not been performed in our case, in international consensus guidelines (17) on NODAT, pretransplantation risk factors should be considered in tailoring immunosuppressive therapy, thereby reducing the individual risk of developing diabetes. Many patient-related factors are known to contribute to NODAT, including age, sex, family history of diabetes, obesity, hepatitis C infection, and the type of immunosuppressant regimen used (1). Genetic susceptibility is a non-modifiable risk factor for NODAT development, and more than 40 SNPs

associated with the development of NODAT have been identified thus far. SNPs in *HNF1A* and *HNF4A* result in MODY3 and MODY1, respectively, both of which are related to NODAT (18, 19). Like HNF1A and HNF4A, HNF1B is involved in pancreatic β -cell function. Moreover, *HNF1B* conditional inactivation in the pancreas leads to a pancreas hypoplasia in mice (20), and *HNF1B* mutations are sometimes associated with pancreas hypoplasia in human (21). Because *HNF1B* mutations can cause both β -cell dysfunction and pancreas dysmorphogenesis, the patients carrying *HNF1B* mutations are thought to be liable to NODAT by immunosuppressants. Mutations of *HNF1B* can cause both diabetes and renal hypodysplasia which in turn is the common underlying disease preceding ESRD in pediatric patients (8). Therefore, a relatively high frequency of *HNF1B* mutations in pediatric kidney transplant recipients can be suspected. Based on these lines of evidence, *HNF1B* mutation may be included among the non-modifiable risk factors for NODAT, especially in pediatric kidney recipients with renal hypodysplasia.

In conclusion, we identified a novel splicing mutation of *HNF1B*, designated c.344 + 2T>C, in a pediatric patient with NODAT. This is the fifth reported case of NODAT attributed to a *HNF1B* mutation and the first human case of HNF1B-associated disease to include a bile duct anomaly. CAKUT is the leading cause of ESRD in children and *HNF1B* mutations can cause both renal hypodysplasia and diabetes. Therefore, *HNF1B* mutations may account for a portion of NODAT cases in pediatric CAKUT patients who have undergone kidney transplantation. Because NODAT is a serious and major complication of solid organ transplantation and is associated with decreased graft survival, for the appropriate management of kidney transplantation, screening for *HNF1B* mutations should be considered in pediatric patients with transplants caused by CAKUT who develop NODAT and show extra-renal symptoms.

Funding source

No funding was secured for this study.

Financial disclosure

All authors have no financial relationships relevant to this article to disclose.

Conflict of interest

All authors have no conflict of interests to disclose.

Authors' contributions

Dr. Kanda: Designed the report and drafted the initial manuscript; Dr. Morisada: performed the genetic analysis and participated in critical review of the manuscript; Dr. Kaneko, Dr. Yabuuchi, Dr. Nawashiro, Dr. Tada, Dr. Nishiyama, Dr. Miyai, Dr. Sugawara, Dr. Ishizuka, Dr. Chikamoto, and Dr. Akioka: Revised the clinical data of the case and participated in critical review of the manuscript; Dr. Iijima: Performed the genetic analysis and participated in critical review of the manuscript; Dr. Hattori: Conceptualized, designed the report, and drafted the initial manuscript; All authors approved the final manuscript as submitted and agreed to be accountable for all aspects of the work.

References

1. SHARIF A, BABOOLAL K. Risk factors for new-onset diabetes after kidney transplantation. *Nat Rev Nephrol* 2010; 6: 415–423.
2. HORIKAWA Y, IWASAKI N, HARA M, et al. Mutation in hepatocyte nuclear factor-1 beta gene (TCF2) associated with MODY. *Nat Genet* 1997; 17: 384–385.
3. CLISSOLD RL, HAMILTON AJ, HATTERSLEY AT, ELLARD S, BINGHAM C. HNF1B-associated renal and extra-renal disease—an expanding clinical spectrum. *Nat Rev Nephrol* 2015; 11: 102–112.
4. ULINSKI T, LESCURE S, BEAUFILS S, et al. Renal phenotypes related to hepatocyte nuclear factor-1β (TCF2) mutations in a pediatric cohort. *J Am Soc Nephrol* 2006; 17: 497–503.
5. WEBER S, MORINIERE V, KNÜPPEL T, et al. Prevalence of mutations in renal developmental genes in children with renal hypodysplasia: Results of the ESCAPE study. *J Am Soc Nephrol* 2006; 17: 2864–2870.
6. NAKAYAMA M, NOZU K, GOTO Y, et al. HNF1B alterations associated with congenital anomalies of the kidney and urinary tract. *Pediatr Nephrol* 2010; 25: 1073–1079.
7. THOMAS R, SANNA-CERCHI S, WARADY BA, FURTH SL, KASKEL FJ, GHARAVI AG. HNF1B and PAX2 mutations are a common cause of renal hypodysplasia in the CKiD cohort. *Pediatr Nephrol* 2011; 26: 897–903.
8. HATTORI M, SAKO M, KANEKO T, et al. End-stage renal disease in Japanese children: A nationwide survey during 2006–2011. *Clin Exp Nephrol* 2015; 19: 933–938.
9. HARAMBAT J, VAN STRALEN KJ, KIM JJ, TIZARD EJ. Epidemiology of chronic kidney disease in children. *Pediatr Nephrol* 2012; 27: 363–373.
10. WALLER SC, REES L, WOOLF AS, et al. Severe hyperglycemia after renal transplantation in a pediatric patient with a mutation of the hepatocyte nuclear factor-1 beta gene. *Am J Kidney Dis* 2002; 40: 1325–1330.
11. ZUBER J, BELLANNÉ-CHANTELOT C, CARETTE C, et al. HNF1B-related diabetes triggered by renal transplantation. *Nat Rev Nephrol* 2009; 5: 480–484.
12. TUDORACHE E, SELLIER-LECLERC AL, LENOIR M, et al. Childhood onset diabetes posttransplant in a girl with TCF2 mutation. *Pediatr Diabetes* 2012; 13: e35–39.
13. FAGUER S, CHASSAING N, BANDIN F, et al. The HNF1B score is a simple tool to select patients for HNF1B gene analysis. *Kidney Int* 2014; 86: 1007–1015.
14. CHEN YZ, GAO Q, ZHAO XZ, et al. Systematic review of TCF2 anomalies in renal cysts and diabetes syndrome/maturity onset diabetes of the young type 5. *Chin Med J* 2010; 123: 3326–3333.
15. COFFINIER C, GRESH L, FIETTE L, et al. Bile system morphogenesis defects and liver dysfunction upon targeted deletion of HNF1beta. *Development* 2002; 129: 1829–1838.
16. GARRO R, WARSHAW B, FELNER E. New-onset diabetes after kidney transplant in children. *Pediatr Nephrol* 2015; 30: 405–416.
17. WILKINSON A, DAVIDSON J, DOTTA F, et al. Guidelines for the treatment and management of new-onset diabetes after transplantation. *Clin Transplant* 2005; 19: 291–298.
18. YANG J, HUTCHINSON II, SHAH T, MIN DI. Genetic and clinical risk factors of new-onset diabetes after transplantation in Hispanic kidney transplant recipients. *Transplantation* 2011; 91: 1114–1119.
19. MCCAUGHAN JA, MCKNIGHT AJ, MAXWELL AP. Genetics of new-onset diabetes after transplantation. *J Am Soc Nephrol* 2014; 25: 1037–1049.
20. MG DE VAS, KOPP JL, HELIOT C, SANDER M, CEREGHINI S, HAUMAITRE C. Hnf1b controls pancreas morphogenesis and the generation of Ngn3+ endocrine progenitors. *Development* 2015; 142: 871–882.
21. HALDORSEN IS, VESTERHUS M, RAEDER H, et al. Lack of pancreatic body and tail in HNF1B mutation carriers. *Diabet Med* 2008; 25: 782–787.

Association between low birth weight and childhood-onset chronic kidney disease in Japan: a combined analysis of a nationwide survey for paediatric chronic kidney disease and the National Vital Statistics Report

Daishi Hirano^{1,2}, Kenji Ishikura³, Osamu Uemura⁴, Shuichi Ito^{3,5}, Naohiro Wada⁶, Motoshi Hattori⁷, Yasuo Ohashi⁸, Yuko Hamasaki⁹, Ryojiro Tanaka¹⁰, Koichi Nakanishi¹¹, Tetsuji Kaneko¹² and Masataka Honda¹³ on behalf of the Pediatric CKD Study Group in Japan in conjunction with the Committee of Measures for Pediatric CKD of the Japanese Society of Pediatric Nephrology

¹Department of Pediatrics, The Jikei University School of Medicine, Tokyo, Japan, ²Department of Biostatistics, School of Public Health, The University of Tokyo, Tokyo, Japan, ³Division of Nephrology and Rheumatology, National Center for Child Health and Development, Tokyo, Japan, ⁴Department of Pediatric Nephrology, Aichi Children's Health and Medical Center, Aichi, Japan, ⁵Department of Pediatrics, Graduate School of Medicine, Yokohama City University, Kanagawa, Japan, ⁶Department of Pediatric Nephrology, Shizuoka Children's Hospital, Shizuoka, Japan, ⁷Department of Pediatric Nephrology, Tokyo Women's Medical University, Tokyo, Japan, ⁸Department of Integrated Science and Technology for Sustainable Society (Faculty of Science and Technology), Chuo University, Tokyo, Japan, ⁹Department of Pediatric Nephrology, Toho University Faculty of Medicine, Tokyo, Japan, ¹⁰Department of Nephrology, Hyogo Prefectural Kobe Children's Hospital, Hyogo, Japan, ¹¹Department of Pediatrics, Wakayama Medical University, Wakayama, Japan, ¹²Department of Clinical Research, Tokyo Metropolitan Children's Medical Center, Tokyo, Japan and ¹³Department of Nephrology, Tokyo Metropolitan Children's Medical Center, Tokyo, Japan

Correspondence and offprint requests to: Daishi Hirano; E-mail: [bxq1976@hotmail.com](mailto:bqx1976@hotmail.com)

ABSTRACT

Background. Although numerous epidemiological surveys performed across several continents and ethnic groups have linked low birth weight (LBW) to increased risk of chronic kidney disease (CKD) in adulthood, the effects of birth weight and prematurity on development of CKD in childhood have not been clearly established.

Methods. Data on sex, LBW incidence and gestational age were compared between paediatric CKD cases and a control group. Paediatric CKD cases were obtained from a nationwide survey conducted by the Pediatric CKD Study Group in Japan. The population attributable fraction was calculated to evaluate the effects of reducing the prevalence of LBW infants (LBWI).

Results. Of 447 individuals born between 1993 and 2010 that fulfilled the eligibility criteria, birth weight data were obtained for 381 (85.2%) (231 boys and 150 girls), 106 (27.8%) of whom were LBWI. The proportion of LBWI in the general population during the same period was much lower (8.6%). Therefore, the risk ratio (RR) for paediatric CKD was significantly higher in

the LBW group [crude RR: 4.10; 95% confidence interval (CI) 3.62–5.01], and the overall impact on paediatric CKD for removal of LBW amounted to 21.1% (95% CI 16.0–26.1%). In addition, 82 patients (21.9%) with paediatric CKD were born prematurely (before 37 weeks of gestation), and as with LBW, a strong correlation was observed between prematurity and CKD (RR: 4.73; 95% CI 3.91–5.73).

Conclusions. Both birth weight and gestational age were strongly associated with childhood-onset CKD in this study.

Keywords: chronic kidney disease, developmental origins of health and disease, intrauterine growth restriction, Japan, low birth weight

INTRODUCTION

The concept of developmental programming of adult chronic diseases [Developmental Origins of Health and Disease (DOHaD)] has been raised over the past two decades [1]. Although various pathophysiological and molecular biological

mechanisms are involved in the initial programming of chronic kidney disease (CKD), only a few have been elucidated. At present, nephron loss (i.e. a deficiency in the number of nephrons) is believed to play an important role in the development of CKD [2–5]. A reduction in nephron number is responsible in adaptive single-nephron glomerular hyperfiltration. Over time, consecutive glomerular hypertension can eventually result in impaired renal function. There is a direct linear correlation between birth weight and nephron number in both adults and children, and the number of nephrons increases with an increase of 257 426 glomeruli per kilogram in birth weight [6], suggesting that the nephron numbers are lower in individuals with a low birth weight (LBW) than those with normal birth weight.

Although the original concept of DOHaD focused on intrauterine growth restriction (IUGR) patients, according to Brenner's hypothesis [7], pre-term kidneys may also have fewer functional nephrons because human nephrogenesis ends at around 36 weeks of gestation, after which no new nephrons can form [8]. Recently, Hodgkin *et al.* reported the first case series of premature infants that developed secondary focal segmental glomerulosclerosis [9]. These patients were all very premature, with gestational ages of 22–30 weeks, and presented with nephrotic-range proteinuria at an average age of 32 years old. Thus, the association of not only IUGR but also pre-term birth (PTB) with later kidney dysfunction in children is subtle and requires investigation.

The impact of the DOHaD theory is considerable as diseases such as CKD and end-stage kidney disease (ESKD) lead to haemodialysis, which is a major cause of high medical expenses. There has been a marked rise in incidence rate of CKD over the past several decades. Therefore, studies on the association between the intrauterine environment and renal disease are required, and it is necessary to determine the relative contributions of prematurity and growth restriction in renal disease.

MATERIALS AND METHODS

Data acquisition

Paediatric chronic kidney disease cases. Since 2010, the Pediatric CKD Study Group in Japan has been conducting a cross-sectional, nationwide, population-based survey in conjunction with the Committee of Measures for Pediatric CKD of the Japanese Society of Pediatric Nephrology [10–14]. Details of the study design have been published previously [10]. Briefly, eligible children aged 3 months to 15 years old with pre-dialysis CKD were included to examine the prevalence of paediatric CKD in Japan. CKD was classified according to the previously established criteria derived from the reference serum creatinine levels in Japanese children [10, 13]. Subjects with available birth history data were included in the study.

General population group

All children born alive in Japan between 1993 and 2010, the same period in which the children with CKD were born, were included as controls. Data on these children were recorded as vital statistics [15] and published annually by the Ministry

of Health, Labour and Welfare, in addition to health data published by the Organization for Economic Cooperation and Development [16].

Exposure variables

According to the International Statistical Classification of Diseases, 10th revision, published by the World Health Organization [17], birth weight was divided into two categories, with 2500 g as the cut-off for normal birth weight and <2500 g as LBW. PTB was defined as live birth before 37 weeks of pregnancy.

Outcome variables

Stage 3–5 CKD was classified using our diagnostic criteria derived from the serum creatinine levels of age- and sex-matched Japanese children described in a previous report [10]. These criteria were already validated by our group using the recently revised abbreviated Schwartz equation [10, 18].

Statistical analysis

The present study had a case-cohort design, in which cases (paediatric CKD patients) were randomly sampled and the control group was the entire Japanese birth population (with a sampling fraction of 1). The results for sex, LBW incidence and gestational age in weeks were compared between the paediatric CKD patients and controls. As the paediatric CKD patients in this study could be considered representative of cases throughout Japan for the same period, the CKD risk ratio (RR) was computed by calculating the odds ratio (OR) in paediatric CKD patients and controls. To take advances in medical technology over the years into consideration, the Mantel–Haenszel (MH) OR was calculated as an adjusted RR with birth year as a categorical variable (MH RR). In addition, to investigate the extent to which LBW and PTB contribute to the onset of paediatric CKD, the population attributable fraction (PAF) was calculated with RR_{MH} as the MH RR and $P_{LBW/PTB}$ as the LBW/PTB proportion in the general population.

$$PAF = \frac{P_{LBW/PTB}(RR_{MH} - 1)}{P_{LBW/PTB}(RR_{MH} - 1) + 1} \times 100$$

The PAF measures provide a measure of the proportion of a particular outcome that can be attributed to a particular exposure or specific characteristic or exposure to a given effector [19]. In the present study, PAF provided an estimate of the proportion of paediatric CKD cases in LBW and PTB individuals that theoretically could be avoided by elimination of LBW and PTB.

Although a marker of poor foetal growth, LBW is a result of not only IUGR but also prematurity with appropriate size for gestational age. Therefore, we repeated RR analysis for IUGR patients defined as those with birth weight below the 10th percentile for gestational age according to the population-based growth curves for primiparas that have traditionally been used in Japan [20]. Unfortunately, accurate incidence data on IUGR for all Japanese infants were not available, and we created scenarios and calculated several values based on previous reports indicating that of all the infants born in developed countries, 4–8% are diagnosed with IUGR [21]. The scenarios

were as follows: (i) 4.0% of all infants are expected to have IUGR; and (ii) 8.0% of all infants are expected to have IUGR.

In addition, we also performed repeated analysis of paediatric CKD for children with congenital anomalies of the kidney and urinary tract (CAKUT) after excluding 143 individuals with recorded non-CAKUT and 34 with recorded syndromic CAKUT listed below, as CAKUT is a potential cause of LBW. Recognizable syndromes were excluded ($n = 34$) as follows: Down syndrome (OMIN, #190685); VATER association (#192350); Kabuki syndrome (#147920); Wolf–Hirschhorn syndrome (#194190); Townes–Brocks syndrome (#107480); prune belly syndrome (#100100); and branchio-oto-renal syndrome (#113650).

Stata version 12.0 (Stata Corp., College Station, TX, USA) was used for statistical analyses. In all analyses, $P < 0.05$ was taken to indicate statistical significance.

This study was conducted in accordance with the ethical principles stipulated in the Declaration of Helsinki and with the ethical guidelines for epidemiological studies issued by the Ministry of Health, Labour and Welfare of Japan. The study was approved by the Ethics Review Committee of the University of Tokyo (ID: 3797). In accordance with the above guidelines, informed consent was not deemed necessary because the data were obtained retrospectively from patients' charts.

RESULTS

Paediatric CKD characteristics

Birth weight data were obtained for 381 (85.2%) of the 447 subjects with Stage 3–5 CKD that fulfilled the eligibility criteria. The patient characteristics are summarized in Table 1. A total of 106 (27.8%) were LBW infants (LBWI) with a median birth weight of 2040 g (range 410–2494 g). In addition, the gestational age data of 374 (83.7%) were also obtained; 81 (22.1%) were found to be premature. The incidence of IUGR was 15.5% among paediatric CKD cases. The primary aetiologies of CKD in the study population are presented in Table 2.

Table 1. Baseline demographics and clinical characteristics of children born in Japan from 1993 to 2010 that developed paediatric CKD compared with the general paediatric population

	Paediatric CKD cases		General population	
	<i>n</i>	%	<i>n</i>	%
All	381	–	20 619 622	–
Sex				
Boys	231	60.6	10 584 354	51.3
Girls	150	39.4	10 035 268	48.7
Birth weight (g)				
<2500	106	27.8	1 776 544	8.6
≥2500	275	72.2	18 843 078	91.4
Gestational age (weeks)				
<37	82	21.9	1 154 699	5.6
37–41	288	77.0	19 341 205	93.8
≥42	4	1.1	123 718	0.6
IUGR	58	15.5	–	–

CKD, chronic kidney disease; IUGR, intrauterine growth restriction; LBW, low birth weight.

CAKUT (238/381; 62.5%) was the most common primary cause of CKD.

General population group

The characteristics of the controls are also given in Table 1. The incidence of LBWI was 1 776 544 of the 20 619 622 births (8.6%) between 1993 and 2010, which was low compared with that of paediatric CKD cases. The data were not aligned with gestational age in all cases; however, premature birth cases were lower than paediatric CKD cases.

Risk ratio of paediatric CKD among LBWI and PTB infants

The RR of paediatric CKD was significantly higher in the LBW group [crude RR: 4.10; 95% confidence interval (CI) 3.62–5.01] (Table 3). The results were stratified into 3-year periods by birth year, and adjusted RR (MH RR) was 4.21 (95% CI 3.37–5.26). Adjustment for birth year did not affect the crude RR for the development of paediatric CKD. In addition, 82 patients (21.9%) with paediatric CKD were born prematurely before 37 weeks of gestation, and in patients with LBW, a strong correlation was observed between prematurity and CKD (RR: 4.73; 95% CI 3.91–5.73).

Estimation of PAF

The PAF of paediatric CKD for LBW and PTB was 21.1% (95% CI 16.0–26.1%) and 18.2% (95% CI 16.5–25.6%), respectively. These data indicate that about 20% of paediatric CKD may be associated with LBW and PTB.

RR analyses for IUGR and CAKUT patients

As given in Table 4, with an expected rate of 4.0 or 8.0% for IUGR among all Japanese infants, the crude RR of IUGR

Table 2. Primary aetiologies of Stage 3–5 paediatric CKD cases

Primary disease	<i>n</i>	%
All	381	–
CAKUT		
CAKUT with obstructive urological malformations	55	14.4
CAKUT without obstructive urological malformations	183	48.0
Cortical necrosis (perinatal period)	39	10.2
Polycystic kidney disease	19	5.0
Nephronophthisis	15	3.9
Drug induced	13	3.4
Other inherited kidney damage	10	2.6
Focal segmental glomerulonephritis	8	2.1
Acute kidney injury	7	1.8
Alport's syndrome	7	1.8
Chronic glomerulonephritis	6	1.6
Other non-inherited kidney damage	5	1.3
Neurogenic bladder	4	1.0
Congenital nephrotic syndrome	2	0.9
Cystinosis	1	0.2
Wilm's tumour	1	0.2
Chronic tubulointerstitial nephritis	1	0.2
Haemolytic uraemic syndrome	1	0.2
Systemic lupus erythematosus	1	0.2
Unknown	4	1.0

CAKUT, congenital anomalies of the kidney and urinary tract; CKD, chronic kidney disease.

Table 3. RR and LBW distribution in paediatric CKD cases and controls stratified by birth year (every 3 years)

Birth year	Birth weight (g)	Paediatric CKD cases (n)	General population (n)	RR (95% CI)	P
1993–95	<2500	11	257 754	4.54 (2.71–7.58)	<0.01
	≥2500	34	3 613 674		
1996–98	<2500	14	282 089	3.19 (2.00–5.19)	<0.01
	≥2500	56	3 601 367		
1999–2001	<2500	29	304 329	6.74 (5.05–9.01)	<0.01
	≥2500	50	3 538 878		
2002–04	<2500	22	310 504	4.61 (3.25–6.55)	<0.01
	≥2500	52	3 388 186		
2005–07	<2500	16	311 549	3.97 (2.61–6.02)	<0.01
	≥2500	42	3 245 022		
2008–10	<2500	14	310 319	3.56 (2.26–5.59)	<0.01
	≥2500	41	3 232 495		
1993–2010 (whole year)	<2500	106	1 776 544	Crude RR	<0.01
	≥2500	275	20 619 622	MH RR 4.10 (3.62–5.01) 4.21 (3.37–5.26)	<0.01

CI, confidence interval; CKD, chronic kidney disease; LBW, low birth weight; MH, Mantel-Haenszel; RR, risk ratio.

among paediatric CKD patients would be 4.40 (95% CI 3.47–5.58) and 2.11 (95% CI 1.67–2.67), respectively. In both cases, a strong association was revealed between IUGR and the development of paediatric CKD.

We analysed the RR of paediatric CKD for children with CAKUT. Overall, the risk factors for CAKUT were almost identical to those for total CKD with similar estimates of RR. The crude RR and adjusted RR of CAKUT among the LBWI were 3.36 (95% CI 2.63–4.29) and 3.31 (95% CI 2.40–4.56), respectively (Table 5).

DISCUSSION

This nationwide study revealed strong associations of not only IUGR but also prematurity with the development of paediatric CKD.

In the 1980s, Barker *et al.* reported an inverse correlation between LBW with IUGR and increased mortality rate due to coronary heart disease [22], and subsequent studies confirmed the associations with increased risk of the development of hypertension and Type 2 diabetes. Brenner’s hypothesis was confirmed in later studies. A subsequent study applying Barker’s theory to the development of CKD, suggested that either an acquired or congenital reduction in nephron number could lead to the development of hypertension or CKD [7]. While cell proliferation occurs before the first, second or third trimester of pregnancy in most organs, the majority of nephrons (60% of the total nephrons) are formed during the third trimester of pregnancy, and nephron formation ceases in normal pregnancy at 36 weeks of gestation [8]. Thus, IUGR and prematurity are both associated with congenital reduction in the nephron number; in turn, reduced nephron number is associated with increased susceptibility to kidney disease. The findings of the present study are consistent with Brenner’s hypothesis.

With or without non-congenital causes, our sensitivity analysis revealed that LBW was itself significantly associated with paediatric CKD. This association may be explained by the

Table 4. Association of IUGR with development of paediatric CKDs

IUGR	Paediatric CKD cases	General population (Scenario 1) ^a	General population (Scenario 2) ^b
Yes	58	824 782	1 649 564
No	316	19 794 764	18 969 982
% of IUGR	15.5	4.0	8.0
Crude RR (95% CI)	–	4.40 (3.47–5.58)	2.11 (1.67–2.67)

IUGR, intrauterine growth restriction; CI, confidence interval; CKD, chronic kidney disease; RR, risk ratio.

^aScenario 1: 4.0% of all infants are expected to have IUGR.

^bScenario 2: 8.0% of all infants are expected to have IUGR.

Table 5. Adjustment for CAKUT

CKD	Low birth weight (<2500 g)	
	Yes	No
Yes	49	155
No	1 773 211	18 846 335
Crude RR (95% CI)	3.36 (2.63–4.29)	
Adjusted RR (95% CI)	3.31 (2.40–4.56) ^a	

CAKUT, congenital anomalies of the kidney and urinary tract; CI, confidence interval; CKD, chronic kidney disease; RR, risk ratio.

^aAdjusted for birth year.

strong association between LBW and ESKD due to congenital or inherited causes that are more common during childhood. In fact, according to a previous study by Ishikura *et al.* and the report of the North American Pediatric Renal Trials and Collaborative Studies, congenital causes are responsible for the greatest percentage of paediatric CKD cases [10, 23]. However, these findings persisted after re-analysing patients without non-CAKUT, and the results indicated that LBW was significantly associated with paediatric CKD with non-congenital causes. This may indicate that a critical shortage of nephrons associated with LBW manifests itself particularly strongly during childhood.

This is the first study to investigate the effects of birth weight and gestational age on the risk of paediatric CKD, and the results confirmed the hypothesis that LBW is associated with an increased risk of renal failure. However, a causal relation between LBW and increased risk of renal failure could not be conclusively demonstrated due to the retrospective nature of the present study. The strength of our study is that the reliability of the data was high and the data were derived from the national registry database of epidemiological research. Our results indicated that LBW and PTB have RR of 4.21 and 4.73 for paediatric CKD, respectively, similar to the findings of sub-analysis performed by Vikse *et al.* [24].

Our study had several limitations that should be mentioned. Foetal/neonatal ultrasonography was the most frequently used method to detect CAKUT. However, the diagnosis of some types of CAKUT, such as obstructive uropathy, may be challenging, resulting in underestimation of its incidence rate. Nevertheless, the prevalence of CAKUT in our study was consistent with those reported in the ItalKid and REPIR II studies (67.5 and 59%, respectively) [25, 26]. We did not consider the diagnosis of CAKUT to be a serious issue because it is rare for CAKUT, undetectable on ultrasonography, to progress into paediatric CKD. Secondly, we used infants in the general population as controls. Although the control group also included paediatric CKD cases, we did not consider this to be a serious problem because paediatric CKD is a rare endpoint with rather conservative results. Thirdly, we were unable to adjust for potential confounding factors such as extreme prematurity, episodes of acute kidney injury and treatment in neonatal intensive care units as these confounders were not measured in the general population group. Fourthly, although we found both birth weight and prematurity were strongly associated with childhood-onset CKD, we were unable to clarify which of IUGR or pre-term appropriate gestational age (AGA) was more closely associated with paediatric CKD as accurate incidence data regarding IUGR and pre-term AGA were not available for the general population group of the present study. We hope to further evaluate this association in a future study.

Physiological nephron drop-out throughout the lifespan of most individuals possessing a good nephron complement at birth does not reach the level of CKD or ESKD unless there is an acquired secondary insult, such as diabetes. The risks of CKD and ESKD are higher in individuals born with a low number of nephrons and are further increased by post-natally acquired insult. Furthermore, PAF results showed that about 20% of paediatric CKD cases may be derived from LBW or PTB. As the first generation of infants born in the era of surfactant use are now reaching young adulthood, it is possible that there is already a silent epidemic of CKD in this population of adults. Therefore, it will be important to reduce the incidence rates of LBW and PTB for the well-being of the public.

The growing pandemic of CKD has attracted a great deal of attention. As birth weight and gestational age were found to be associated with childhood-onset Stage 3–5 CKD, greater attention should be given to the structure of the kidneys and the results of urinary screening in children with LBW or PTB. Understanding the risk factors and implementing screening programmes in populations at risk will increase early detection

and allow initiation of treatment of modifiable risk factors for ESKD, along with appropriate treatment for CKD. In addition, the economic burden caused by the cost of renal replacement therapy may be mitigated by early detection of CKD risk factors.

ACKNOWLEDGEMENTS

The authors thank Takuhito Nagai (Aichi), Kenichi Satomura (Osaka), Tomoo Kise (Okinawa), Takuji Yamada (Aichi), Midori Awazu (Tokyo), Hiroshi Asanuma (Tokyo), Toshiyuki Ohta (Hiroshima), Kazumoto Iijima (Kobe), Takeshi Matsuyama (Tokyo), Hidefumi Nakamura (Tokyo), Mayumi Sako (Tokyo), Tomoyuki Sakai (Shiga), Yusuke Okuda (Shiga), Shunsuke Shinozuka (Saitama), Yoshinobu Nagaoka (Hokkaido), Shuichiro Fujinaga (Saitama), Hiroshi Kitayama (Shizuoka), Naoya Fujita (Shizuoka), Masataka Hisano (Chiba), Yuko Akioka (Tokyo), Naoaki Mikami (Tokyo), Hiroshi Hataya (Tokyo), Hiroyuki Satoh (Tokyo), Tae Omori (Tokyo), Takashi Sekine (Tokyo), Yoshimitsu Goto (Aichi), Yohei Ikezumi (Niigata), Takeshi Yamada (Niigata) and Akira Matsunaga (Yamagata) of The Pediatric CKD Study Group in Japan for their contributions to the study. The authors also thank all the institutions that participated in the surveys, and Masaaki Kurihara, Chie Matsuda, Naomi Miyamoto and Takako Arai of the Japan Clinical Research Support Unit (Tokyo) for their help with data management. The authors also wish to thank statistician Yutaka Matsuyama and Tomohiro Shinozaki for their valuable advice in the statistical analysis. The results of the present study have not previously been published, in whole or in part, except in abstract form.

FUNDING

This work was supported by a Health and Labour Sciences Research Grant for Research in Rare and Intractable Diseases from the Ministry of Health, Labour, and Welfare, Japan (H25-nanchitou(nan)-ippan-017).

CONFLICT OF INTEREST STATEMENT


K.I. has received lecture fees from Novartis Pharma and Asahi Kasei Pharma. O.U. has received lecture fees from Asahi Kasei Pharma, Kyowa Hakko Kirin, Takeda Pharmaceutical and Siemens Group in Japan. M. Hattori has received research grants from Astellas Pharma and Chugai Pharmaceutical. Y.O. has received consulting fees from Kyowa Hakko Kirin and Chugai Pharmaceutical. Y.H. has received research grants from Novartis Pharma, and lecture fees from Novartis Pharma, Astellas Pharma and Pfizer Japan. R.T. has received lecture fees from Pfizer Japan and Asahi Kasei Pharma. K.N. has received lecture fees from Otsuka Pharmaceutical Co., Asahi Kasei Pharma and Astellas Pharma. M. Honda has received lecture fees from Novartis Pharma, Asahi Kasei Pharma, Takeda Pharmaceutical and Chugai Pharmaceutical.

REFERENCES

- Barker DJ, Eriksson JG, Forsén T *et al.* Fetal origins of adult disease: strength of effects and biological basis. *Int J Epidemiol* 2002; 31: 1235–1239
- McMillen IC, Robinson JS. Developmental origins of the metabolic syndrome: prediction, plasticity, and programming. *Physiol Rev* 2005; 85: 571–633
- Simeoni U, Ligi I, Buffat C *et al.* Adverse consequences of accelerated neonatal growth: cardiovascular and renal issues. *Pediatr Nephrol* 2011; 26: 493–508
- Vehaskari VM, Woods LL. Prenatal programming of hypertension: lessons from experimental models. *J Am Soc Nephrol* 2005; 16: 2545–2556
- Brenner BM, Chertow GM. Congenital oligonephropathy and the etiology of adult hypertension and progressive renal injury. *Am J Kidney Dis* 1994; 23: 171–175
- Hughson M, Farris AB, III, Douglas-Denton R *et al.* Glomerular number and size in autopsy kidneys: the relationship to birth weight. *Kidney Int* 2003; 63: 2113–2122
- Zandi-Nejad K, Luyckx VA, Brenner BM. Adult hypertension and kidney disease: the role of fetal programming. *Hypertension* 2006; 47: 502–508
- Hinchliffe SA, Sargent PH, Howard CV *et al.* Human intrauterine renal growth expressed in absolute number of glomeruli assessed by the disector method and Cavalieri principle. *Lab Invest* 1991; 64: 777–784
- Hodgin JB, Rasoulopour M, Markowitz GS *et al.* Very low birth weight is a risk factor for secondary focal segmental glomerulosclerosis. *Clin J Am Soc Nephrol* 2009; 4: 71–76
- Ishikura K, Uemura O, Ito S *et al.* Pre-dialysis chronic kidney disease in children: results of a nationwide survey in Japan. *Nephrol Dial Transplant* 2013; 28: 2345–2355
- Ishikura K, Uemura O, Hamasaki Y *et al.* Progression to end-stage kidney disease in Japanese children with chronic kidney disease: results of a nationwide prospective cohort study. *Nephrol Dial Transplant* 2014; 29: 878–884
- Hamasaki Y, Ishikura K, Uemura O *et al.* Growth impairment in children with pre-dialysis chronic kidney disease in Japan. *Clin Exp Nephrol* 2015; 19: 1142–1148
- Uemura O, Honda M, Matsuyama T *et al.* Age, gender, and body length effects on reference serum creatinine levels determined by an enzymatic method in Japanese children: a multicenter study. *Clin Exp Nephrol* 2011; 15: 694–699
- Ishikura K, Uemura O, Hamasaki Y *et al.* Insignificant impact of VUR on the progression of CKD in children with CAKUT. *Pediatr Nephrol* 2016; 31: 105–112
- Vital, Health and Social Statistics Division, Statistics and Information Department, Minister's Secretariat, Ministry of Health, Labour and Welfare. *Vital Statistics of Japan*. <http://www.mhlw.go.jp/english/database/db-hw/vs01.html> (21 March 2014, date last accessed)
- OECD Health at a Glance 2011. <http://www.oecd.org/health/healthataglance> (21 March 2014, date last accessed)
- WHO. International Statistical Classification of Diseases and Related Health Problems. *Tenth Revision*. Geneva: World Health Organization, 1994
- Schwartz GJ, Muñoz A, Schneider MF *et al.* New equations to estimate GFR in children with CKD. *J Am Soc Nephrol* 2009; 20: 629–637
- Woodward M. *Epidemiology Study Design and Data Analysis, 2nd edn*. London: Chapman and Hall, 2005
- Itabashi K, Fujimura M, Kusuda S *et al.* New standard values of birth weight and height for gestational age. *Nihon Shonika Gakkai Zasshi* 2010; 114: 1271–1293
- Kramer MS. Determinants of low birth weight: methodological assessment and meta-analysis. *Bull World Health Organ* 1987; 65: 663–737
- Barker DJP, Winter PD, Osmond C *et al.* Weight in infancy and death from ischaemic heart disease. *Lancet* 1989; 9: 577–580
- Warady BA, Chadha V. Chronic kidney disease in children: the global perspective. *Pediatr Nephrol* 2007; 22: 1999–2009
- Vikse BE, Irgens LM, Leivestad T *et al.* Low birth weight increases risk for end-stage renal disease. *J Am Soc Nephrol* 2008; 19: 151–157
- Ardissino G, Daccò V, Testa S *et al.* Epidemiology of chronic renal failure in children: data from the ItalKid project. *Pediatrics* 2003; 111: e382–e387
- Areses Trapote R, Sanahuja Ibáñez MJ, Navarro M *et al.* Epidemiology of chronic kidney disease in Spanish pediatric population. REPIR II Project. *Nefrologia* 2010; 30: 508–517 (in Spanish)

Received for publication: 8.8.2015; Accepted in revised form: 22.11.2015

Rare renal ciliopathies in non-consanguineous families that were identified by targeted resequencing

Tomohiko Yamamura¹ · Naoya Morisada^{1,2}  · Kandai Nozu¹ · Shogo Minamikawa¹ · Shingo Ishimori³ · Daisaku Toyoshima⁴ · Takeshi Ninchoji¹ · Masato Yasui⁵ · Mariko Taniguchi-Ikeda¹ · Ichiro Morioka¹ · Koichi Nakanishi⁶ · Hisahide Nishio² · Kazumoto Iijima¹

Received: 25 November 2015 / Accepted: 29 February 2016 / Published online: 11 March 2016
© Japanese Society of Nephrology 2016

Abstract

Background Nephronophthisis-related ciliopathies (NPHP-RC) are a frequent cause of renal failure for children and adolescents. Although diagnosing these diseases clinically is difficult, a comprehensive genetic screening approach of targeted resequencing can uncover the genetic background in this complicated family of diseases.

Methods We studied three Japanese female patients with renal insufficiency from non-consanguineous parents. A renal biopsy for clinical reasons was not performed. Therefore, we did not know the diagnosis of these patients from a clinical aspect. We performed comprehensive genetic analysis using the TruSight One Sequencing Panel next generation sequencing technique.

Results We identified three different rare NPHP-RC variants in the following genes: *SDCCAG8*, *MKKS*, and *WDR35*. Patient 1 with *SDCCAG8* homozygous deletions

showed no ciliopathy-specific extrarenal manifestations, such as retinitis pigmentosa or polydactyly prior to genetic analysis. Patient 2 with a *MKKS* splice site homozygous mutation and a subsequent 39-amino acid deletion in the substrate-binding apical domain, had clinical symptoms of Bardet–Biedl syndrome. She and her deceased elder brother had severe renal insufficiency soon after birth. Patient 3 with a compound heterozygous *WDR35* mutation had ocular coloboma and intellectual disability.

Conclusions Our results suggest that a comprehensive genetic screening system using target resequencing is useful and non-invasive for the diagnosis of patients with an unknown cause of pediatric end-stage renal disease.

Keywords Nephronophthisis-related ciliopathy · Targeted resequencing · Next generation sequencing · *SDCCAG8* · *MKKS* · *WDR35*

✉ Naoya Morisada
morisada@med.kobe-u.ac.jp

¹ Department of Pediatrics, Kobe University Graduate School of Medicine, 7-5-1 Kusunoki-cho, Chuo-ku, Kobe 650-0017, Japan

² Department of Community Medicine and Social Healthcare Science, Kobe University Graduate School of Medicine, 7-5-1 Kusunoki-cho, Chuo-ku, Kobe 650-0017, Japan

³ Department of Pediatrics, Kakogawa West City Hospital, 384-1, Hiratsu, Yoneda-cho, Kakogawa 675-8611, Japan

⁴ Department of Child Neurology, Hyogo Prefectural Kobe Children's Hospital, 1-1-1, Takakuradai, Suma-ku, Kobe 654-0081, Japan

⁵ Department of Pediatrics, Fukuyama Capital Hospital, 5-23-1, Zao-cho, Fukuyama 721-0971, Japan

⁶ Department of Pediatrics, Wakayama Medical College, 811-1, Kimiidera, Wakayama 641-8509, Japan

Introduction

Nephronophthisis-related ciliopathy (NPHP-RC) is an autosomal recessive cystic kidney disease and a common cause of end-stage renal disease (ESRD) in childhood and adolescence [1]. More than 20 genes have been reported as the causative genes of NPHP-RC [2] and over 40 genes have been reported to be associated with ciliopathies. These genes encode proteins located in primary cilia and related structures [3]. The cause of NPHP-RC is dysfunction of primary cilia, which are non-motile cilia in cells. The most frequent causative gene in NPHP-RC is *NPHP1* [4]. Three quarters of patients with an *NPHP1* homozygous deletion show isolated renal manifestations. However, NPHP-RC is often complicated by extrarenal manifestations, such as retinitis pigmentosa in Senior–Løken

syndrome, cerebellar vermis aplasia or hypoplasia in Joubert syndrome, multiple organ involvement and neurodegeneration in Meckel (or Meckel–Gruber) syndrome, and Bardet–Biedl syndrome (BBS) characterized by intellectual disability, obesity, and retinitis pigmentosa. Cranioectodermal dysplasia (CED), otherwise known as Sensenbrenner syndrome, is a ciliopathy with features of craniofacial abnormalities, metaphyseal dysplasia, ectodermal anomalies, retinal dystrophy, and hepatic disorders [5]. Leber’s congenital amaurosis and oral-facial-digital syndrome are also ciliopathy-related disorders [6]. All types of ciliopathies may involve renal manifestations. In the genetic mechanism, gene locus heterogeneity is more important for determining the disease phenotype than allelism or modifier genes [4].

NPHP-RC is pathologically characterized as interstitial fibrosis, irregular thickening or disruption of the tubular basement membrane, and cystic formation in the cortex or medulla [1]. The most frequent cause of ESRD in childhood is congenital anomalies of the kidney and urinary tract, especially renal hypoplasia or dysplasia (RHD), and this is an important cause of ESRD according to North American Pediatric Renal Trials and Collaborative Studies (NAPRTCS, <http://spitfire.emmes.com/study/ped/index.htm>). RHD is characterized by a reduction in the number of glomeruli or oligomeganephronia. Most of the causative genes of RHD, such as *PAX2*, *HNF1B*, *SIX1*, *EYA1*, and *SALL1*, are all autosomal dominant [7]. Patients with these gene mutations sometimes show extrarenal manifestations as with NPHP-RC, including visual impairment, hearing loss, or intellectual disability. RHD and NPHP may be pathologically or clinically distinguishable. However, in the stage of severe renal insufficiency or if a renal biopsy cannot be performed for clinical reasons, clearly distinguishing between RHD and NPHP is difficult.

Recently, next generation sequencing (NGS) has become available in clinical medicine. NGS is able to analyze the whole genome sequence or whole exome sequence (WES). NGS is useful not only to discover new pathogenic genes for an unknown cause of genetic disease, but also to comprehensively analyze known causative genes simultaneously. Gee et al. identified the causative genes using WES in seven of 10 NPHP-RC patients with renal histological or ultrasonographic diagnosis of NPHP-RC before genetic analysis [8]. NGS may be extremely useful for identification of the cause of ESRD in childhood, even when a renal biopsy cannot be performed.

We studied three Japanese patients with ESRD in childhood to identify the causative genes using NGS. All of the patients were born from non-consanguineous parents on inquiry and they did not have a renal biopsy performed for clinical reasons.

Materials and methods

Ethics

All procedures were reviewed and approved by the Institutional Review Board of Kobe University School of Medicine (approval #65), and they were performed in accordance with the ethical standards laid down in the 1964 Declaration of Helsinki. Informed consents were obtained from all patients or their legal guardians.

Patients

Patient 1

A 3-year and 6-month-old girl with intellectual disability was admitted to a former local hospital because of afebrile generalized seizures. She was born to unrelated parents as the first child. She was diagnosed with epilepsy and mild renal insufficiency at that time. Her serum creatinine levels gradually increased from 0.59 mg/dl at the first admission to 1.09 mg/dl in 3 months. Her renal insufficiency deteriorated rapidly and hypertension and oliguria were observed. She was transferred to our hospital at the age of 3 years and 9 months. Her serum creatinine level was 3.21 mg/dl and blood urea nitrogen level was 62.2 mg/dl. An emergency operation of placing a peritoneal dialysis (PD) catheter was performed at the day of transfer. Because her respiratory condition was poor, we could not perform a renal biopsy. A renal ultrasound revealed bilateral mild enlarged kidneys and no obvious cyst. She required continuous PD because of anuria. She did not have obesity and polydactyly. Retinitis pigmentosa was identified by an ocular examination after genetic diagnosis. She took levetiracetam for her epilepsy. Brain and cerebellar magnetic resonance imaging (MRI) showed no abnormal findings, including molar tooth sign (Fig. 1a).

Patient 2

Patient 2 was a 27-year-old woman. She was born to unrelated parents as the second child. Her elder brother died soon after birth because of bilateral polycystic kidneys, severe renal dysfunction and pulmonary hypoplasia. Patient 2 was referred to our hospital because of bilateral polycystic kidneys and severe renal insufficiency in the neonatal period. She had postaxial polydactyly in her right hand and left foot, and they were treated by resection. Her visual performance was low and she was diagnosed with bilateral retinitis pigmentosa. Her renal function progressively deteriorated, and she started PD at the age of 3 years. She had living-donor renal transplantation from

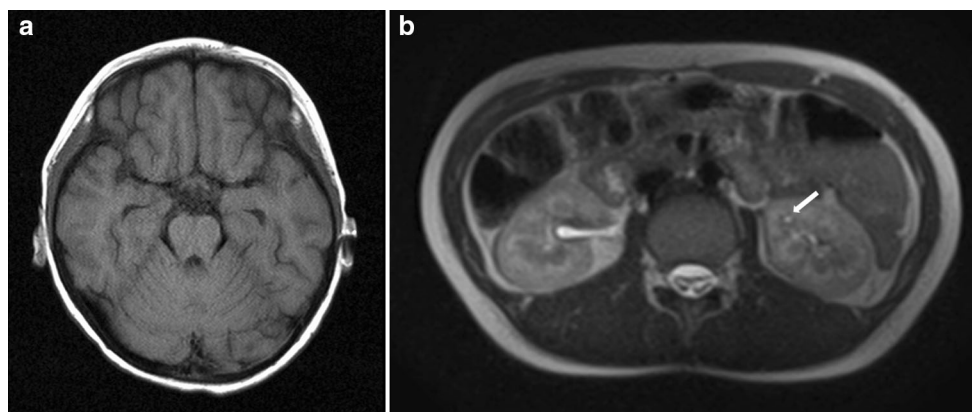


Fig. 1 MRI findings of the patients. **a** Brain MRI of Patient 1. No remarkable changes, including molar tooth sign, were observed. **b** Abdominal MRI of Patient 3. A small renal cyst was observed in the corticomedullary junction in the left kidney (arrow)

her mother at the age of 4 years. Her intellectual disability was mild to moderate. She was obese. She received oophorectomy because of ovarian cystoma. She did not have any congenital heart anomalies. Her father died from liver cell carcinoma.

Patient 3

Patient 3 was a 15-year-old girl. She was born to non-consanguineous parents as the first child, and had no family history. She was diagnosed with developmental delay with autism spectrum disorder and bilateral mild optic disc edema. She did not have a short stature and she did not have any polydactyly. Brain MRI was normal. At the age of 13 years, non-nephrotic range proteinuria was observed at an annual urinary test in a Japanese school for the first time. A recent urinary protein and creatinine ratio was 0.74 g/g creatinine. Serum creatinine and urinary beta-microglobulin levels were elevated (1.24 mg/dl and 2.48 mg/g creatinine, respectively). A renal ultrasonographic examination and abdominal MRI showed a few small cysts at the corticomedullary junction in bilateral kidneys (Fig. 1b). Recently, the estimated glomerular filtration rate was 29.9 ml/min/1.73 m², indicating chronic kidney disease stage 4. Renal biopsy was not performed. She received an angiotensin II type 1 receptor blocker and alfacalcidol. Patient 3 was clinically considered as having papillorenal syndrome (OMIM#120330), but there was no major mutation in *PAX2* by direct sequencing.

Preparation of the patients' DNA and NGS

Genomic DNA samples were extracted from peripheral blood mononuclear cells using the QuickGene whole blood kit S (Kurabo, Osaka, Japan). For library preparation in NGS, we used a commercially available targeted

resequencing kit, the TruSight One Sequencing Panel, on a MiSeq platform (Illumina, San Diego, CA, USA). By using the TruSight One Sequencing Panel kit, we are able to analyze 4813 target genes associated with human genetic disorders (<http://www.illumina.com/products/trusight-one-sequencing-panel.html>). All procedures were prepared according to the manufacturers' instructions. In brief, 50 ng of genomic DNA samples were tagged by the Nextera transposome (Nextera DNA Library preparation Kit, Illumina). The libraries containing double-strand DNA were then denatured into single-strand DNA. Biotin-labeled probes were hybridized to the targeted region for the first rapid capture. The pool of mixed samples was enriched for the target regions by adding streptavidin beads. Biotinylated DNA fragments that were combined with the streptavidin beads were pulled down magnetically from the solution. The enriched DNA fragments were then eluted from the beads and hybridized for the second rapid capture. The prepared library was applied to MiSeq Flowcell for sequencing. The sequence data that were generated were analyzed using MiSeq Reporter software (Illumina).

Complementary DNA analysis

For mRNA analysis, total RNA was extracted from blood leukocytes using the NucleoSpin RNA Blood kit (Macherey–Nagel GmbH & Co. KG, Düren, Germany). The reverse transcribed cDNA was generated using random hexamers and the Superscript III kit (ThermoFisher Scientific, Waltham, MA, USA). The cDNA was amplified by nested PCR using the following McKusick–Kaufman syndrome (MKKS) primer pairs: for the first PCR, the forward primer was 5'-GTGCTTT GATCCTGAGAGCCT-3' and the reverse primer was 5'-GG GCACTGCAAATGCTTCA-3'; for the second PCR, the forward primer was 5'-ATCAACTGCCCTCAAGGTGG-3' and the reverse primer was 5'-GTACAGCCACCTCCCAAC

AA-3'. PCR-amplified products were purified and subjected to Sanger sequencing.

Data analysis

For data analysis, we used VariantStudio ver. 2.2.1 (Illumina) and Integrative Genomics Viewer software ver. 2.3.57 (Broad Institute, Cambridge, MA, USA). Mutations were confirmed by standard Sanger sequencing using the 3130 genetic analyzer (Thermo Fisher Scientific). Sanger sequence data were analyzed by the CLC main workbench ver. 6.7.1 (QIAGEN, Hilden, Germany). Allele frequency is available in the Single Nucleotide Polymorphism Database (dbSNP, <http://www.ncbi.nlm.nih.gov/SNP/>) and the Human Genome Variation Browser (HGVB, <http://www.genome.med.kyoto-u.ac.jp/SnpDB/index.html?>) in the Japanese population.

Results

We identified three different mutations by NGS. All of these mutations were confirmed by Sanger sequencing (Fig. 2). In Patient 1, we found a homozygous four-base pair deletion in *SDCCAG8* (serologically defined colon cancer antigen 8, NPHP10, 1q43) termed NM_006642.3:c.845_848delTTTG, C283X. This deletion was identified in each parent as heterozygous. In Patient 2, we identified a homozygous splice acceptor site mutation in *MKKS* (20p12.2) termed NM_018848.3:c.986-1G>A. Sequencing of cDNA from Patient 2 revealed aberrant transcripts of *MKKS* by a new splice acceptor site within exon 4, and this consequently induced a 117-bp deletion in the transcript product of *MKKS* (Fig. 3a, b). We did not perform segregation analysis of her family. In Patient 3,

WDR35 compound heterozygous mutations were identified and termed NM_001006657.1:c.622G>C, A208P and NM_001006657.1:c.2134delC, L712Y fsTer20. Both mutations were not found in the dbSNP and HGVB. A208P was a novel missense mutation, and three missense mutation prediction websites, Mutation Taster (<http://www.mutationtaster.org/>), PolyPhen2 (<http://genetics.bwh.harvard.edu/pph2/>), and SIFT (<http://sift.jcvi.org/>), all identified it as a pathogenic mutation. Her father had A208P, and her mother had L712YfsTer20.

Discussion

We identified rare causative genes for NPHP-RC in three patients from non-consanguineous parents by targeted resequencing panels. To the best of our knowledge, there are no reports on patients with NPHP-RC with the three rare genes found in the current study in the East-Asian population. All of the three patients were not able to undergo a renal biopsy for medical reasons. Patients 1 and 3 were not considered as having NPHP-RC before genetic analysis because there were no specific clinical symptoms, including renal and extrarenal manifestations.

Patient 1 had a homozygous four-base pair deletion in *SDCCAG8*. A homozygous or compound heterozygous mutation in *SDCCAG8* is a cause of BBS16 (OMIM#615993) or Senior-Løken syndrome 7 (OMIM#613615) as reported by Otto et al. [9]. They reported 12 different truncating mutations of *SDCCAG8* in patients with NPHP-RC. *SDCCAG8* protein is located in primary cilia, and directly interacts with oral-facial-digital syndrome 1 protein, which is also a causative gene of NPHP-RC in an X dominant manner. Although polydactyly tends to be a complication in other types of BBS,

Fig. 2 Results of genetic analysis confirmed by Sanger methods

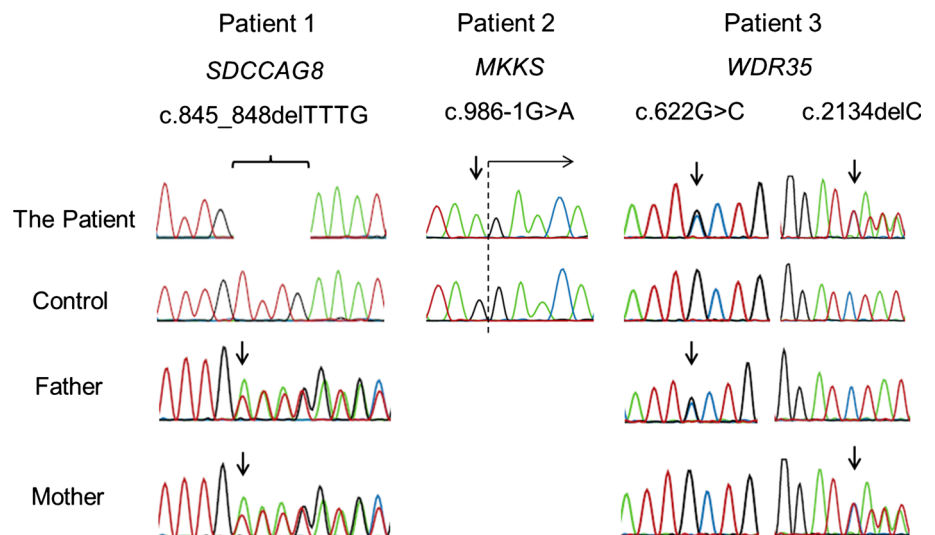
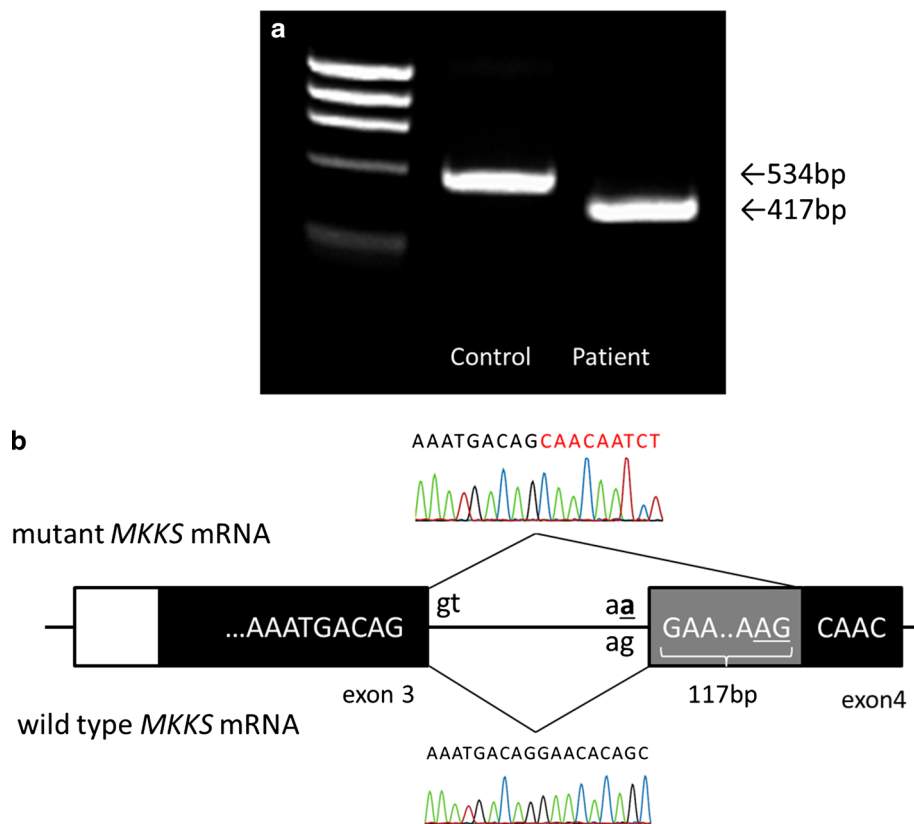


Fig. 3 Analysis of cDNA for *MKKS* in Patient 2. **a** PCR amplification for cDNA using primers annealing to exons 3 and 5 of *MKKS* showed a 117-bp deletion in Patient 2. **b** Schematic representation of the changing splice acceptor site in mutant *MKKS* mRNA



patients with NPHP-RC associated with *SDCCAG8* do not have polydactyly [10]. *SDCCAG8* protein plays an important role in repair of DNA damage and DNA replication in the S-phase cell cycle [11]. The allele frequency of NM_006642.3:c.845_848delTTTG is 0.002 in the Japanese population according to the HGVB. There are no data of this deletion in the dbSNP. This suggests that patients with the same mutation as that in Patient 1 may appear with the probability of 0.000004 in the Japanese population.

Patient 2 had a homozygous splice acceptor site mutation in *MKKS*, which encodes a chaperone-like protein. This mutation has been registered in the dbSNP as rs200633158, but the minor allele frequency and clinical significance are unknown. There are no data in the HGVB. Our cDNA analysis revealed a 117-bp deletion in *MKKS* and a subsequent 39-amino acid deletion, NP_061336.1:G329_E367del. This deleted lesion is located in the substrate-binding apical domain of *MKKS* protein, and mutations in this domain cause cellular mislocalization [12]. Homozygous or compound heterozygous mutations of *MKKS*, which encodes a chaperon-like protein, have been reported in *BBS6* (OMIM#605231) or *MKKS* (OMIM#236700). *MKKS* was first reported by McKusick in 1964 [13]. *MKKS* is characterized by genitourinary malformations, especially hydrometrocolpos, postaxial

polydactyly, and congenital heart disease. The clinical features of *BBS6* are associated with obesity, retinitis pigmentosa, intellectual disability, and renal and urogenital anomalies [14]. Patient 2 had mild obesity, but this may have been due to oral prednisolone therapy for immune suppression after renal transplantation. Her eyes were suspected as having retinitis pigmentosa. Urogenital anomalies, including uterine malformations, are major features in *MKKS*. These findings suggest the spectrum disorder of *MKKS* mutation. *MKKS* homozygous mutations have been reported in approximately 2 % of the Amish population and this disorder is rare elsewhere [15]. Patient 2, her deceased brother, and her parents were from the Japanese population. This is the first report of *MKKS* patients in Japan. We could not perform genetic analysis in the parents. Because the sibling of the proband died owing to cystic kidney and subsequent respiratory failure, the parents might have the same heterozygous mutation in *MKKS*.

Patient 3 had a compound heterozygous mutation in *WDR35*. *WDR35* which is involved in intraflagellar transport [16] is the responsible gene of *CED2* (OMIM#613610) or short-rib thoracic dysplasia 7 with or without polydactyly (*SRTD7*, OMIM#614091). *CED* includes craniosynostosis, and facial ectodermal and skeletal anomalies. Occasionally, *CED* is complicated by NPHP-RC, hepatic

Table 1 Clinical phenotype and genotype in the patients

	Patient 1	Patient 2	Patient 3
Age in diagnosis	3	37	15
Age in ESRD	3	0	Not yet
Gender	Female	Female	Female
Responsible gene	<i>SDCCAG8</i>	<i>MKKS</i>	<i>WDR35</i>
Mutation	c.845_848delTTTG	c.986-1G>A	c.622G>C/c.2134delC
Intellectual disability	+	+	+
Brain MRI findings	NAA	NAA	NAA
Polydactyly	None	+	None
Ocular lesion	None	+	+
Obesity	None	+	None
Other	Epilepsy	Polycystic ovary Pulmonary nodular lesion	None

ESRD end-stage renal disease, NAA no apparent abnormalities

fibrosis, or retinitis pigmentosa [16]. Several gene mutations in CED have been reported, including *IFT122* (CED1), *IFT43* (CED3), and *WDR19* (CED4). These genes are associated with intraflagellar transport in cilia. In the same family, their clinical phenotypes may be different [17]. Renal manifestations with *WDR35* mutations may be chronic kidney disease [18]. *WDR35* protein is present at the renal tubules, but not at glomeruli, according to the Human Protein Atlas (<http://www.proteinatlas.org>) [19]. Patient 3 had optic coloboma, intellectual disability, and cystic kidney, which were compatible with ciliopathy. However, she had no apparent skeletal anomalies, including a narrow thorax or cranial abnormalities. She might have papillorenal syndrome according to coloboma and renal dysfunction, but there was no pathogenic mutation in *PAX2*. Patients with papillorenal manifestation without *PAX2* mutation may have NPHP-RC (Table 1).

We performed genetic analysis using a commercially based targeted resequencing kit, TruSight One. The TruSight One Sequencing Panel can analyze 4813 genes, which are associated with clinically relevant genes (<http://www.illumina.com/products/trusight-one-sequencing-panel.html>). This kit contains 14 NPHP-related genes (NPHP1–13, 19) or other ciliopathy-related genes. Although targeted resequencing cannot be used to investigate all human genes, it can provide data associated with disease-specific gene variants, and it is more cost-effective than the whole genome sequence or WES.

Distinguishing NPHP-RC and RHD is clinically important. Most cases of NPHP-RC have autosomal recessive inheritance, and most congenital anomalies of the kidney and urinary tract, including RHD, are autosomal dominant in manner. This difference is important in genetic counseling for the family. Furthermore, recent pharmacological approaches for NPHP-RC have attempted to delay aggravation of renal function using paclitaxel or histone

deacetylase inhibitors [20]. Early diagnosis using NGS may help improve the patient's prognosis.

Conclusion

In conclusion, our results suggest that comprehensive analysis using NGS with a targeted resequencing panel is useful and non-invasive for patients with unknown causes of ESRD.

Acknowledgments The authors thank all participants and their families in this study, as well as Tetsuko Yamanouchi and Ming Juan Ye for their excellent technical assistance.

Compliance with ethical standards

Conflict of interest KI received grants from Daiichi Sankyo Co. Ltd., and Clio Co. Ltd.


Sources of funding This study was supported by a JSPS KAKENHI Grant (Number 15K09261) for NM and Ministry of Health, Labour and Welfare Japan (grant number 26070201) for KI.

References

- Halbritter J, Porath JD, Diaz KA, Braun DA, Kohl S, Chaki M, Allen SJ, Soliman NA, Hildebrandt F, Otto EA, G. P. N. Study Group. Identification of 99 novel mutations in a worldwide cohort of 1,056 patients with a nephronophthisis-related ciliopathy. *Hum Genet.* 2013;132:865–84.
- Wolf MT. Nephronophthisis and related syndromes. *Curr Opin Pediatr.* 2015;27:201–11.
- Hildebrandt F, Benzing T, Katsanis N. Ciliopathies. *N Engl J Med.* 2011;364:1533–43.
- Chaki M, Hoefele J, Allen SJ, Ramaswami G, Janssen S, Bergmann C, Heckenlively JR, Otto EA, Hildebrandt F. Genotype-phenotype correlation in 440 patients with NPHP-related ciliopathies. *Kidney Int.* 2011;80:1239–45.

5. Lin AE, Traum AZ, Sahai I, Keppler-Noreuil K, Kukolich MK, Adam MP, Westra SJ, Arts HH. Sensenbrenner syndrome (cranioectodermal dysplasia): clinical and molecular analyses of 39 patients including two new patients. *Am J Med Genet A*. 2013;161A:2762–76.
6. Waters AM, Beales PL. Ciliopathies: an expanding disease spectrum. *Pediatr Nephrol*. 2011;26:1039–56.
7. Weber S, Moriniere V, Knuppel T, Charbit M, Dusek J, Ghiggeri GM, Jankauskiene A, Mir S, Montini G, Peco-Antic A, Wuhl E, Zurowska AM, Mehls O, Antignac C, Schaefer F, Salomon R. Prevalence of mutations in renal developmental genes in children with renal hypodysplasia: results of the ESCAPE study. *J Am Soc Nephrol*. 2006;17:2864–70.
8. Gee HY, Otto EA, Hurd TW, Ashraf S, Chaki M, Cluckey A, Vega-Warner V, Saisawat P, Diaz KA, Fang H, Kohl S, Allen SJ, Airik R, Zhou W, Ramaswami G, Janssen S, Fu C, Innis JL, Weber S, Vester U, Davis EE, Katsanis N, Fathy HM, Jeck N, Klaus G, Nayir A, Rahim KA, Al Attrach I, Al Hassoun I, Ozturk S, Drozd D, Helmchen U, O'Toole JF, Attanasio M, Lewis RA, Nurnberg G, Nurnberg P, Washburn J, MacDonald J, Innis JW, Levy S, Hildebrandt F. Whole-exome resequencing distinguishes cystic kidney diseases from phenocopies in renal ciliopathies. *Kidney Int*. 2014;85:880–7.
9. Otto EA, Hurd TW, Airik R, Chaki M, Zhou W, Stoetzel C, Patil SB, Levy S, Ghosh AK, Murga-Zamalloa CA, van Rieuwijk J, Letteboer SJ, Sang L, Giles RH, Liu Q, Coene KL, Estrada-Cuzcano A, Collin RW, McLaughlin HM, Held S, Kasanuki JM, Ramaswami G, Conte J, Lopez I, Washburn J, Macdonald J, Hu J, Yamashita Y, Maher ER, Guay-Woodford LM, Neumann HP, Obermuller N, Koenekoop RK, Bergmann C, Bei X, Lewis RA, Katsanis N, Lopes V, Williams DS, Lyons RH, Dang CV, Brito DA, Dias MB, Zhang X, Cavalcoli JD, Nurnberg G, Nurnberg P, Pierce EA, Jackson PK, Antignac C, Saunier S, Roepman R, Dollfus H, Khanna H, Hildebrandt F. Candidate exome capture identifies mutation of SDCCAG8 as the cause of a retinal-renal ciliopathy. *Nat Genet*. 2010;42:840–50.
10. Schaefer E, Zaloszczyk A, Lauer J, Durand M, Stutzmann F, Perdomo-Trujillo Y, Redin C, Bennouna Greene V, Toutain A, Perrin L, Gerard M, Caillard S, Bei X, Lewis RA, Christmann D, Letsch J, Kribs M, Mutter C, Muller J, Stoetzel C, Fischbach M, Marion V, Katsanis N, Dollfus H. Mutations in SDCCAG8/NPHP10 cause Bardet–Biedl syndrome and are associated with penetrant renal disease and absent polydactyly. *Mol Syndromol*. 2011;1:273–81.
11. Airik R, Slaats GG, Guo Z, Weiss AC, Khan N, Ghosh A, Hurd TW, Bekker-Jensen S, Schroder JM, Elledge SJ, Andersen JS, Kispert A, Castelli M, Boletta A, Giles RH, Hildebrandt F. Renal-retinal ciliopathy gene Sdccag8 regulates DNA damage response signaling. *J Am Soc Nephrol*. 2014;25:2573–83.
12. Kim JC, Ou YY, Badano JL, Esmail MA, Leitch CC, Fiedrich E, Beales PL, Archibald JM, Katsanis N, Rattner JB, Leroux MR. MKKS/BBS6, a divergent chaperonin-like protein linked to the obesity disorder Bardet–Biedl syndrome, is a novel centrosomal component required for cytokinesis. *J Cell Sci*. 2005;118:1007–20.
13. McKusick VA, Bauer RL, Koop CE, Scott RB. Hydrometrocolpos as a simply inherited malformation. *JAMA*. 1964;189:813–6.
14. Beales PL, Elcioglu N, Woolf AS, Parker D, Flinter FA. New criteria for improved diagnosis of Bardet–Biedl syndrome: results of a population survey. *J Med Genet*. 1999;36:437–46.
15. Schaefer E, Durand M, Stoetzel C, Doray B, Viville B, Helle S, Danse JM, Hamel C, Bitoun P, Goldenberg A, Finck S, Faivre L, Sigaudy S, Holder M, Vincent MC, Marion V, Bonneau D, Verloes A, Nisand I, Mandel JL, Dollfus H. Molecular diagnosis reveals genetic heterogeneity for the overlapping MKKS and BBS phenotypes. *Eur J Med Genet*. 2011;54:157–60.
16. Gilissen C, Arts HH, Hoischen A, Spruijt L, Mans DA, Arts P, van Lier B, Steehouwer M, van Rieuwijk J, Kant SG, Roepman R, Knoers NV, Veltman JA, Brunner HG. Exome sequencing identifies WDR35 variants involved in Sensenbrenner syndrome. *Am J Hum Genet*. 2010;87:418–23.
17. Bacino CA, Dhar SU, Brunetti-Pierri N, Lee B, Bonnen PE. WDR35 mutation in siblings with Sensenbrenner syndrome: a ciliopathy with variable phenotype. *Am J Med Genet A*. 2012;158A:2917–24.
18. Hoffer JL, Fryssira H, Konstantinidou AE, Ropers HH, Tzschach A. Novel WDR35 mutations in patients with cranioectodermal dysplasia (Sensenbrenner syndrome). *Clin Genet*. 2013;83:92–5.
19. Uhlén M, Fagerberg L, Hallström BM, Lindskog C, Oksvold P, Mardinoglu A, Sivertsson Å, Kampf C, Sjöstedt E, Asplund A, Olsson I, Edlund K, Lundberg E, Navani S, Szigartyo CA, Odeberg J, Djureinovic D, Takanen JO, Hober S, Alm T, Edqvist PH, Berling H, Tegel H, Mulder J, Rockberg J, Nilsson P, Schwenk JM, Hamsten M, von Feilitzen K, Forsberg M, Persson L, Johansson F, Zwahlen M, von Heijne G, Nielsen J, Pontén F. Proteomics. Tissue-based map of the human proteome. *Science*. 2015;347:1260419.
20. Slaats GG, Lilien MR, Giles RH. Nephronophthisis: should we target cysts or fibrosis? *Pediatr Nephrol*. 2015;. doi:[10.1007/s00467-015-3162-y](https://doi.org/10.1007/s00467-015-3162-y).

A pure chloride channel mutant of CLC-5 causes Dent's disease via insufficient V-ATPase activation

Nobuhiko Satoh¹ · Hideomi Yamada¹ · Osamu Yamazaki² · Masashi Suzuki¹ · Motonobu Nakamura¹ · Atsushi Suzuki¹ · Akira Ashida³ · Daisuke Yamamoto⁴ · Yoshitsugu Kaku⁵ · Takashi Sekine⁶ · George Seki⁷ · Shoko Horita¹ 

Received: 25 December 2015 / Revised: 2 February 2016 / Accepted: 8 March 2016 / Published online: 5 April 2016
© Springer-Verlag Berlin Heidelberg 2016

Abstract Dent's disease is characterized by defective endocytosis in renal proximal tubules (PTs) and caused by mutations in the $2\text{Cl}^-/\text{H}^+$ exchanger, CLC-5. However, the pathological role of endosomal acidification in endocytosis has recently come into question. To clarify the mechanism of pathogenesis for Dent's disease, we examined the effects of a novel gating glutamate mutation, E211Q, on CLC-5 functions and endosomal acidification. In *Xenopus* oocytes, wild-type (WT) CLC-5 showed outward-rectifying currents that were inhibited by extracellular acidosis, but E211Q and an artificial pure Cl^-

channel mutant, E211A, showed linear currents that were insensitive to extracellular acidosis. Moreover, depolarizing pulse trains induced a robust reduction in the surface pH of oocytes expressing WT CLC-5 but not E211Q or E211A, indicating that the E211Q mutant functions as a pure Cl^- channel similar to E211A. In HEK293 cells, E211A and E211Q stimulated endosomal acidification and hypotonicity-inducible vacuolar-type H^+ -ATPase (V-ATPase) activation at the plasma membrane. However, the stimulatory effects of these mutants were reduced compared with WT CLC-5. Furthermore, gene silencing experiments confirmed the functional coupling between V-ATPase and CLC-5 at the plasma membrane of isolated mouse PTs. These results reveal for the first time that the conversion of CLC-5 from a $2\text{Cl}^-/\text{H}^+$ exchanger into a Cl^- channel induces Dent's disease in humans. In addition, defective endosomal acidification as a result of insufficient V-ATPase activation may still be important in the pathogenesis of Dent's disease.

Daisuke Yamamoto deceased.

Parts of this paper were taken from the thesis written in English by Nobuhiko Satoh. The title of the thesis, which is in Japanese, is as follows: “CLC-5の $2\text{Cl}^-/\text{H}^+$ 交換輸送機能はV-ATPaseを介する効率的エンドゾーム酸性化に必要である”. The summary (in Japanese) of the thesis is accessible at http://repository.dl.itc.u-tokyo.ac.jp/index_e.html

✉ Shoko Horita
shorita-tky@umin.ac.jp

Keywords CLC-5 · Gating glutamate · Dent's disease · V-ATPase · Endocytosis · Endosomal acidification

- ¹ Department of Internal Medicine, Faculty of Medicine, The University of Tokyo Hospital, 7-3-1 Hongo, Bunkyo-ku, Tokyo 113-0033, Japan
- ² Apheresis and Dialysis Center, General Medicine, School of Medicine, Keio University, Tokyo, Japan
- ³ Department of Pediatrics, Osaka Medical College, Takatsuki, Osaka, Japan
- ⁴ Biomedical Computation Center, Osaka Medical College, Takatsuki, Osaka, Japan
- ⁵ Department of Nephrology, Fukuoka Children's Hospital, Fukuoka, Japan
- ⁶ Department of Pediatrics, Ohashi Medical Center, Toho University, Meguro-ku, Tokyo, Japan
- ⁷ Yaizu City Hospital, Yaizu, Japan

Introduction

Dent's disease is an X-linked disorder that causes a dysfunction in renal proximal tubules (PTs) and is characterized by low-molecular-weight proteinuria (LMWP), hypercalciuria, nephrocalcinosis, nephrolithiasis, and renal failure [6, 8, 9, 48, 51]. The etiology of Dent's disease has been associated with mutations in the *CLCN5* gene that encodes the electrogenic $2\text{Cl}^-/\text{H}^+$ exchanger CLC-5 [22, 31, 36, 56].

CLC-5 belongs to the CLC family [20] and is abundantly expressed in early endosomes of the PT, where it is co-localized with vacuolar-type H^+ -ATPase (V-ATPase) [14, 35]. Several lines of evidence indicate that CLC-5 plays an essential role in

normal PT endocytosis by facilitating V-ATPase-mediated endosomal acidification [25]. Indeed, previous studies showed that two different CLC-5 knockout (KO) mice exhibited defective endosomal acidification and LMWP due to defective endocytosis [15, 16, 32, 49]. Therefore, a hypothesis was proposed that CLC-5 provides a Cl^- shunt pathway required for maximal endosomal acidification by V-ATPase.

The identification of CLC-5 as a $2\text{Cl}^-/\text{H}^+$ exchanger rather than a Cl^- channel [31, 36, 56] has posed a challenge to the above hypothesis, because endosomal Cl^- transport by the $2\text{Cl}^-/\text{H}^+$ exchanger may waste energy by recycling H^+ between endosomes and the cytoplasm. Nevertheless, simulation studies suggested that the $2\text{Cl}^-/\text{H}^+$ exchange mode of CLC-7, rather than the simple Cl^- conductance, would be more efficient in lysosomal acidification, and this is applicable to the situation of CLC-5 in endosomes [19, 50]. In contrast, Smith and Lippiat proposed that CLC-5 directly acidifies endosomes by transporting H^+ into endosomes in exchange of Cl^- [41].

In the $2\text{Cl}^-/\text{H}^+$ exchanger CLC-ec1 of *Escherichia coli*, a glutamate residue in the selectivity filter (E148) acts not only as the outside Cl^- gate but also as the extracellular H^+ acceptor [10, 11]. Replacement of this conserved “gating glutamate,” which corresponds to E211 in CLC-5, with alanine converts $2\text{Cl}^-/\text{H}^+$ exchangers to pure Cl^- channels [1, 2, 31, 36]. Interestingly, in transgenic mice, the E211A mutation of CLC-5 acts as an artificial pure Cl^- channel mutant and causes defective PT endocytosis similar to that of CLC-5 KO mice. Unlike CLC-5 KO mice, however, the E211A mice completely preserved normal endosomal acidification, suggesting that endosomal Cl^- accumulation is more important for PT endocytosis than endosomal acidification [29].

While more than 150 mutations in *CLCN5* have been identified [9, 24], mutations in the “gating glutamate” have not been reported to date. Notably, a recent genetic study of Japanese patients with typical Dent’s disease identified a previously unrecognized CLC-5 E211Q mutation [39]. Interestingly, the E148Q mutant in CLC-ec1, like the E148A mutant, was shown to behave as a pure Cl^- channel. In this study, we aimed to clarify the mechanism of pathogenesis for Dent’s disease by analyzing the effects of the E211Q mutation on CLC-5 functions and endosomal acidification.

Methods

Patient description

The patient was a 7-year-old boy who presented with high urinary β 2-microglobulin (37,580 $\mu\text{g}/\text{L}$; normal range $<230 \mu\text{g}/\text{L}$), hypercalciuria (calcium/creatinine 0.313 mg/mg; normal range $<0.2 \text{ mg}/\text{mg}$), and renal calcification without renal failure. The genetic analysis identified a codon change c.631G>C resulting in the CLC-5 E211Q mutation [39].

Animals

All animal procedures including sacrifice were approved by the University of Tokyo Ethics Committee for Animal Experiments and conformed to the guidelines for animal experiments of the University of Tokyo.

Molecular modeling of CLC-5

A three-dimensional model of the human CLC-5 transmembrane domains was constructed as previously reported [52] based on X-ray crystallographic data for CLC-ec1 [10, 11]. This model utilized the optimization of the molecular structure by energy minimization and molecular dynamic simulation. Molecular modeling and analysis were performed using a package for molecular structure analyses, Molecular Operating Environment (MOE 2011.10, Chemical Computing Group Inc., Québec, Canada <http://www.chemcomp.com/>). The E211Q and E211A mutant models were also constructed by the same manner.

Preparation of CLC-5-expressing constructs

Hemagglutinin (HA)-tagged human wild-type (WT) CLC-5 subcloned into pTLN [13] and pcDNA3.1 vectors were used for expression in *Xenopus laevis* oocytes and HEK293 cells, respectively. Both of the vectors were kindly provided by Dr. T. J. Jentsch (Leibniz-Institut für Molekulare Pharmakologie, Berlin, Germany). To introduce mutations, the QuickChange II XL Site-Directed Mutagenesis kit (Agilent Technologies, Santa Clara, CA, USA) was used and the complete cDNA sequences were verified by DNA sequencing.

Expression in oocytes

The mMACHINE high-yield Capped RNA Transcription kit (Thermo Fisher Scientific, Waltham, MA, USA) was used to synthesize capped cRNAs from the CLC-5 constructs. Female *X. laevis* were anesthetized before surgery by immersion in 0.2 % tricaine methanesulfonate (MS-222, Sigma-Aldrich, St. Louis, MO, USA) solution for 30 min. Oocytes were surgically collected from ovaries, treated with collagenase as described [17, 40, 47], and injected with 5 ng of each cRNA, while the frogs were kept in separate tanks for 2 days after the suture and put back in the aquarium. Electrophysiological experiments were performed 3–4 days after cRNA injection.

Voltage clamp in oocytes

An oocyte was placed in a perfusion chamber and superfused with nominally HCO_3^- -free ND96 solution (96 mM NaCl, 2 mM KCl, 1 mM MgCl_2 , 1.8 mM CaCl_2 , and 5 mM

HEPES) that was adjusted to pH 7.4. To measure the CLC-5 current, a two-electrode voltage clamp method consisting of 20 mV steps from -80 to $+80$ mV during 100 ms from a folding potential of -25 mV was performed with a model OC-725C oocyte clamp (Warner Instruments, Hamden, CT, USA) controlled by the Clampex module of pCLAMP software (Molecular Devices, Sunnyvale, CA, USA). Using the same voltage clamp method, we measured the CLC-5 current in perfusates of various pH (5.4, 6.4, 7.4, and 8.4) to examine its sensitivity to extracellular acidosis. For pH 6.4 and 5.4 solutions, 5 mM HEPES was replaced by 5 mM 2-(*N*-morpholino)-ethanesulfonic acid (MES). To exclude a contribution of any leaky endogenous currents, a reduction in current amplitude to the replacement of 80 mM Cl^- in ND96 by equivalent amounts of Γ^- was routinely confirmed [46].

Surface pH measurement in oocytes

An oocyte was voltage clamped and the surface pH of the oocyte was measured by pH-sensitive and reference microelectrodes connected to a Duo773 high-input impedance differential electrometer (WPI, Sarasota, FL, USA). Tips of pH-sensitive microelectrodes were siliconized with dichlorodimethylsilane vapor

(Serva, Heidelberg, Germany) and filled with the ionophore cocktail (95293, Sigma-Aldrich) as described [21, 38], and only electrodes responding with a slope larger than 50 mV per pH unit were used. For these measurements, HEPES concentration in perfusates was reduced to 0.5 mM as described [31].

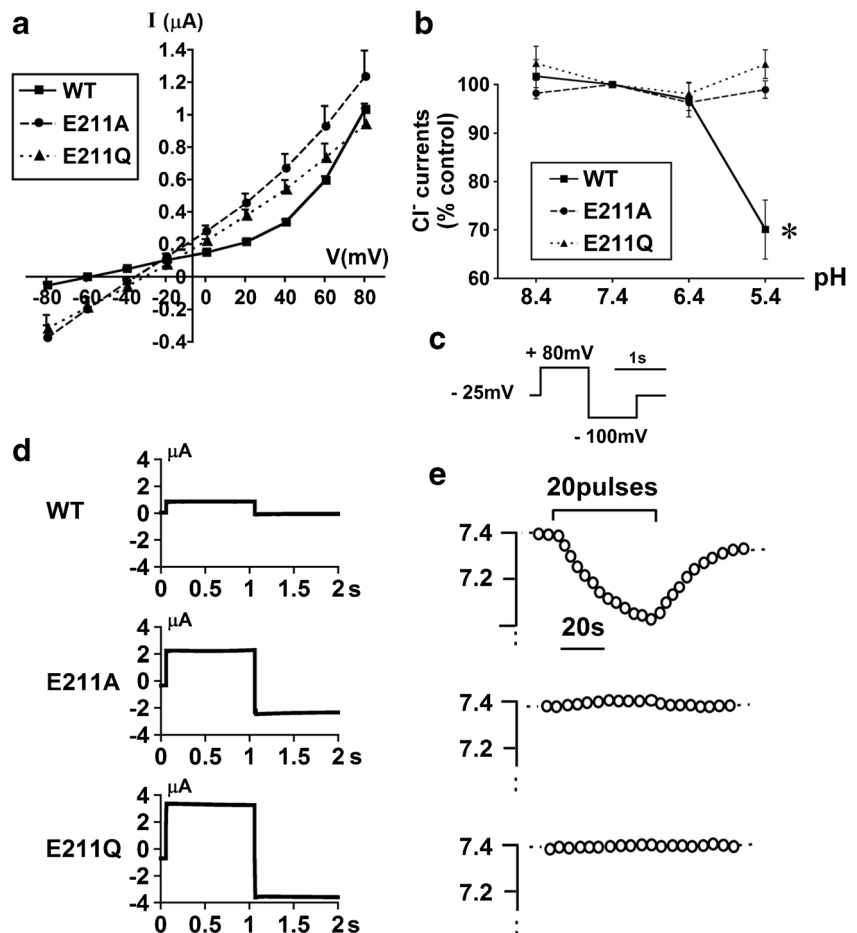
Expression in HEK293 cells

HEK293 cells were transfected with CLC-5 constructs using Lipofectamine 2000 (Thermo Fisher Scientific). To facilitate the expression of CLC-5 constructs, Dulbecco's modified Eagle's medium (DMEM) supplemented with 10 % fetal calf serum and 5 mM sodium butyrate was used [7]. Measurements of cell and endosomal pH, immunoblotting, or immunofluorescence analysis were performed 48 h after transfection.

Measurement of V-ATPase activity in HEK293 cells

HEPES-buffered solution (127 mM NaCl, 5 mM KCl, 1.5 mM CaCl_2 , 1 mM MgCl_2 , 2 mM NaH_2PO_4 , 1 mM Na_2SO_4 , 25 mM HEPES, and 5.5 mM glucose) was adjusted to pH 7.4. In isotonic Na^+ -free solution, Na^+ was replaced by equivalent amounts of *N*-methyl-D-glucamine. In hypotonic Na^+ -free solution, the

Fig. 1 Electrophysiological properties of WT and CLC-5 mutants. **a** Steady-state current–voltage relationships of oocytes expressing WT CLC-5 ($n=8$), E211A ($n=9$), and E211Q mutants ($n=6$). **b** Current sensitivity to changes in external pH. Currents at 80 mV were monitored for each oocyte expressing WT CLC-5 ($n=6$), the E211A mutant ($n=7$), or the E211Q mutant ($n=7$) ($*p<0.05$ versus pH 7.4). Each data point is normalized to the current value at pH 7.4. **c** A protocol of each single depolarizing pulse. **d** A representative CLC-5 current elicited by a single depolarizing pulse. **e** Changes in surface pH of oocytes in response to repetitive depolarizing pulse trains measured with pH-sensitive and reference microelectrodes



osmolality was reduced to 210 mOsm [33]. In NH_4Cl solution, 30 mM NaCl in HEPES-buffered solution was replaced by equimolar amounts of NH_4Cl . Cellular pH was measured by detecting fluorescence emissions from the pH dye acetoxymethylester of bis(carboxyethyl)carboxyfluorescein (BCECF/AM; Dojin, Kumamoto, Japan) with a photometry system (OSP-10; Olympus, Tokyo, Japan) [17, 47, 53]. To induce intracellular acidification, cells were first pulsed with 30 mM NH_4Cl for 3 min. Afterwards, the solution was exchanged for isotonic Na^+ -free solution followed by hypotonic Na^+ -free solution, which was previously shown to activate V-ATPase [3, 33]. Intracellular pH was calibrated by incubating the cells with solutions containing 120 mM KCl, 20 mM NaCl, and 10 μM nigericin adjusted to pH 6.5 to 7.5 [54].

Measurement of endosomal pH in HEK293 cells

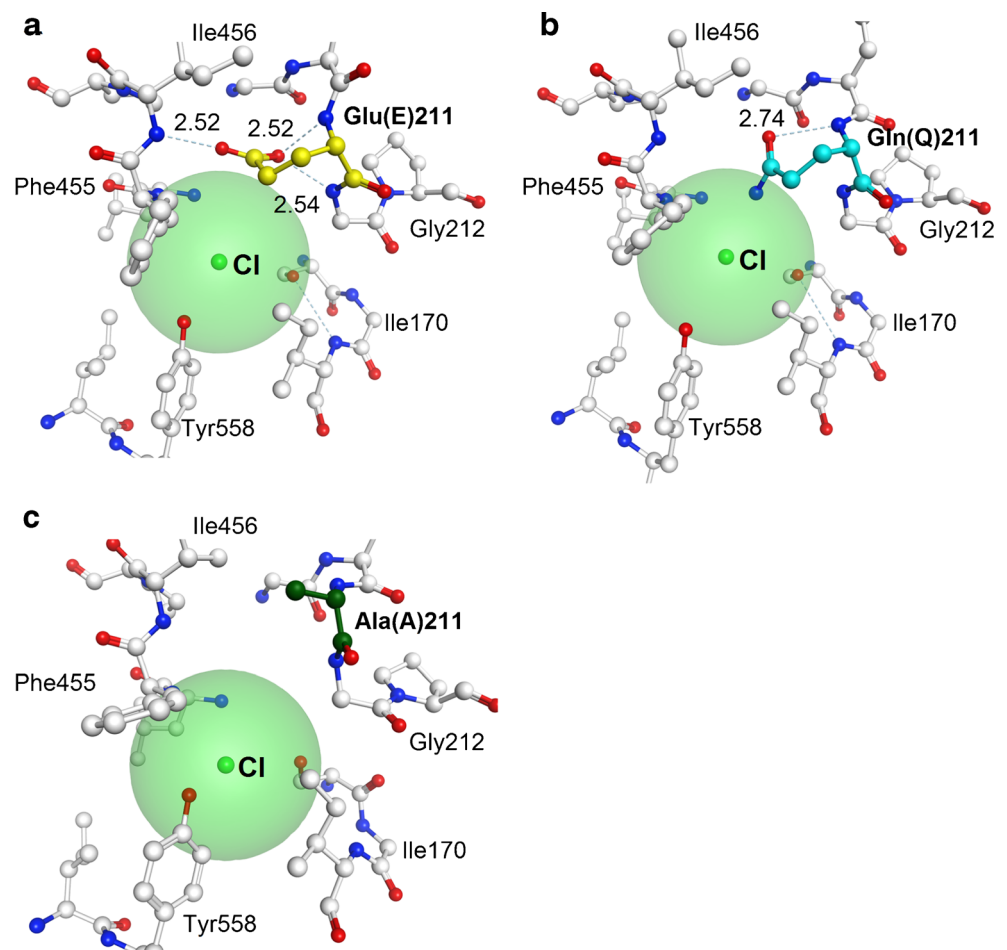
To measure endosomal pH, we used a ratiometric biosensor comprised of the pH-sensitive GFP mutant pHluorin fused to the vesicle-associated membrane protein VAMP2, kindly provided by Dr. J. D. Lippiat (University of Leeds, Leeds, UK) [26, 41]. HEK293 cells were cotransfected with VAMP2-pHluorin and CLC-5 constructs. A Leica TCS SP5II confocal

microscope (Leica Microsystems, Wetzlar, Germany) was used to excite VAMP2-pHluorin at 405 and 488 nm. Emissions were measured through a long-pass filter covering 505 to 696 nm. Endosomal pH was determined in two or three vesicles in a single cell across ≥ 20 cells that were transfected with CLC-5 constructs or a blank vector control. To convert the 405-/488-nm fluorescence ratio to pH, in situ pH calibration was performed as described [43].

Sample preparation, cell surface biotinylation, and immunoblotting

HEK293 cells were grown on a 10-cm culture dish, transfected with the CLC-5 constructs, collected, lysed with the lysis buffer (Tris/pH 8.0, 150 mM NaCl, 1 % Nonidet P-40, 0.5 % sodium deoxycholate, 0.1 % SDS, and 1 mM PMSF), and subjected to immunoblotting of total cellular fractions. To examine the effect of hypotonicity on plasma membrane V-ATPase expression, HEK293 cells transfected with each CLC-5 construct were superfused with 30 mM NH_4Cl solution for 3 min, isotonic Na^+ -free solution for 90 s, and hypotonic Na^+ -free solution (210 mOsm) for 1 min at 37 °C. Thereafter, cell surface biotinylation was performed using the

Fig. 2 Predicted molecular structures of CLC-5 constructs. Transmembrane domain molecular structure of WT human CLC-5, E211Q, and E211A were predicted on X-ray crystallographic data of CLC-ec1 and shown in **a**, **b**, and **c**, respectively. E211 (WT), Q211 (mutant), and A211 (mutant) are colored in *yellow*, *light blue*, and *deep green*. Oxygen, nitrogen, and chloride are colored in *red*, *blue*, and *light green*, respectively. Hydrogen atoms are not described. Theoretical van der Waals surface of chloride ions are described in *light green*. Hydrogen bonds and distances related to side-chains of E211 and Q211 are shown by *green dashed lines* with the lengths (\AA)



Pierce Cell Surface Protein Isolation Kit (Thermo Scientific) as described [47, 53] and samples were subjected to biotinylation western blotting. Immunoblotting of total cellular fractions or cell surface fractions was performed by using antibodies against HA (Roche Diagnostics, Meyland, France), B2 subunit of V-ATPase (Santa Cruz Biotechnology, Dallas, TX, USA), β -actin (Merck Millipore), or Na/K pump α 1 (Merck Millipore, Darmstadt, Germany).

Immunofluorescence

HEK293 cells were cotransfected with CLC-5 constructs and VAMP2-pHluorin and grown on polylysine-coated coverslips. After fixation with 4 % paraformaldehyde in PBS, cells were permeabilized with 0.1 % Triton X-100 (Sigma-Aldrich) and stained with a rabbit polyclonal anti-HA antibody (BETHYL, Montgomery, TX, USA) followed by an Alexa Fluor 546 goat anti-rabbit IgG (Molecular Probes) secondary antibody. The Leica TCS SP5II confocal microscope was used to visualize VAMP2-pHluorin (488 nm) and CLC-5 constructs (543 nm).

Measurement of luminal Na^+/H^+ exchanger (NHE) and V-ATPase activities in isolated mouse PTs

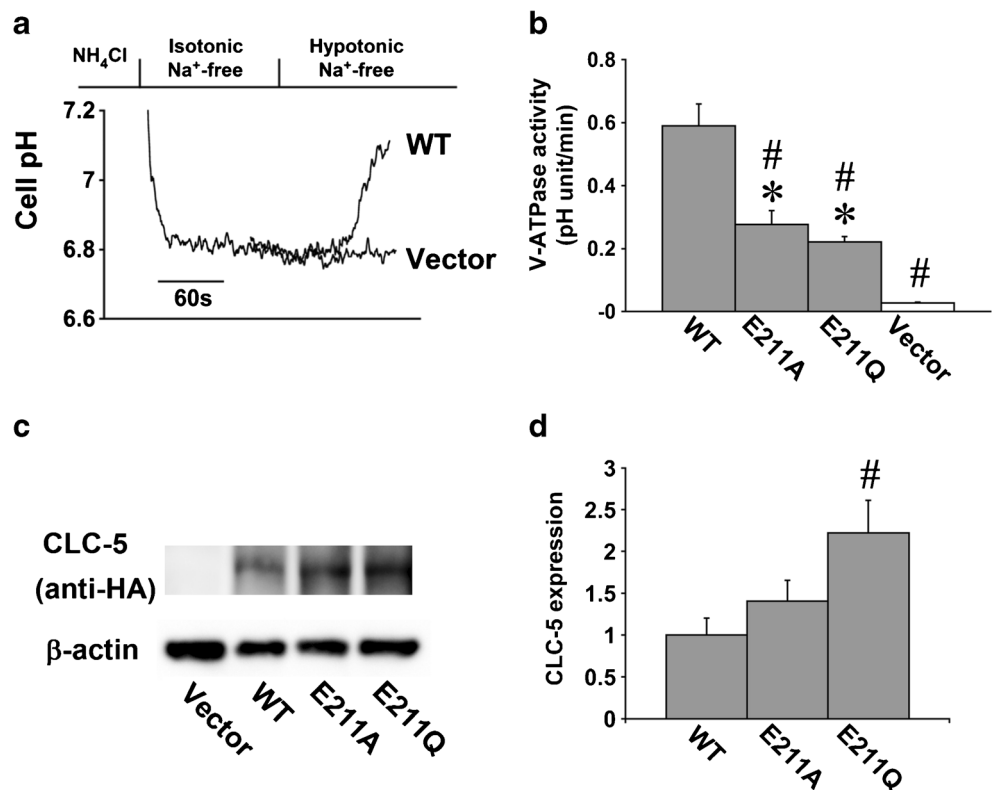
PTs were isolated from 6-week-old C57BL/6 mice which were sacrificed by intraperitoneal injection of excessive amounts of

pentobarbital and attached to a glass coverslip coated with Cell-Tak glue (Corning, NY, USA). A capillary glass was used to expose the luminal surface as described for isolated mouse distal tubules [37]. To measure luminal V-ATPase and NHE activities, intracellular pH was monitored with an inverted fluorescence microscope equipped with MetaFluor 7.7 software (Molecular Devices, Sunnyvale, CA, USA) similar to the measurements of V-ATPase activity in HEK293 cells. In brief, isolated and split-opened mouse PTs in the chamber were first loaded with BCECF/AM in HEPES-buffered solution for 5 to 10 min, and then the perfusate was switched to isotonic Na^+ -free solution. After intracellular acidification was achieved by the NHE activities, the solution was replaced with hypotonic Na^+ -free solution to activate plasma membrane V-ATPase. The V-ATPase activity was determined by the rates of cellular pH recovery that was observed both in isotonic and hypotonic Na^+ -free solutions. For the calculation of the activity, the cellular pH change during the initial 30 s was measured.

siRNA treatment in isolated mouse PTs

Freshly isolated mouse PTs were treated with siRNA for the V-ATPase B2 subunit, CLC-5, or scrambled negative control (all from Santa Cruz Biotechnology, Dallas, TX, USA) using Lipofectamine 2000 and were incubated overnight in DMEM supplemented with 10 % FBS as previously reported [27].

Fig. 3 Effects of CLC-5 constructs on V-ATPase in HEK293 cells. **a** Intracellular pH tracings of WT or the control vector are shown. Note that WT, but not vector, exhibited a rapid cell pH recovery in hypotonic Na^+ -free solution. **b** V-ATPase activity determined by the rates of intracellular pH recovery in hypotonic Na^+ -free solution (* $p < 0.05$ versus vector, and # $p < 0.05$ versus WT). **c** Total cellular expression of CLC-5 constructs and β -actin in HEK293 cells. **d** Intensity data for CLC-5 constructs/ β -actin semi-quantified by densitometry and normalized to the average value of WT ($n = 5$ for each construct) (# $p < 0.05$ versus WT)



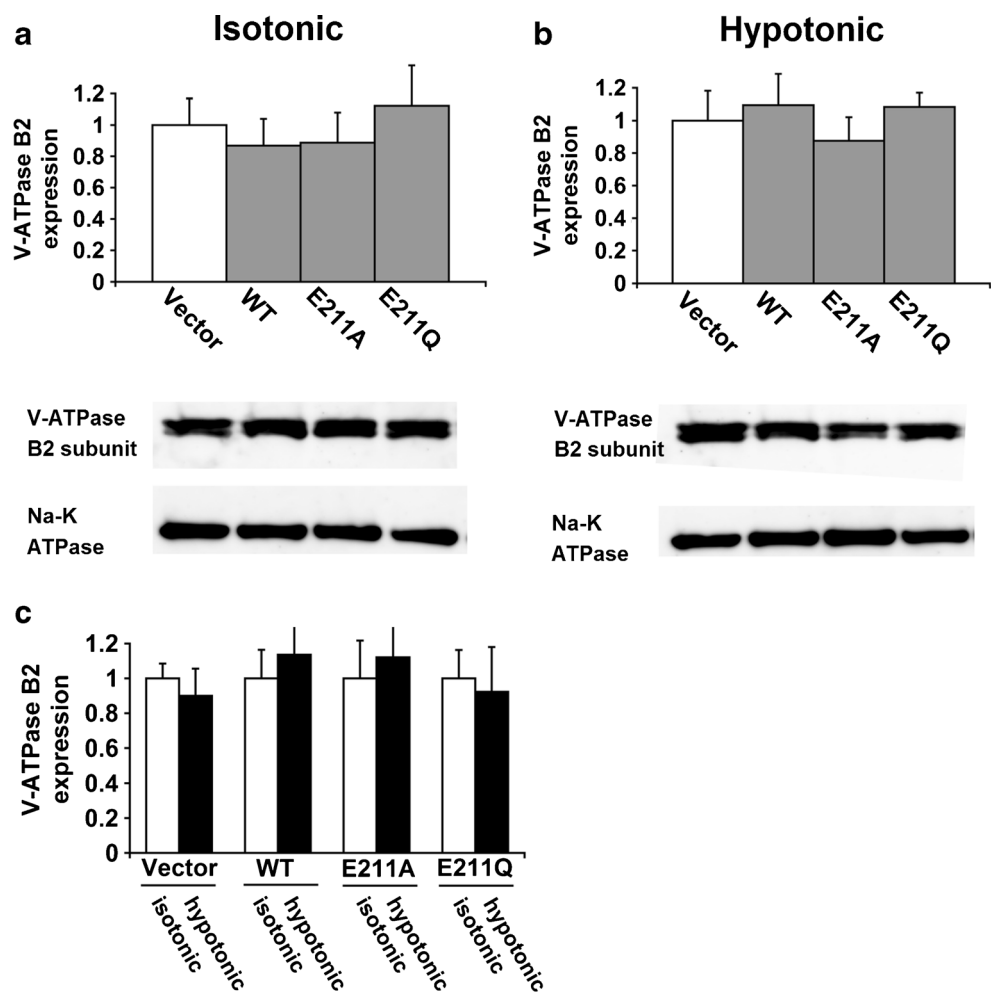
RNA extraction and quantitative PCR analysis

Total RNA was extracted from isolated mouse PTs by using Isogen II (Nippon Gene, Tokyo, Japan), and cDNA was synthesized with the cDNA Synthesis Kit (Takara, Tokyo, Japan) as previously described [27]. Quantitative PCR was performed with TaqMan Gene Expression Master Mix (Applied Biosystems, Foster City, CA, USA), TaqMan Gene Expression Assays (Mm00431987_ml for V-ATPase B2, Mm00443851_ml for CLC-5, and Mm00607939_sl for β -actin; all from Applied Biosystems), and sequence detection system (7500 Fast Real-time PCR System; Applied Biosystems). The expression level was quantified relative to the abundance of β -actin cDNA.

Statistical analysis

The data were presented as the mean \pm SEM. Unpaired Student's *t* test or ANOVA with Bonferroni's correction were used to determine significant differences as appropriate. Statistical significance was set at $p < 0.05$.

Fig. 4 Surface expression of endogenous V-ATPase B2 subunit in HEK293 cells. **a** Biotinylation western blotting in isotonic Na^+ -free solution. Intensity data for V-ATPase B2 subunit/ Na^+ - K^+ ATPase were semi-quantified by densitometry and normalized to the average value of the vector ($n = 4$ for each construct). **b** Biotinylation western blotting in hypotonic Na^+ -free solution. Intensity data for V-ATPase B2 subunit/ Na^+ - K^+ ATPase were semi-quantified by densitometry and normalized to the average value of the vector ($n = 4$ for each construct). **c** Effects of hypotonicity on surface expression of B2 subunit. *Open bars* represent data in isotonic solution, and *closed bars* represent data in hypotonic solution ($n = 4$ for each construct)



Results

Functional analysis of E211Q in *Xenopus* oocytes

We first examined the functional properties of the CLC-5 E211Q mutant. Figure 1a shows the current–voltage relationships of oocytes expressing WT CLC-5, the E211Q mutant, or the artificial E211A mutant. WT CLC-5 showed strongly outwardly rectifying currents as previously reported [13, 46]. In contrast, the pure Cl^- channel E211A mutant showed nearly linear currents [31, 36]. Notably, the E211Q mutant also showed linear currents similar to that of E211A. Although extracellular acidosis significantly reduced the WT currents, E211A and E211Q mutants had no reduction in currents as shown in Fig. 1b. These results suggest that the E211Q mutant behaves as a pure Cl^- channel.

To further characterize the properties of the E211Q mutant, we examined changes in the surface pH of oocytes in response to trains of depolarizing pulses (Fig. 1c). As shown in Fig. 1d, e, WT CLC-5 elicited an immediate and reversible reduction in surface pH by 0.31 ± 0.04 ($n = 4$) in response to the pulse trains, consistent with its function as a $2\text{Cl}^-/\text{H}^+$ exchanger [31]. In

contrast, either the E211A mutant ($n=7$) or the E211Q ($n=7$) mutant failed to elicit changes in surface pH in response to the pulse trains. These results confirmed that the E211Q mutation, like E211A, converts CLC-5 into the pure Cl^- channel.

Effects of E211Q and E211A mutations on CLC-5 gating structure

To gain insight into molecular mechanism underlying the mutation-based changes in CLC-5 function, we also performed simulation analysis on the gating structure. Transmembrane domain molecular structures of WT CLC-5, E211Q, and E211A mutant were predicted based on X-ray crystallographic data of CLC-ec1 [10, 11].

Figure 2a shows that carboxyl group of E211 in WT CLC-5 was fixed by hydrogen bonds to main-chain NH groups of E211, G212, and I456. The homologous E148 in CLC-ec1 has also similar interaction to neighboring main-chain [23]. Figure 2b illustrates the structural effects of the E211Q mutation. In the case of Q211, the side-chain direction was changed, and only hydrogen bond to Q211 main-chain NH group remained. The NH_2 group of Q211 would break the hydrogen bonds to G212 and I456, and its partially positive charge weakly interacted to a neighboring chloride ion. This “open conformation,” as also observed in CLC-ec1 E148Q mutation [23], is

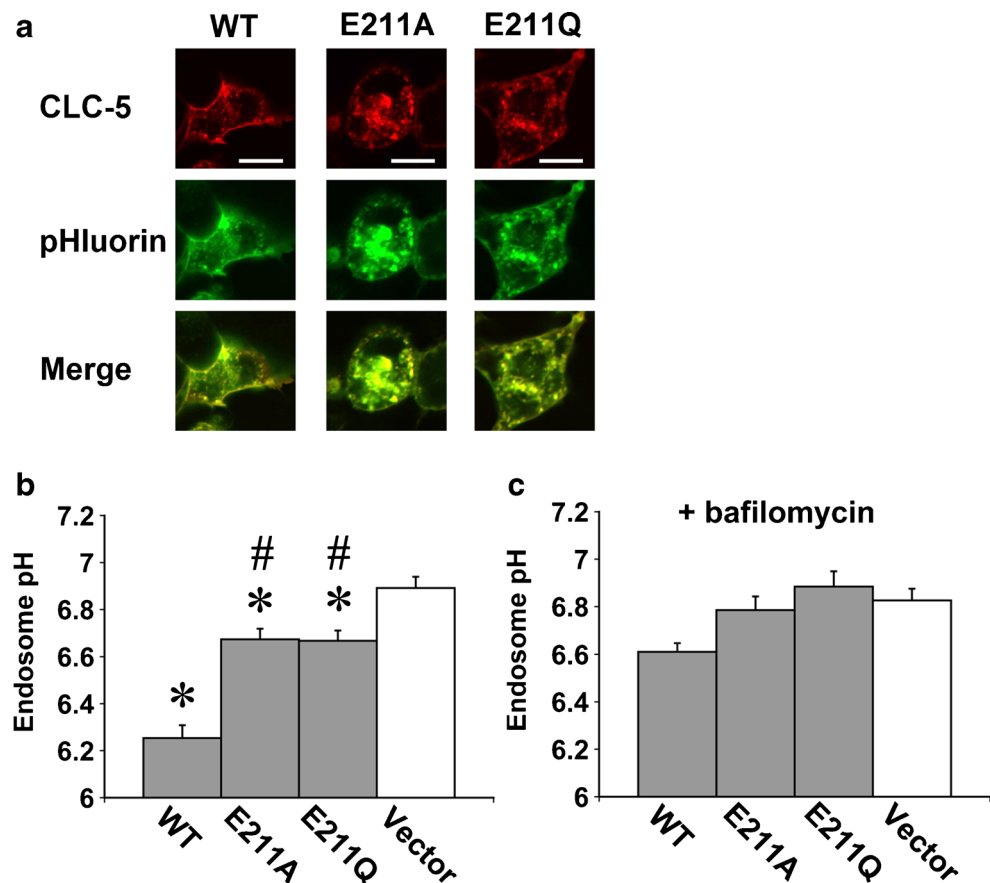
similar to the structure of a temporary protonated E211 in the theoretical model of human CLC-5 proton transformation [55]. Figure 2c also illustrates the structural effects of the E211A mutation. In this model, A211 main-chain was shifted away from F455-I456 due to its small side-chain. Thus, the conformational shift of neighboring side-chains (including F455, I456, and Y558) in the E211A mutant was significantly larger enough to form slightly wider “open conformation” than that in the E211Q mutant. The similar main-chain shift was also observed in the CLC-ec1 E148A mutation [28]. Unlike the E211Q mutant, the E211A mutant failed to directly interact with a chloride ion due to the lack of NH_2 group.

These structural analyses confirmed that the protonation of E211 played a key role in the gating mechanism for Cl^- transport [30, 55]. Furthermore, E211Q and E211A mutations were expected to induce similar changes in the gating structure, resulting in an “open conformation” that allowed for free Cl^- transport even in the absence of E211 protonation.

Effects of CLC-5 constructs on V-ATPase in HEK293 cells

We next examined the impact of WT and mutant CLC-5 constructs on plasma membrane V-ATPase activity in HEK293 cells. Cellular pH recovery from acid load was monitored in the absence of Na^+ , and V-ATPase was activated by

Fig. 5 Effects of CLC-5 constructs on endosomal pH. **a** Co-localization of HA-CLC-5 constructs and VAMP2-pHluorin. Confocal images of HEK293 cells showed that each CLC-5 construct (red) and VAMP-2 pHluorin (green) localized in endosomes and also at the plasma membrane. Scale bars = 10 μm . **b** Endosomal pH measured by the ratiometric VAMP2-pHluorin analysis. (* $p < 0.05$ versus Vector and # $p < 0.05$ versus WT). **c** Endosomal pH in the presence of 200 nM bafilomycin



hypotonicity as previously reported [3, 33]. As shown in Fig. 3a, superfusion with isotonic Na^+ -free solution after NH_4Cl pulse decreased cellular pH to approximately 6.8. While the subsequent hypotonic Na^+ -free solution had a negligible effect on pH recovery in cells transfected with the control vector alone, WT CLC-5 induced a rapid pH recovery that was completely inhibited by 200 nM bafilomycin, an effect that is consistent with the activation of V-ATPase [3, 33]. Both of the E211A and E211Q mutants also activated V-ATPase, but the magnitude of V-ATPase activation was reduced compared with WT CLC-5 (Fig. 3b). Western blot analysis confirmed that E211A levels were comparable to that of WT CLC-5, and E211Q levels were higher than WT CLC-5 as shown in Fig. 3c, d. This indicates that the reduced activation

of V-ATPase by E211A and E211Q mutants was not due to a difference in protein expression levels of these mutants.

We also examined the surface expression of the V-ATPase B2 subunit. Figure 4a shows that the CLC-5 constructs had no effect on the surface expression of endogenous V-ATPase. In addition, Fig. 4b, c shows that incubation with hypotonic Na^+ -free solution did not impact the surface expression of V-ATPase. These results indicate that the difference in surface expression of V-ATPase cannot account for the difference in the degree of V-ATPase activation by CLC-5 constructs. These data also confirmed that hypotonicity stimulates V-ATPase activity without altering V-ATPase surface expression as previously reported [3, 33].

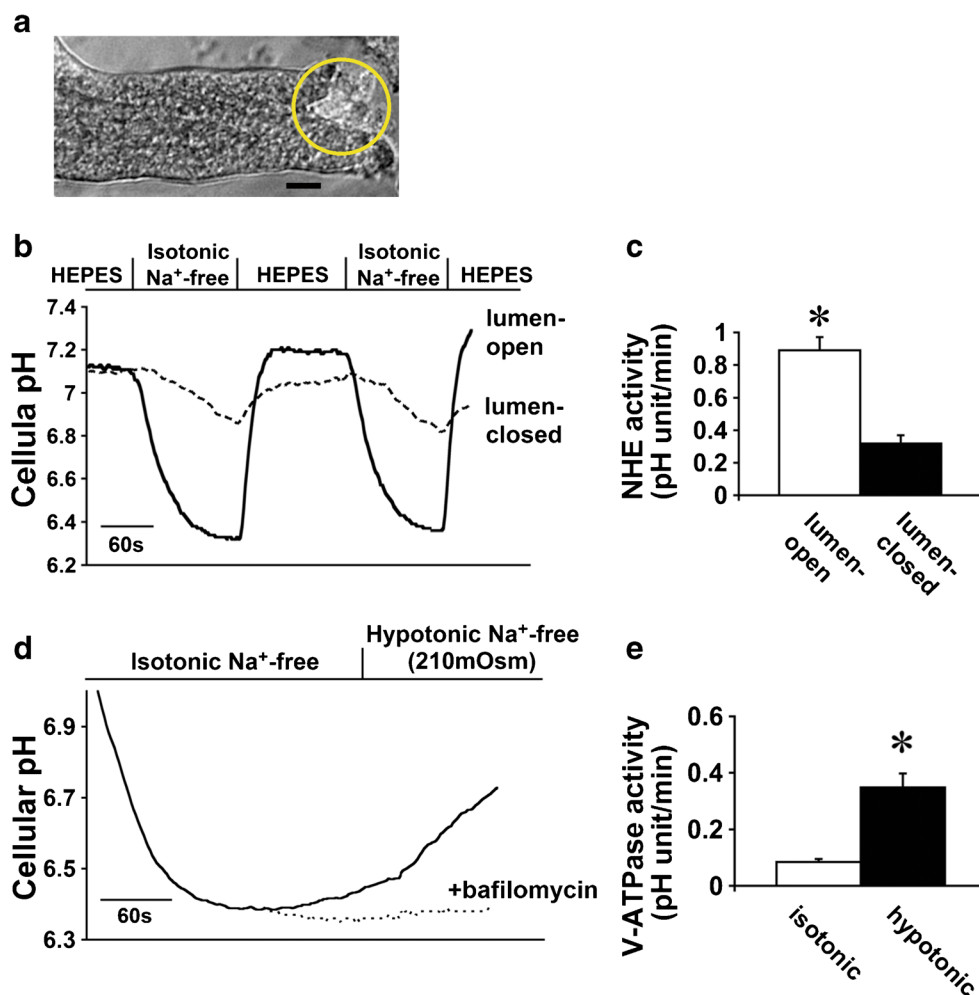


Fig. 6 Activities of luminal transporters in freshly isolated and split-opened mouse PTs. **a** An image of an isolated and split-opened mouse PT. It was attached to a glass coverslip by a tissue adhesive, and one side was split by a glass pipet (shown in a yellow circle). **a** Scale bar = 10 μm . **b** Intracellular pH tracings of lumen-open and lumen-closed mouse PTs in response to Na^+ removal. Lumen-open PTs exhibited a faster and greater pH decrease by Na^+ removal, which reflected the higher NHE activity. **c** NHE activity determined by the rates of cellular pH decrease in response

to Na^+ removal. *Open and closed bars* indicate data from lumen-open and lumen-closed PTs, respectively ($n=6$ for each and $*p<0.05$ versus lumen-closed). **d** Hypotonicity-inducible luminal V-ATPase activation in lumen-open mouse PTs. **e** Bafilomycin-sensitive V-ATPase activity in lumen-open mouse PTs. *Open and closed bars* indicate data in isotonic ($n=6$) and hypotonic ($n=7$) Na^+ -free solution, respectively ($*p<0.05$ versus isotonic)

Effects of CLC-5 constructs on endosomal acidification in HEK293 cells

We next examined the effects of CLC-5 constructs on endosomal acidification in HEK293 cells by using VAMP2-pHluorin [41]. Figure 5a illustrates the localization of CLC-5 and VAMP2-pHluorin in HEK293 cells transfected with each CLC-5 construct. As can be seen in these images, WT CLC-5, E211A, and E211Q showed similar intracellular localization in endosomes and at the plasma membrane. Figure 5b shows that while all of the CLC-5 constructs significantly reduced endosomal pH, the magnitude of acidification by E211A and E211Q was reduced compared with WT. Given that bafilomycin abolished the effects of the CLC-5 constructs on endosomal acidification (Fig. 5c), CLC-5-induced endosomal acidification reflected V-ATPase activity at the endosome.

Effects of CLC-5 on plasma membrane V-ATPase in isolated mouse PTs

While the activation of endosomal V-ATPase by CLC-5 has been well established [14, 42], the activation of plasma membrane V-ATPase by CLC-5 is rather unexpected. Therefore, we examined whether CLC-5 was required for the plasma membrane V-ATPase activation in isolated mouse PTs.

Figure 6a shows an isolated and split-opened mouse PT. In this preparation, luminal NHE activity was reliably measured

(Fig. 6b, c). Moreover, Fig. 6d, e shows that hypotonicity activated bafilomycin-sensitive V-ATPase also in isolated mouse PTs. As shown in Fig. 7, luminal NHE and V-ATPase activities were largely preserved after overnight incubation with control small interference RNA (siRNA), consistent with the functional preservation of cultured PTs through the duration of the experiments [27].

Figure 8a, b shows that treatment with siRNA against V-ATPase B2 subunit or CLC-5 effectively and selectively suppressed the mRNA expression of B2 subunit or CLC-5, respectively. Consistent with the predominant role of the B2 subunit in V-ATPase in PTs [4], siRNA against B2 markedly suppressed hypotonicity-induced V-ATPase activity in PTs and, moreover, siRNA against CLC-5 also largely suppressed V-ATPase activity as shown in Fig. 8c, d. These results indicate that CLC-5 is required for plasma membrane V-ATPase activity not only in cultured cells but also in intact PTs.

Discussion

We performed the functional characterization of the “gating glutamate” mutation E211Q in CLC-5 identified in a typical Dent’s disease patient. In *Xenopus* oocytes, WT CLC-5 showed outward-rectifying currents that were inhibited by extracellular acidosis. On the other hand, E211Q, like the artificial mutant E211A, displayed linear currents that were

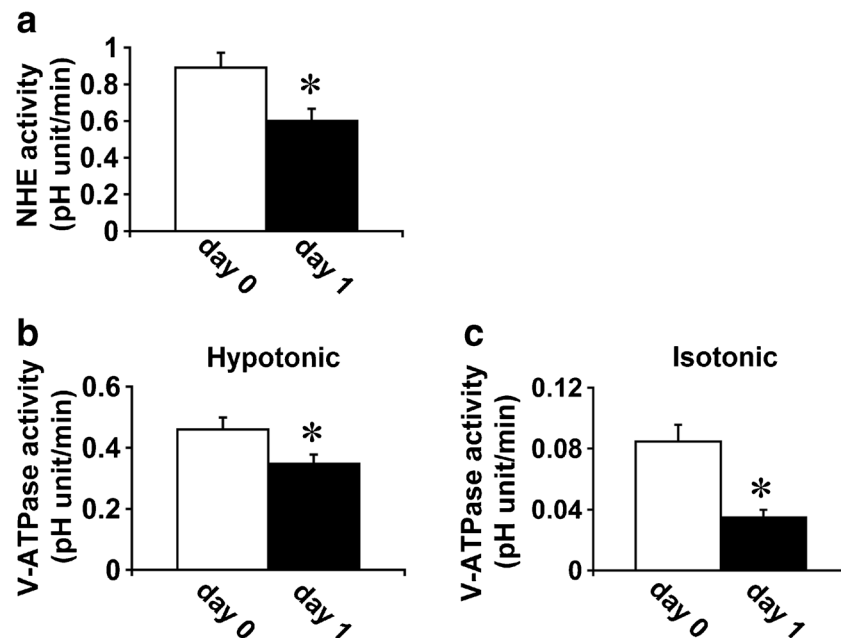


Fig. 7 Preserved activities of luminal transporters in isolated mouse PTs after overnight incubation with control small interference RNA (siRNA). **a** NHE activity of freshly isolated PTs (day 0) and PTs treated with control siRNA (day 1). *Open and closed bars* indicate data from day 0 and day 1, respectively ($n=6$ for each and $*p<0.05$ versus day 0). **b** Plasma membrane V-ATPase activity of freshly isolated PTs (day 0) and PTs treated with control siRNA (day 1), activated by hypotonic solution.

Open and closed bars indicate data from day 0 and day 1, respectively ($n=7$ for day 0, $n=6$ for day 1, and $*p=0.046$ versus day 0). **c** Plasma membrane V-ATPase activity of freshly isolated PTs (day 0) and PTs treated with control siRNA (day 1) in isotonic solution. *Open and closed bars* indicate data from day 0 and day 1, respectively ($n=6$ for each and $*p<0.05$ versus day 0)

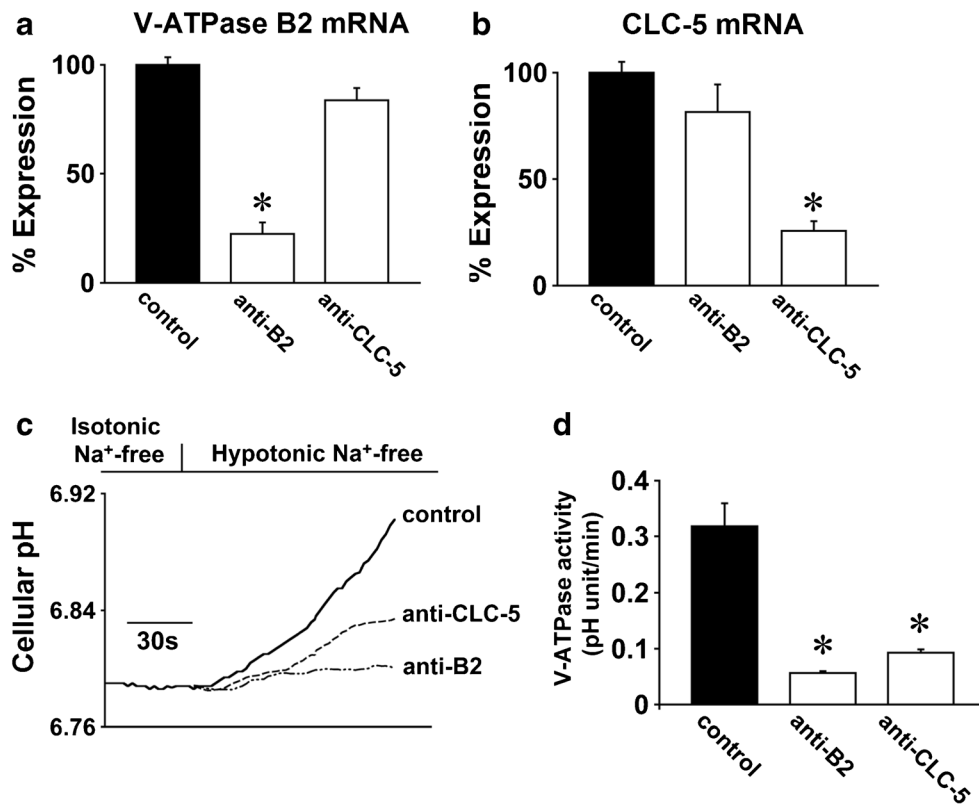


Fig. 8 V-ATPase activity in isolated mouse PTs requires CLC-5. Isolated mouse PTs were treated with scrambled siRNA (control), siRNA against V-ATPase B2 subunit (anti-B2), or siRNA against CLC-5 (anti-CLC-5). **a** mRNA expression level of V-ATPase B2 subunit ($n=4$). Each data point is normalized to the average value of control. **b** mRNA expression level of CLC-5 ($n=4$). Each data point is normalized to the average value of

control. **c** Intracellular pH tracings of siRNA-treated PTs. Note that cell pH recovery in hypotonic Na⁺-free solution was markedly suppressed by anti-B2 or anti-CLC-5 siRNA. **d** Summary data for V-ATPase activity (8 for control, $n=7$ for V-ATPase anti-B2 subunit, $n=8$ for anti-CLC-5 and $*p<0.05$ versus control)

insensitive to extracellular acidosis. While WT CLC-5 induced a robust decrease in surface pH in response to the depolarizing pulses, E211Q and E211A failed to induce such changes in surface pH. These results indicate that the E211Q mutant behaves as a Cl⁻ channel similar to the E211A mutant. Simulation analysis based on the structure model of CLC-5 further supports this conclusion. Previously, the E211A mutant was shown to cause defective endocytosis in PTs of transgenic mice [29]. This study is the first to show that the E211Q mutation also converts the functional mode of CLC-5 from a 2Cl⁻/H⁺ exchanger into a Cl⁻ channel, which leads to the pathogenesis of Dent's disease in humans. Traditionally, endosomal acidification via functional coupling between CLC-5 and V-ATPase has been considered to be essential for normal endocytosis [25]. However, endosomal acidification of vesicles purified from PTs was reported to be completely preserved even in E211A mice. This seemed to suggest that Cl⁻ accumulation might be critical for normal endocytosis rather than endosomal acidification [29, 50]. Nevertheless, our present study indicates that defective endosomal acidification due to insufficient V-ATPase activation still plays an important role in the pathogenesis of Dent's disease.

In HEK293 cells, we observed that both of the E211Q and E211A mutants caused a moderate reduction in endosomal pH. However, endosomal acidification by these mutants was significantly less than that by WT CLC-5, in contrast to previous findings in E211A mice. Methodological differences may account for this discrepancy. For example, significant acidification could still be detected in endosomal vesicles prepared from mouse PT fractions even in the complete absence of CLC-5 [15]. In contrast, basal V-ATPase activity was negligible in HEK293 cells, lacking the endogenous CLC-5 activity [41]. Accordingly, the difference in endosomal acidification by the CLC-5 constructs as detected in the present study might have been missed in vesicles prepared from the E211A mice [29]. Some compensatory mechanisms might have also emerged in the gene-targeted mice. While the involvement of cell type-specific factors cannot be excluded, lack of basal V-ATPase activity in HEK293 cells may support the functional coupling of V-ATPase and CLC-5 at the plasma membrane as will be discussed below. On the other hand, our study confirms the model that the Cl⁻ shunt pathway can facilitate endosomal acidification by V-ATPase [25, 34]. Although this observation

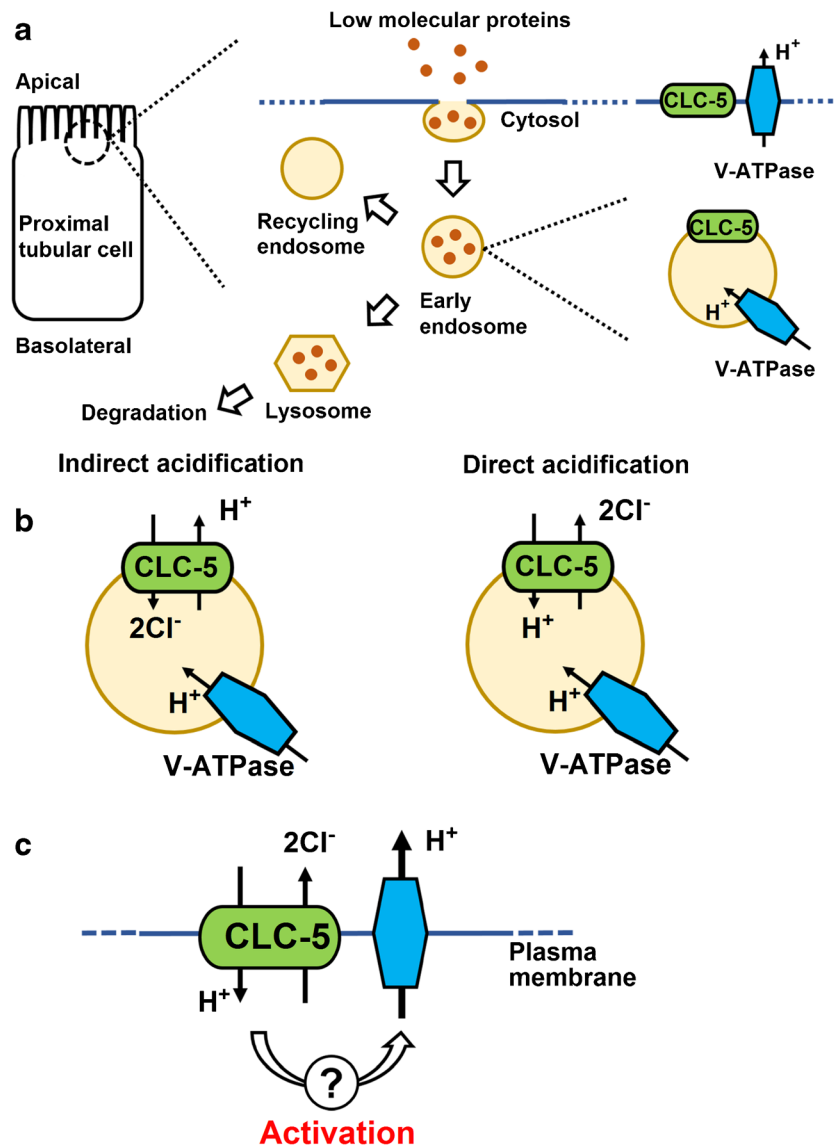


Fig. 9 Hypothetical models for the functional coupling between V-ATPase and CLC-5 in endosomes and plasma membrane. **a** A schematic model of endocytosis and localization of CLC-5 and V-ATPase in a renal proximal tubular cell. CLC-5 expressed in early endosomes with V-ATPase is involved in normal endocytosis, while it is also expressed in the plasma membrane with V-ATPase. Mutations in the coding gene *CLCN5* cause Dent's disease that is characterized primarily by low-molecular-weight proteinuria (LMWP). **b** Proposed models for roles of CLC-5 in endosome. In indirect acidification model, CLC-5 activates V-ATPase indirectly by functioning as a Cl^- shunt

pathway. Although the results of our present study supports this model, we cannot exclude that Cl^- accumulation into endosome rather than Cl^- shunting is more important in the same model. In direct acidification model, on the other hand, CLC-5 functions in the opposite direction as a Cl^- exit pathway. **c** Functional coupling of V-ATPase and CLC-5 in the plasma membrane. CLC-5 activates V-ATPase in the plasma membrane via unknown mechanisms that require the $2\text{Cl}^-/\text{H}^+$ exchange activity. This type of functional coupling between V-ATPase and CLC-5 is presumed to exist even in endosomes

contradicts the idea of direct endosomal acidification by CLC-5 [41], theoretical considerations also put the direct acidification theory in doubt [44, 45].

The previous simulation studies on lysosomal acidification support the advantage of the $2\text{Cl}^-/\text{H}^+$ exchange mode. Thus, CLC-7 as an antiporter provides more negative intravesicular potential than a pure Cl^- conductor, resulting in the electrochemical environments that are more favorable for V-ATPase [19, 50]. Such indirect activation of V-ATPase is one possible

explanation for the more efficient endosomal acidification by WT CLC-5 than by the E211Q and E211A mutants. However, the present study raised another intriguing possibility that the $2\text{Cl}^-/\text{H}^+$ exchange mode of WT CLC-5 directly activates V-ATPase.

At usual inside negative cell membrane potentials, the simple linear Cl^- channel should provide a negative charge shunt by exporting Cl^- from inside cells, leading to the acceleration of H^+ extrusion. Conversely, the

outwardly rectifying $2\text{Cl}^-/\text{H}^+$ exchanger should be nearly inactive at this potential according to the current–voltage relationship (Fig. 1a) and would induce no changes in electrochemical gradients for H^+ . Nevertheless, WT actually activated plasma membrane V-ATPase in HEK293 cells more efficiently than the E211Q and E211A mutants. Moreover, silencing of CLC-5 by siRNA in isolated mouse PTs significantly reduced plasma membrane V-ATPase activity without changing the expression level of the B2 subunit. These results support the view that tight functional coupling between V-ATPase and CLC-5 exists also in the plasma membrane.

How did WT CLC-5 activate plasma membrane V-ATPase more efficiently than the Cl^- channel mutants? The answer to this question is currently unknown, but V-ATPase is known to have multiple functions. For example, V-ATPase may be critical for endosomal pH-sensing mechanism by interacting with the small GTPase Afr6 and ARNO [18]. Moreover, a multi-protein complex including V-ATPase senses amino acids in lysosomes and thereby activates target of rapamycin (mTOR) kinase [57], which may in turn regulate megalin-mediated PT endocytosis [12]. It is therefore possible that the $2\text{Cl}^-/\text{H}^+$ exchange mode of CLC-5 induces the maximal plasma membrane V-ATPase activation by recruiting unknown cellular factors and/or modifying V-ATPase functions. A previous study using immortalized rat renal proximal tubule cells also supports this view [5]. Hypothetical models for the functional coupling between V-ATPase and CLC-5 in both endosomes and plasma membrane were summarized in Fig. 9. On the other hand, it is unclear whether our present in vitro data directly corresponds to in vivo condition where many compensatory functions will happen. To clarify this issue, future studies on E211Q knock-in mice or PT cells from the patient carrying the E211Q mutation will be required.

In summary, our present study revealed that the conversion of CLC-5 $2\text{Cl}^-/\text{H}^+$ exchanger into the pure Cl^- channel indeed induces Dent's disease in humans. We found that the $2\text{Cl}^-/\text{H}^+$ exchange mode of CLC-5 is required for the maximal V-ATPase activation in both endosome and plasma membrane. While we cannot exclude the potential involvement of endosomal Cl^- accumulation, our data support the critical role of defective endosomal acidification due to insufficient V-ATPase activation in the pathogenesis of Dent's disease.

Acknowledgments This study was supported in part by grants from the Ministry of Education, Culture, Sports, Science and Technology of Japan.

Compliance with ethical standards

Conflict of interest The authors declare that they have no competing interests.

References

- Accardi A, Kolmakova-Partensky L, Williams C, Miller C (2004) Ionic currents mediated by a prokaryotic homologue of CLC Cl^- channels. *J Gen Physiol* 123:109–19. doi:10.1085/jgp.200308935
- Accardi A, Miller C (2004) Secondary active transport mediated by a prokaryotic homologue of CLC Cl^- channels. *Nature* 427:803–7. doi:10.1038/nature02314
- Amlal H, Goel A, Soleimani M (1998) Activation of H^+ -ATPase by hypotonicity: a novel regulatory mechanism for H^+ secretion in IMCD cells. *Am J Physiol* 275:F487–501
- Cao X, Yang Q, Qin J, Zhao S, Li X, Fan J, Chen W, Zhou Y, Mao H, Yu X (2012) V-ATPase promotes transforming growth factor-beta-induced epithelial-mesenchymal transition of rat proximal tubular epithelial cells. *Am J Physiol Renal Physiol* 302:F1121–32. doi:10.1152/ajprenal.00278.2011
- Carraro-Lacroix LR, Lessa LM, Bezerra CN, Pessoa TD, Souza-Menezes J, Morales MM, Girardi AC, Malnic G (2010) Role of CFTR and CIC-5 in modulating vacuolar H^+ -ATPase activity in kidney proximal tubule. *Cell Physiol Biochem* 26:563–76. doi:10.1159/000322324
- Claverie-Martin F, Ramos-Trujillo E, Garcia-Nieto V (2011) Dent's disease: clinical features and molecular basis. *Pediatr Nephrol* 26:693–704. doi:10.1007/s00467-010-1657-0
- D'Antonio C, Molinski S, Ahmadi S, Huan LJ, Wellhauser L, Bear CE (2013) Conformational defects underlie proteasomal degradation of Dent's disease-causing mutants of CLC-5. *Biochem J* 452:391–400. doi:10.1042/BJ20121848
- Dent CE, Friedman M (1964) Hypercalcuric rickets associated with renal tubular damage. *Arch Dis Child* 39:240–9
- Devuyst O, Thakker RV (2010) Dent's disease. *Orphanet J Rare Dis* 5:28. doi:10.1186/1750-1172-5-28
- Dutzler R, Campbell EB, Cadene M, Chait BT, MacKinnon R (2002) X-ray structure of a CLC chloride channel at 3.0 Å reveals the molecular basis of anion selectivity. *Nature* 415:287–94. doi:10.1038/415287a
- Dutzler R, Campbell EB, MacKinnon R (2003) Gating the selectivity filter in CLC chloride channels. *Science* 300:108–12. doi:10.1126/science.1082708
- Gleixner EM, Canaud G, Hermlé T, Guida MC, Kretz O, Helmstadter M, Huber TB, Eimer S, Terzi F, Simons M (2014) V-ATPase/mTOR signaling regulates megalin-mediated apical endocytosis. *Cell Rep* 8:10–9. doi:10.1016/j.celrep.2014.05.035
- Grand T, Mordasini D, L'Hoste S, Pennaforte T, Genete M, Biyeyeme MJ, Vargas-Poussou R, Blanchard A, Teulon J, Lourdel S (2009) Novel CLCN5 mutations in patients with Dent's disease result in altered ion currents or impaired exchanger processing. *Kidney Int* 76:999–1005. doi:10.1038/ki.2009.305
- Gunther W, Luchow A, Cluzeaud F, Vandewalle A, Jentsch TJ (1998) CLC-5, the chloride channel mutated in Dent's disease, colocalizes with the proton pump in endocytotically active kidney cells. *Proc Natl Acad Sci U S A* 95:8075–80
- Gunther W, Piwon N, Jentsch TJ (2003) The CLC-5 chloride channel knock-out mouse—an animal model for Dent's disease. *Pflugers Arch* 445:456–62. doi:10.1007/s00424-002-0950-6
- Hara-Chikuma M, Wang Y, Guggino SE, Guggino WB, Verkman AS (2005) Impaired acidification in early endosomes of CLC-5 deficient proximal tubule. *Biochem Biophys Res Commun* 329:941–6. doi:10.1016/j.bbrc.2005.02.060
- Horita S, Yamada H, Inatomi J, Moriyama N, Sekine T, Igarashi T, Endo Y, Dasouki M, Ekim M, Al-Gazali L, Shimadzu M, Seki G, Fujita T (2005) Functional analysis of NBC1 mutants associated with proximal renal tubular acidosis and ocular abnormalities. *J Am Soc Nephrol* 16:2270–8. doi:10.1681/ASN.2004080667

18. Hurtado-Lorenzo A, Skinner M, El Annan J, Futai M, Sun-Wada GH, Bourgoin S, Casanova J, Wildeman A, Bechoua S, Ausiello DA, Brown D, Marshansky V (2006) V-ATPase interacts with ARNO and Arf6 in early endosomes and regulates the protein degradative pathway. *Nat Cell Biol* 8:124–36. doi:10.1038/ncb1348
19. Ishida Y, Nayak S, Mindell JA, Grabe M (2013) A model of lysosomal pH regulation. *J Gen Physiol* 141:705–20. doi:10.1085/jgp.201210930
20. Jentsch TJ, Steinmeyer K, Schwarz G (1990) Primary structure of Torpedo marmorata chloride channel isolated by expression cloning in *Xenopus* oocytes. *Nature* 348:510–4. doi:10.1038/348510a0
21. Kondo Y, Fromter E (1987) Axial heterogeneity of sodium-bicarbonate cotransport in proximal straight tubule of rabbit kidney. *Pflugers Arch* 410:481–6
22. Lloyd SE, Pearce SH, Fisher SE, Steinmeyer K, Schwappach B, Scheinman SJ, Harding B, Bolino A, Devoto M, Goodyer P, Rigden SP, Wrong O, Jentsch TJ, Craig IW, Thakker RV (1996) A common molecular basis for three inherited kidney stone diseases. *Nature* 379:445–9. doi:10.1038/379445a0
23. Lobet S, Dutzler R (2006) Ion-binding properties of the CLC chloride selectivity filter. *EMBO J* 25:24–33. doi:10.1038/sj.emboj.7600909
24. Lourdel S, Grand T, Burgos J, Gonzalez W, Sepulveda FV, Teulon J (2012) CLC-5 mutations associated with Dent's disease: a major role of the dimer interface. *Pflugers Arch* 463:247–56. doi:10.1007/s00424-011-1052-0
25. Mellman I, Fuchs R, Helenius A (1986) Acidification of the endocytic and exocytic pathways. *Annu Rev Biochem* 55:663–700. doi:10.1146/annurev.bi.55.070186.003311
26. Miesenböck G, De Angelis DA, Rothman JE (1998) Visualizing secretion and synaptic transmission with pH-sensitive green fluorescent proteins. *Nature* 394:192–5. doi:10.1038/28190
27. Nakamura M, Yamazaki O, Shirai A, Horita S, Satoh N, Suzuki M, Hamasaki Y, Noiri E, Kume H, Enomoto Y, Homma Y, Seki G (2015) Preserved Na/HCO₃ cotransporter sensitivity to insulin may promote hypertension in metabolic syndrome. *Kidney Int* 87:535–42. doi:10.1038/ki.2014.351
28. Nguitragool W, Miller C (2006) Uncoupling of a CLC Cl⁻/H⁺ exchange transporter by polyatomic anions. *J Mol Biol* 362:682–90. doi:10.1016/j.jmb.2006.07.006
29. Novarino G, Weinert S, Rickheit G, Jentsch TJ (2010) Endosomal chloride-proton exchange rather than chloride conductance is crucial for renal endocytosis. *Science* 328:1398–401. doi:10.1126/science.1188070
30. Picollo A, Malvezzi M, Accardi A (2010) Proton block of the CLC-5 Cl⁻/H⁺ exchanger. *J Gen Physiol* 135:653–9. doi:10.1085/jgp.201010428
31. Picollo A, Pusch M (2005) Chloride/proton antiporter activity of mammalian CLC proteins CLC-4 and CLC-5. *Nature* 436:420–3. doi:10.1038/nature03720
32. Piwon N, Gunther W, Schwake M, Bosl MR, Jentsch TJ (2000) CLC-5 Cl⁻-channel disruption impairs endocytosis in a mouse model for Dent's disease. *Nature* 408:369–73. doi:10.1038/35042597
33. Rahmati N, Kunzelmann K, Xu J, Barone S, Sirianant L, De Zeeuw CI, Soleimani M (2013) Slc26a11 is prominently expressed in the brain and functions as a chloride channel: expression in Purkinje cells and stimulation of V H⁺-ATPase. *Pflugers Arch* 465:1583–97. doi:10.1007/s00424-013-1300-6
34. Sabolic I, Burekhardt G (1986) Characteristics of the proton pump in rat renal cortical endocytotic vesicles. *Am J Physiol* 250:F817–26
35. Sakamoto H, Sado Y, Naito I, Kwon TH, Inoue S, Endo K, Kawasaki M, Uchida S, Nielsen S, Sasaki S, Marumo F (1999) Cellular and subcellular immunolocalization of CLC-5 channel in mouse kidney: colocalization with H⁺-ATPase. *Am J Physiol* 277:F957–65
36. Scheel O, Zdebek AA, Lourdel S, Jentsch TJ (2005) Voltage-dependent electrogenic chloride/proton exchange by endosomal CLC proteins. *Nature* 436:424–7. doi:10.1038/nature03860
37. Schodel J, Klanke B, Weidemann A, Buchholz B, Bernhardt W, Bertog M, Amann K, Korbmacher C, Wiesener M, Warnecke C, Kurtz A, Eckardt KU, Willam C (2009) HIF-prolyl hydroxylases in the rat kidney: physiologic expression patterns and regulation in acute kidney injury. *Am J Pathol* 174:1663–74. doi:10.2353/ajpath.2009.080687
38. Seki G, Fromter E (1990) The chloride/base exchanger in the basolateral cell membrane of rabbit renal proximal tubule S3 segment requires bicarbonate to operate. *Pflugers Arch* 417:37–41
39. Sekine T, Komoda F, Miura K, Takita J, Shimadzu M, Matsuyama T, Ashida A, Igarashi T (2014) Japanese Dent disease has a wider clinical spectrum than Dent disease in Europe/USA: genetic and clinical studies of 86 unrelated patients with low-molecular-weight proteinuria. *Nephrol Dial Transplant* 29:376–84. doi:10.1093/ndt/gft394
40. Shirakabe K, Priori G, Yamada H, Ando H, Horita S, Fujita T, Fujimoto I, Mizutani A, Seki G, Mikoshiba K (2006) IRBIT, an inositol 1,4,5-trisphosphate receptor-binding protein, specifically binds to and activates pancreas-type Na⁺/HCO₃⁻ cotransporter 1 (pNBC1). *Proc Natl Acad Sci U S A* 103:9542–7. doi:10.1073/pnas.0602250103
41. Smith AJ, Lippiat JD (2010) Direct endosomal acidification by the outwardly rectifying CLC-5 Cl⁻/H⁺ exchanger. *J Physiol* 588:2033–45. doi:10.1113/jphysiol.2010.188540
42. Smith AJ, Reed AA, Loh NY, Thakker RV, Lippiat JD (2009) Characterization of Dent's disease mutations of CLC-5 reveals a correlation between functional and cell biological consequences and protein structure. *Am J Physiol Renal Physiol* 296:F390–7. doi:10.1152/ajprenal.90526.2008
43. Sonawane ND, Thiagarajah JR, Verkman AS (2002) Chloride concentration in endosomes measured using a ratioable fluorescent Cl⁻ indicator: evidence for chloride accumulation during acidification. *J Biol Chem* 277:5506–13. doi:10.1074/jbc.M110818200
44. Stauber T, Jentsch TJ (2013) Chloride in vesicular trafficking and function. *Annu Rev Physiol* 75:453–77. doi:10.1146/annurev-physiol-030212-183702
45. Stauber T, Weinert S, Jentsch TJ (2012) Cell biology and physiology of CLC chloride channels and transporters. *Compr Physiol* 2:1701–44. doi:10.1002/cphy.c110038
46. Steinmeyer K, Schwappach B, Bens M, Vandewalle A, Jentsch TJ (1995) Cloning and functional expression of rat CLC-5, a chloride channel related to kidney disease. *J Biol Chem* 270:31172–7
47. Suzuki M, Vaisbich MH, Yamada H, Horita S, Li Y, Sekine T, Moriyama N, Igarashi T, Endo Y, Cardoso TP, de Sa LC, Koch VH, Seki G, Fujita T (2008) Functional analysis of a novel missense NBC1 mutation and of other mutations causing proximal renal tubular acidosis. *Pflugers Arch* 455:583–93. doi:10.1007/s00424-007-0319-y
48. Thakker RV (2000) Pathogenesis of Dent's disease and related syndromes of X-linked nephrolithiasis. *Kidney Int* 57:787–93. doi:10.1046/j.1523-1755.2000.00916.x
49. Wang SS, Devuyst O, Courtoy PJ, Wang XT, Wang H, Wang Y, Thakker RV, Guggino S, Guggino WB (2000) Mice lacking renal chloride channel, CLC-5, are a model for Dent's disease, a nephrolithiasis disorder associated with defective receptor-mediated endocytosis. *Hum Mol Genet* 9:2937–45
50. Weinert S, Jabs S, Supancharat C, Schweizer M, Gimber N, Richter M, Rademann J, Stauber T, Kornak U, Jentsch TJ (2010) Lysosomal pathology and osteopetrosis upon loss of H⁺-driven lysosomal Cl⁻ accumulation. *Science* 328:1401–3. doi:10.1126/science.1188072
51. Wrong OM, Norden AG, Feest TG (1994) Dent's disease; a familial proximal renal tubular syndrome with low-molecular-weight

- proteinuria, hypercalciuria, nephrocalcinosis, metabolic bone disease, progressive renal failure and a marked male predominance. *QJM* 87:473–93
52. Wu F, Roche P, Christie PT, Loh NY, Reed AA, Esnouf RM, Thakker RV (2003) Modeling study of human renal chloride channel (hCLC-5) mutations suggests a structural-functional relationship. *Kidney Int* 63:1426–32. doi:[10.1046/j.1523-1755.2003.00859.x](https://doi.org/10.1046/j.1523-1755.2003.00859.x)
53. Yamazaki O, Yamada H, Suzuki M, Horita S, Shirai A, Nakamura M, Satoh N, Fujita T, Seki G (2013) Identification of dominant negative effect of L522P mutation in the electrogenic $\text{Na}^+\text{-HCO}_3^-$ cotransporter NBCe1. *Pflugers Arch* 465:1281–91. doi:[10.1007/s00424-013-1277-1](https://doi.org/10.1007/s00424-013-1277-1)
54. Yamazaki O, Yamada H, Suzuki M, Horita S, Shirai A, Nakamura M, Seki G, Fujita T (2011) Functional characterization of nonsynonymous single nucleotide polymorphisms in the electrogenic $\text{Na}^+\text{-HCO}_3^-$ cotransporter NBCe1A. *Pflugers Arch* 461:249–59. doi:[10.1007/s00424-010-0918-x](https://doi.org/10.1007/s00424-010-0918-x)
55. Zifarelli G, De Stefano S, Zanardi I, Pusch M (2012) On the mechanism of gating charge movement of ClC-5, a human Cl^-/H^+ antiporter. *Biophys J* 102:2060–9. doi:[10.1016/j.bpj.2012.03.067](https://doi.org/10.1016/j.bpj.2012.03.067)
56. Zifarelli G, Pusch M (2009) Conversion of the 2 $\text{Cl}^-/1 \text{H}^+$ antiporter ClC-5 in a NO_3^-/H^+ antiporter by a single point mutation. *EMBO J* 28:175–82. doi:[10.1038/emboj.2008.284](https://doi.org/10.1038/emboj.2008.284)
57. Zoncu R, Bar-Peled L, Efeyan A, Wang S, Sancak Y, Sabatini DM (2011) mTORC1 senses lysosomal amino acids through an inside-out mechanism that requires the vacuolar H^+ -ATPase. *Science* 334:678–83. doi:[10.1126/science.1207056](https://doi.org/10.1126/science.1207056)